



**AGRICULTURAL UNIVERSITY OF ATHENS
DEPARTMENT OF BIOTECHNOLOGY
LABORATORY OF CELL TECHNOLOGY**

Doctoral thesis

Development of an integrated biosensor system for Toxicology and
Pharmacology applications

Georgia A. Paivana

Supervisor:

Spyridon Kintzios, Professor AUA

Three-member advisory committee

Spyridon Kintzios, Professor AUA

Konstantinos Yialouris, Professor AUA

Grigoris Kaltsas, Professor UNIWA

ATHENS

2022

**AGRICULTURAL UNIVERSITY OF ATHENS
DEPARTMENT OF BIOTECHNOLOGY
LABORATORY OF CELL TECHNOLOGY**

Doctoral thesis

Development of an integrated biosensor system for Toxicology and
Pharmacology applications

Ανάπτυξη ολοκληρωμένου συστήματος βιοαισθητήρα για
εφαρμογές στην Τοξικολογία και Φαρμακολογία

Georgia A. Paivana

Seven-member selection committee

Spyridon Kintzios, Professor AUA (Supervisor)

Grigoris Kaltsas, Professor UNIWA

Konstantinos Yialouris, Professor AUA

Nikolaos Lamprou, Professor AUA

Eleni Ntouni, Associate Professor AUA

Georgia Moschopoulou, Assistant Professor AUA

Sophia Mavrikou, Assistant Professor AUA

Development of an integrated biosensor system for toxicology and pharmacology applications

*Department of Biotechnology
Laboratory of Cell Technology*

Abstract

This thesis presents an analytical study regarding electrical impedance measurements on various cell lines. Based on the principles of Electrochemical Impedance Spectroscopy (EIS) as a technique mostly applied for biological assays, the electrical properties of the solution tested were evaluated. The characterization of complex resistance and its variations as a function of application field is described by impedance. A common approach in different medical areas is bio-impedance as a non-invasive and simultaneously cost-effective method. The application of different substances that considerably affect the cell culture confirmed the significance of this method. Moreover, impedance measurements provide important information about the culture's properties tested under cells' immobilization conditions. Specific custom-made electrodes were used for the evaluation of impedance measurements in combination with custom-made 3D printed well.

The first experimental section presents the application of a particular catecholamine neurotransmitter. More specifically, dopamine (DA) was used as a stimulant to immobilized cell culture for the evaluation of the effects of this bioactive substance. The extraction of calibration curves in a specific frequency range with the application of known DA concentrations with the use of an impedance meter is the key aim of this section. The behaviour of immobilized and non-immobilized cells with the presence of the same DA concentrations as well as the behaviour of respective DA solutions without cells were assessed for comparison purposes. The results indicated that the electrical response of the cell medium is affected by the presence of frequency, thus the immobilization conditions can be considered as a crucial factor in cell cultures. In addition, the electrical response appeared to interfere with dopamine's absorption from cells, information that can be taken into account for medical evaluation regarding schizophrenia, Parkinson's disease, etc.

In the second experimental section, the interactions of immobilized cells under either two-dimensional (2D) or three-dimensional (3D) conditions treated to a bioactive substance are evaluated. In particular, these two types of cell

immobilization arrangements are able to mimic in vivo tissue conditions. The impedance analysis was implemented in murine neuroblastoma cells treated to a specific stimulant. From the results of the previous experimental section, DA was chosen once again as a bioactive substance for further investigation. The main objective of this section is again the extraction of calibration curves in various frequencies for the analytical description of the dopamine's behaviour, this time applied to 2D and 3D immobilized cell cultures. For both immobilization matrices, the mean impedance value was assessed in every frequency tested. The differential responses highlighted the influence of the impedance when a frequency is applied for both immobilization cases and especially in the 2D immobilization matrix where the impedance has higher values. Moreover, the results showed that the increase in dopamine concentration is related to a decrease in impedance for the case of the 3D immobilization matrix, although the opposite behavior is noticed in the 2D case.

The third and last experimental section is focused on anticancer drug research and assessment. In literature, scientists have pointed out the essential role of cancer cell lines as they can provide significant information from real-time impedance measurements, regarding cell viability. Four different adherent mammalian cancer cell lines (SK-N-SH, HeLa, HEK293, and MCF-7) immobilized in three-dimensional (3D) for three different populations (50.000, 100.000, and 200.000 cells/100 μ l) using calcium alginate hydrogel matrix conditions were formed in order to be evaluated by Electric Impedance Spectroscopy analysis. 5-fluorouracil (5-FU) was used as a standard cytostatic agent in every cell culture. This section aims to evaluate the behavior of the abovementioned cell lines after the application of 5-FU by extracting the mean impedance values in various frequencies. For comparison purposes, the same impedance measurements were carried out for pure immobilized cell cultures. The obtained results displayed a relation concerning the cell population for every cell line in conjunction with the frequency-dependent impedance. In addition, the impedance range can indicate the possibility to detect tumor cells along with the results of chemotherapy using impedance measurements. This can be explained by the ability of this method to differentiate the alterations among population densities and cell morphologies.

The contribution of this research work to the field of pharmacology and toxicology is the development and the characterization of a biosensor system based on electrical impedance measurements. The proposed biosensor system constitutes a cost-effective and efficient solution for the implementation of impedance measurements on various cell lines. All experimental approaches indicated a sufficient device-response regarding the solution tested in conjunction with the

impedance meter. Despite the fact that the meter used for each experiment allowed the selection of only five frequencies, the results from the mean impedance calculated using the magnitude values of each solution demonstrated a pattern able to discriminate the alterations of cells' morphology with or without the presence of a bioactive substance. Thus, the proposed biosensor system is considered promising for future research concerning improvements on specific parameters such as the type of electrodes, the size of the well, etc.

Scientific area: biosensor development

Keywords: toxicology, pharmacology, biosensor, applications, development, integrated system

Ανάπτυξη ολοκληρωμένου συστήματος βιοαισθητήρα για εφαρμογές στην Τοξικολογία και Φαρμακολογία

*Τμήμα Βιοτεχνολογίας
Εργαστήριο Κυτταρικής Τεχνολογίας*

Περίληψη

Η παρούσα διδακτορική διατριβή παρουσιάζει μια αναλυτική μελέτη σχετικά με τις ηλεκτρικές μετρήσεις σύνθετης αντίστασης (εμπέδησης) σε διάφορες κυτταρικές σειρές. Με βάση τις αρχές της Φασματοσκοπίας Ηλεκτροχημικής Εμπέδησης (EIS) ως μια τεχνική που εφαρμόζεται κυρίως για βιολογικές δοκιμές, αξιολογήθηκαν οι ηλεκτρικές ιδιότητες του διαλύματος προς δοκιμή. Ο χαρακτηρισμός της σύνθετης αντίστασης καθώς και οι παραλλαγές της ανά πεδίο εφαρμογής περιγράφονται από την εμπέδηση. Μια κοινή προσέγγιση για διαφορετικούς ιατρικούς τομείς αποτελεί η βιο-εμπέδηση ως μια μέθοδος μη επεμβατική και παράλληλα οικονομικά αποδοτική. Η εφαρμογή διάφορων ουσιών που επηρεάζουν σημαντικά τις κυτταροκαλλιέργειες επιβεβαιώνει την σημασία αυτής της μεθόδου. Επιπρόσθετα, οι μετρήσεις εμπέδησης παρέχουν σημαντικές πληροφορίες για τις ιδιότητες της καλλιέργειας που δοκιμάστηκαν υπό συνθήκες ακινητοποίησης των κυττάρων. Για την εκτέλεση των μετρήσεων εμπέδησης χρησιμοποιήθηκαν συγκεκριμένα ειδικά προσαρμοσμένα ηλεκτρόδια από διαφορετικά υλικά σε συνδυασμό με ειδικά κατασκευασμένα τρισδιάστατα εκτυπωμένα κοιλότητα.

Η πρώτη πειραματική ενότητα παρουσιάζει την εφαρμογή ενός συγκεκριμένου νευροδιαβιβαστή κατεχολαμίνης. Πιο συγκεκριμένα, η ντοπαμίνη (DA) χρησιμοποιήθηκε ως διεγερτικό συστατικό στην ακινητοποιημένη κυτταρική καλλιέργεια για την αξιολόγηση των επιδράσεων της συγκεκριμένης βιοδραστικής ουσίας. Ο βασικός στόχος αυτής της ενότητας είναι η εξαγωγή των καμπυλών βαθμονόμησης για ένα συγκεκριμένο πεδίο συχνοτήτων με την εφαρμογή γνωστών συγκεντρώσεων ντοπαμίνης χρησιμοποιώντας μια συσκευή μέτρησης εμπέδησης. Για λόγους σύγκρισης, πραγματοποιήθηκαν μετρήσεις που αφορούν την συμπεριφορά ακινητοποιημένων κυττάρων και μη με την παρουσία των ίδιων συγκεντρώσεων

ντοπαμίνης καθώς επίσης και μετρήσεις που αφορούν την συμπεριφορά των αντίστοιχων διαλυμάτων ντοπαμίνης χωρίς την παρουσία κυττάρων. Τα αποτελέσματα έδειξαν ότι η ηλεκτρική απόκριση του κυτταρικού μέσου εξαρτάται από την συχνότητα, θεωρώντας έτσι τις συνθήκες ακινητοποίησης ως κρίσιμο παράγοντα στις κυτταρικές καλλιέργειες. Επιπλέον, η ηλεκτρική απόκριση φαίνεται να επηρεάζεται από την απορρόφηση της ντοπαμίνης από τα κύτταρα, πληροφορία που πρέπει να ληφθεί υπόψιν για την ιατρική αξιολόγηση σχετικά με την σχιζοφρένεια, την νόσο του Πάρκινσον κτλ.

Στην δεύτερη πειραματική ενότητα αξιολογούνται οι αντιδράσεις των ακινητοποιημένων κυττάρων υπό συνθήκες δύο διαστάσεων ή τριών διαστάσεων κατά την εφαρμογή μιας βιοδραστικής ουσίας. Συγκεκριμένα, οι δυο τύποι των κυτταρικών διατάξεων ακινητοποίησης είναι ικανοί να μιμούνται *in vivo* συνθήκες ιστού. Η ανάλυση της εμπέδησης διεξήχθη σε κύτταρα νευροβλαστώματος ποντικίου που υποβλήθηκαν σε ένα συγκεκριμένο διεγερτικό στοιχείο. Από τα αποτελέσματα της προηγούμενης πειραματικής ενότητας, η ντοπαμίνη επιλέχθηκε και πάλι ως βιοδραστική ουσία για περαιτέρω έρευνα. Ο κύριος στόχος αυτής της ενότητας είναι η εξαγωγή καμπυλών βαθμονόμησης για διάφορες συχνότητες για την αναλυτική περιγραφή της συμπεριφοράς της ντοπαμίνης, αυτή τη φορά κατά την εφαρμογή της σε δισδιάστατες και τρισδιάστατες ακινητοποιημένες κυτταρικές καλλιέργειες. Η μέση τιμή της εμπέδησης αξιολογήθηκε για κάθε συχνότητα και για τους δυο τύπους ακινητοποίησης. Οι διαφορικές αποκρίσεις απέδειξαν την επίδραση της εμπέδησης όταν εφαρμόζεται μια συχνότητα και για τις δυο μεθόδους ακινητοποίησης και ειδικά για την περίπτωση της δυσδιάστατης ακινητοποίησης όπου η εμπέδηση είχε υψηλότερες τιμές. Επιπροσθέτως, τα αποτελέσματα έδειξαν ότι η αύξηση στην συγκέντρωση της ντοπαμίνης σχετίζεται με την μείωση στην εμπέδηση για την περίπτωση της τρισδιάστατης ακινητοποίησης των κυττάρων, παρόλο που η δυσδιάστατη ακινητοποίηση παρουσίασε την αντίθετη συμπεριφορά.

Η τρίτη και τελευταία πειραματική ενότητα εστιάζεται στην έρευνα και την αξιολόγηση αντικαρκινικών φαρμάκων. Στην βιβλιογραφία, οι επιστήμονες έχουν επισημάνει τον ουσιαστικό ρόλο που παίζουν οι καρκινικές κυτταρικές σειρές καθώς παρέχουν σημαντικές πληροφορίες από τις μετρήσεις εμπέδησης σε πραγματικό χρόνο σχετικά με την βιωσιμότητα των κυττάρων. Τέσσερις διαφορετικές προσκολλημένες καρκινικές κυτταρικές σειρές θηλαστικών (SK-N-SH, HeLa, HEK293, and MCF-7) που ακινητοποιήθηκαν τρισδιάστατα σε τρεις διαφορετικούς πληθυσμούς (50.000, 100.000, and 200.000 cells/100μl)

χρησιμοποιώντας υδρογέλη αλγινικού ασβεστίου εξετάστηκαν μέσω φασματοσκοπίας ηλεκτροχημικής εμπέδησης. Η ουσία 5-φθοροουρακίλη (5-FU) χρησιμοποιήθηκε ως βασικός κυτταροστατικός παράγοντας σε κάθε κυτταρική καλλιέργεια. Η ενότητα αυτή στοχεύει στην αξιολόγηση της συμπεριφοράς των προαναφερθεισών κυτταρικών σειρών μετά την εφαρμογή του 5-FU εξάγοντας τις τιμές μέσης εμπέδησης για διαφορετικές συχνότητες. Για λόγους σύγκρισης, οι ίδιες μετρήσεις εμπέδησης διεξήχθησαν για καθαρές ακινητοποιημένες κυτταρικές καλλιέργειες. Τα αποτελέσματα που λήφθηκαν καταδεικνύουν μια σχέση ανάλογα με τον κυτταρικό πληθυσμό μεταξύ κάθε κυτταρικής σειράς και της αντίστασης που εξαρτάται από την συχνότητα. Επίσης, το εύρος της εμπέδησης μπορεί να υποδεικνύει την δυνατότητα ανίχνευσης καρκινικών κυττάρων μαζί με τα αποτελέσματα της χημειοθεραπείας χρησιμοποιώντας μετρήσεις εμπέδησης. Αυτό μπορεί να εξηγηθεί λόγω της ικανότητας της μεθόδου να διαφοροποιεί τις μεταβολές μεταξύ της πυκνότητας του πληθυσμού και των μορφολογιών των κυττάρων.

Η συμβολή της παρούσας ερευνητικής μελέτης περιλαμβάνει την ανάπτυξη καθώς επίσης και τον χαρακτηρισμό ενός συστήματος βιοαισθητήρα που βασίζεται σε μετρήσεις ηλεκτρικής αντίστασης στον τομέα της φαρμακολογίας και της τοξικολογίας. Το προτεινόμενο σύστημα βιοαισθητήρα αποτελεί μια οικονομική, αποδοτική και αποτελεσματική λύση για την εκτέλεση μετρήσεων εμπέδησης σε διάφορες κυτταρικές σειρές. Όλες οι πειραματικές προσεγγίσεις παρουσίασαν μια επαρκή απόκριση του βιοαισθητήρα σχετικά με το διάλυμα που δοκιμάστηκε σε συνδυασμό με την συσκευή μέτρησης της εμπέδησης. Παρόλο που η συσκευή που χρησιμοποιήθηκε για κάθε πείραμα επιτρέπει την επιλογή πέντε μόνο συχνοτήτων, τα αποτελέσματα της μέσης τιμής της εμπέδησης που υπολογίστηκαν χρησιμοποιώντας τις τιμές του πλάτους για κάθε διάλυμα παρουσίασαν ένα μοτίβο ικανό να διακρίνει τις μεταβολές στην μορφολογία των κυττάρων με ή χωρίς την παρουσία βιοδραστικής ουσίας όταν εφαρμόζεται συχνότητα. Συνεπώς, το προτεινόμενο σύστημα βιοαισθητήρα θεωρείται πολλά υποσχόμενο για μελλοντική έρευνα μετά την εφαρμογή βελτιώσεων που αφορούν παράγοντες όπως ο τύπος των ηλεκτροδίων, το μέγεθος της κοιλότητας κτλ.

Επιστημονικό πεδίο: ανάπτυξη βιοαισθητήρα

Λέξεις κλειδιά: τοξικολογία, φαρμακολογία, βιοαισθητήρας, εφαρμογές, ανάπτυξη, ολοκληρωμένο σύστημα

Acknowledgements

I would like to thank all those people who have contributed throughout to the completion of my thesis. I would like to thank the rest members who agreed to participate in my committee and being at my disposal for constructive comments. My sincere appreciation to my supervisor Prof. Spyridon Kintzios for giving me the opportunity to be one of his PhD candidates in his laboratory. In addition, I wish to thank my thesis committee members, Prof. Konstantinos Yialouris, and Prof. Grigoris Kaltsas for their help and their advice. All my professors provided me with their guidance and their knowledge in conjunction with efficient studying, scientific thinking, and problem solving. I am grateful to them being willing to kindly answer and explain my questions anytime during my dissertation.

With this opportunity, I would like to thank all the members of the Laboratory of Cell Technology, and especially Prof. Georgia Moschopoulou, Dr. Theofylaktos Apostolou and Mr. Vasilis Tsekouras and for their help and contribution during my doctoral dissertation. I would like to give special thanks to Prof. Sophie Mavrikou, both as a colleague and personal friend, for her help and support. Her ideas along with the suggestions and discussions helped me make my thesis stronger.

In addition, I would like to thank all the members of microSENSES Lab, and especially Dr. Dimitris Barmpakos, Mr. Tzoulia Koutsis and Mr. Damianos Marinatos for being good friends and helping me during my dissertation.

Lastly, I am thankful to both my parents and my husband for their constant support, encouragement and understanding given to me during the whole period of my studies, and especially during my dissertation.

With my permission, the present work was checked by the Examination Committee through the plagiarism detection software available by GPA and its validity and originality were cross-checked.

Table of contents

Contents

| | |
|--|----|
| Abstract | 1 |
| Περίληψη | 4 |
| Acknowledgements | 8 |
| Table of contents | 9 |
| List of figures | 12 |
| List of tables | 16 |
| List of papers | 18 |
| Chapter 1: Introduction to Toxicology | 19 |
| 1.1 Introduction | 20 |
| 1.2 Toxicology as an applied science | 21 |
| 1.3 Toxicology research: Current scientific topics in toxicology | 23 |
| 1.3.1 Toxicology in the past | 23 |
| 1.3.2 Current toxicological research – Carcinogenesis | 23 |
| 1.3.3 Toxicity of mixtures of substances | 24 |
| 1.3.4 Immunotoxicity | 24 |
| 1.4 In vitro methods | 25 |
| 1.4.1 Introduction | 25 |
| 1.4.2 In vitro models as alternative tests | 26 |
| 1.4.3 Three-dimensional (3D) cell culture models | 26 |
| Chapter 2: Introduction to Sensors | 30 |
| 2.1 Introduction | 31 |
| 2.2 Types of sensors | 32 |
| 2.2.1 Chemical Sensors | 32 |
| 2.2.2 Optical sensors | 33 |
| 2.2.3 Biosensors | 33 |
| 2.2.4 Bioelectric sensors | 34 |
| 2.2.5 Biosensors based on impedance | 36 |
| 2.2.6 Impedimetric Biosensors | 36 |
| 2.2.7 Cell-based impedimetric biosensors | 37 |

| | |
|---|----|
| 2.3 Conclusion | 37 |
| Chapter 3: Introduction to Impedance..... | 39 |
| 3.1 Introduction | 40 |
| 3.2 Bio-impedance – Theory | 41 |
| 3.3 Electrical properties of biological tissues..... | 43 |
| 3.4 Common electrode configurations for bioimpedance measurements | 45 |
| 3.5 Electrode configurations | 46 |
| 3.5.1 Two-electrode configuration | 46 |
| 3.5.2 Three-electrode configuration..... | 47 |
| 3.5.3 Four-electrode configuration..... | 48 |
| 3.6 Different types of tissue engineered constructs..... | 48 |
| 3.6.1 Two-Dimensional (2D) cell culture | 49 |
| 3.6.2 Three-Dimensional (3D) cell culture | 50 |
| 3.7 EIS (Electrical/ Electrochemical Impedance Spectroscopy) | 51 |
| 3.7.1 Description..... | 51 |
| 3.7.2 Strength and weaknesses | 52 |
| 3.8 ECIS (Electric Cell-substrate Impedance Sensors) / Impedance-Based Assays..... | 52 |
| 3.8.1 Description..... | 52 |
| 3.8.2 Strength and weaknesses | 53 |
| 3.9 Conclusion | 54 |
| Chapter 4: Study of the dopamine effect into cell solutions by Impedance Analysis..... | 56 |
| 4. 1. Introduction | 57 |
| 4.2. Materials and methods..... | 58 |
| 4.2.1. Cell culture..... | 58 |
| 4.2.2. Cells’ preparation/immobilization..... | 59 |
| 4.2.3. Experimental setup..... | 59 |
| 4.2.4. Data analysis and experimental design | 60 |
| 4.3. Results and Discussion..... | 60 |
| 4.4. Conclusion | 65 |
| Chapter 5: Impedance Study of Dopamine Effects after Application on 2D and 3D Neuroblastoma Cell Cultures Developed on a 3D-Printed Well | 67 |
| 5.1. Introduction | 68 |

| | |
|---|-----|
| 5.2. Materials and Methods..... | 70 |
| 5.2.1. Cells Preparation/ Immobilization | 70 |
| 5.2.2. Experimental Setup..... | 70 |
| 5.2.3. Experiment design and data analysis | 71 |
| 5.3. Results..... | 72 |
| 5.3.1. Impedance Comparative Results from 2D and 3D Cell Cultures | 72 |
| 5.3.2. nM DA Effects on Cells Immobilized in Bactoagar Matrix..... | 75 |
| 5.3.3. uM DA Effects on Cells Immobilized in PLL..... | 78 |
| 5.4. Discussion | 80 |
| 5.5. Conclusions..... | 81 |
| Chapter 6: Impedance Analysis of various cancer cell types immobilized in 3D matrix and cultured in 3D-Printed Well | 83 |
| 6.1. Introduction | 84 |
| 6.2. Materials and Methods..... | 86 |
| 6.2.1. Cells Preparation/ Immobilization | 86 |
| 6.2.2. Cell Viability Assay..... | 86 |
| 6.2.3. Experimental Setup..... | 87 |
| 6.2.4. Experimental design and data analysis | 88 |
| 6.3. Results..... | 89 |
| 6.3.1. Cell proliferation | 89 |
| 6.3.2. Impedance results in comparison to various immobilized cell lines..... | 94 |
| 6.3.3. Impedance results in comparison to various immobilized cell lines treated with 5-FU97 | |
| 6.4. Discussion | 101 |
| 6.5. Conclusions..... | 103 |
| Chapter 7: Summary – Discussion..... | 104 |
| References | 114 |

List of figures

| | |
|--|----|
| Figure 1: Electrical current's flow among biological tissue: At lower frequency range, current flows between the cells and through the extracellular fluid (a), at high frequency range, current flows through the cell membranes and penetrates intracellular and extracellular fluid (b)..... | 44 |
| Figure 2: Schematic diagram of a two-electrode configuration set up. Both electrodes are used for current carrying (CC) and voltage pick up (PU)..... | 47 |
| Figure 3: Schematic diagram of a three-electrode configuration set up. An external voltage is applied between the reference (RE) and the working electrode (WE), and the electric current is passed from the counter electrode (CE) to the working electrode (WE)..... | 47 |
| Figure 4: Schematic diagram of a four-electrode configuration set up. PU1 and PU2 are the voltage pick up electrodes where the CC1 and CC2 are the current carrying electrodes. | 49 |
| Figure 5: 2D cell culture schematic representation. Cells are seeded as individual cell into a cell culture dish. | 50 |
| Figure 6: Scaffold free 3D cell culture schematic representation of in the form of spheroids. | 51 |
| Figure 7: Schematic representation of an Electric Cell Substrate Impedance Sensing system (ECIS)..... | 54 |
| Figure 8: Experimental setup of the specific electrode assay | 59 |
| Figure 9: Response of monolayer DA solution to different frequencies (1 KHz, 10 KHz, 100 KHz) with increasing DA concentrations with \pm SD values | 61 |
| Figure 10: Response of N2a cells cultured in monolayer to different frequencies (1 KHz, 10 KHz, 100 KHz) with increasing DA concentrations with \pm SD values..... | 61 |
| Figure 11: Response of DA solution applied to the 3D matrix in different frequencies (1 KHz, 10 KHz, 100 KHz) with increasing DA concentrations with \pm SD values..... | 63 |
| Figure 12: Response of 3D immobilized N2a cells to different frequencies (1 KHz, 10 KHz, 100 KHz) with increasing DA concentrations with \pm SD values | 63 |
| Figure 13: Experimental setup of the particular electrode assembly. | 71 |
| Figure 14: Mean impedance magnitude values (n = 3) for cells in 3D (red lines) and 2D (black lines) cultures treated with dopamine (DA) at five different frequencies: (a) 100 Hz, (b) 120 Hz, (c) 1 KHz, (d) 10 KHz, (e) 100 KHz, with \pm SD values..... | 73 |

Figure 15: Mean impedance magnitude values for cells in 3D (GEL) culture treated with DA at five different frequencies (100 Hz, 120 Hz, 1 KHz, 10 KHz, 100 KHz), with \pm SD values... 74

Figure 16: Mean impedance magnitude values for cells in 2D (PLL) culture treated with DA at five different frequencies (100 Hz, 120 Hz, 1 KHz, 10 KHz, 100 KHz), with \pm SD values... 75

Figure 17: Mean impedance values for cells immobilized in Bactoagar matrix treated with nM DA concentrations (1, 10, 50, 100, 200 nM) at five different frequencies. 76

Figure 18: Mean impedance values for cells immobilized in PLL matrix treated with μ M DA concentrations (1, 10, 50, 100, 200 μ M) at five different frequencies..... 79

Figure 19: Experimental set up. Schematic representation of the 3D cell immobilization matrix (a); Connection of the 3D printed assembly to the LCR meter (b). 88

Figure 20: Panoramic view of SK-N-SH cells in 3D immobilization matrix after treatment with MTT for 24 h, indicating the viability in three various populations: 50,000 cells (a); 100,000 cells (b); and 200,000 cells (c). Scale bars = 50 μ m..... 89

Figure 21: Panoramic view of HEK293 cells in 3D immobilization matrix after treatment with MTT for 24 h, indicating the viability in three various populations: 50,000 cells (a); 100,000 cells (b); and 200,000 cells (c). Scale bars = 50 μ m..... 90

Figure 22: Panoramic view of HeLa cells in 3D immobilization matrix after treatment with MTT for 24 h, indicating the viability in three various populations: 50,000 cells (a); 100,000 cells (b); and 200,000 cells (c). Scale bars = 50 μ m..... 90

Figure 23: Panoramic view of MCF-7 cells in 3D immobilization matrix after treatment with MTT for 24 h, indicating the viability in three various populations: 50,000 cells (a); 100,000 cells (b); and 200,000 cells (c). Scale bars = 50 μ m..... 90

Figure 24: Cellular viability of SK-N-SH cells immobilized in 3D matrix after treatment with MTT for 24h showing the viability in three different population densities (50,000, 100,000, 200,000 cells/100 μ L) \pm STD: (a) untreated cells (control), (b) cells treated with 5-FU. ## < 0.01 significantly different from 100,000 cells/100 μ L. 91

Figure 25: Cellular viability of HEK293 cells immobilized in 3D matrix after treatment with MTT for 24h showing the viability in three different population densities (50,000, 100,000, 200,000 cells/100 μ L) \pm STD: (a) untreated cells (control), (b) cells treated with 5-FU. * < 0.05 significantly different from 50,000 cells, ## < 0.01 significantly different from 100,000 cells/100 μ L..... 91

Figure 26: Cellular viability of HeLa cells immobilized in 3D matrix after treatment with MTT for 24h showing the viability in three different population densities (50,000, 100,000, 200,000 cells/100 uL) \pm STD: (a) untreated cells (control), (b) cells treated with 5-FU. * < 0.05, ** < 0.01 significantly different from 50,000 cells, # < 0.05, ### < 0.001 significantly different from 100,000 cells/100 ul. 92

Figure 27: Cellular viability of MCF-7 cells immobilized in 3D matrix after treatment with MTT for 24h showing the viability in three different population densities (50,000, 100,000, 200,000 cells/100 uL) \pm STD: (a) untreated cells (control), (b) cells treated with 5-FU. * < 0.05, ** < 0.01, *** < 0.001 significantly different from 50,000 cells/100 ul..... 92

Figure 28: Normalized values of the mean impedance magnitude for untreated (control) immobilized SK-N-SH cancer cell lines tested at three frequencies (1 KHz, 10 KHz, 100 KHz) for three different population densities \pm STD: (a) 50,000 cells, (b) 100,000 cells and (c) 200,000 cells/100 ul. 94

Figure 29: Normalized values of the mean impedance magnitude for untreated (control) immobilized HEK293 cancer cell lines tested at three frequencies (1 KHz, 10 KHz, 100 KHz) for three different population densities \pm STD: (a) 50,000 cells, (b) 100,000 cells and (c) 200,000 cells/100 ul. 95

Figure 30: Normalized values of the mean impedance magnitude for untreated (control) immobilized HeLa cancer cell lines tested at three frequencies (1 KHz, 10 KHz, 100 KHz) for three different population densities \pm STD: (a) 50,000 cells, (b) 100,000 cells and (c) 200,000 cells/100 ul. 95

Figure 31: Normalized values of the mean impedance magnitude for untreated (control) immobilized MCF-7 cancer cell lines tested at three frequencies (1 KHz, 10 KHz, 100 KHz) for three different population densities: (a) 50,000 cells, (b) 100,000 cells and (c) 200,000 cells/100 ul. 96

Figure 32: Normalized values of the mean impedance magnitude for control immobilized SK-N-SH cells (blue bars) and immobilized SK-N-SH cells treated with 5-FU (grey bars), tested at three different cell population densities \pm STD: (a) 50,000, (b) 100,000 and (c) 200,000/100uL for three different frequencies (1 KHz, 10 KHz, 100 KHz)..... 97

Figure 33: Normalized values of the mean impedance magnitude for control immobilized HEK293 cells (blue bars) and immobilized HEK293 cells treated with 5-FU (grey bars), tested

at three different cell population densities \pm STD: (a) 50,000, (b) 100,000 and (c) 200,000/100uL for three different frequencies (1 KHz, 10 KHz, 100 KHz)..... 98

Figure 34: Normalized values of the mean impedance magnitude for control immobilized HeLa cells (blue bars) and immobilized HeLa cells treated with 5-FU (grey bars), tested at three different cell population densities \pm STD: (a) 50,000, (b) 100,000 and (c) 200,000/100uL for three different frequencies (1 KHz, 10 KHz, 100 KHz)..... 99

Figure 35: Normalized values of the mean impedance magnitude for control immobilized MCF-7 cells (blue bars) and immobilized MCF-7 cells treated with 5-FU (grey bars), tested at three different cell population densities \pm STD: (a) 50,000, (b) 100,000 and (c) 200,000/100uL for three different frequencies (1 KHz, 10 KHz, 100 KHz)..... 100

List of tables

| | |
|--|----|
| Table 1: R ² values for mean impedance responses regarding DA monolayer solution and N2a cell culture in monolayer treated with the same uM increasing DA concentrations in three frequencies tested (1 KHz, 10 KHz, 100 KHz)..... | 62 |
| Table 2: R ² values for mean impedance responses regarding DA solution applied to the 3D immobilization matrix and N2a immobilized cells treated with the same uM increasing DA concentrations in three frequencies tested (1 KHz, 10 KHz, 100 KHz). | 63 |
| Table 3: Significant differences (Student's T-test) in all solutions tested in different DA concentrations, including control solution, between N2a cells in monolayer and 3D immobilized N2a cells at 1 KHz frequency. * < 0.05, ** < 0.01, *** < 0.001..... | 64 |
| Table 4: Significant differences (Student's T-test) in all solutions tested in different DA concentrations, including control solution, between N2a cells in monolayer and 3D immobilized N2a cells at 10 KHz frequency. ** < 0.01, *** < 0.001. | 64 |
| Table 5: Significant differences (Student's T-test) in all solutions tested in different DA concentrations, including control solution, between N2a cells in monolayer and 3D immobilized N2a cells at 100 KHz frequency. * < 0.05, ** < 0.01, *** < 0.001..... | 65 |
| Table 6: R ² values for mean cell impedance responses in gel and polylysine (PLL) matrices after application of increasing DA concentrations..... | 74 |
| Table 7: Significant differences (Student's T-test) in all combinations of solutions tested between N2a immobilized cells in bactoagar gel (G) and N2a immobilized cells in PLL (P) in all five frequencies. * < 0.05, ** < 0.01, *** < 0.001. | 75 |
| Table 8: R ² values for mean cell impedance responses in gel for nM and PLL for uM DA concentrations..... | 76 |
| Table 9: Significant differences (Student's T-test) in all combinations of solutions tested in N2a immobilized cells in bactoagar gel in all five frequencies. * < 0.05, ** < 0.01, *** < 0.001. 77 | 77 |
| Table 10: Correlation matrix of correlation coefficients for the means values of the 3D immobilized cells for all five frequencies tested..... | 77 |
| Table 11: Correlation matrix of correlation coefficients for the means values of the 3D immobilized cells for increasing nM DA concentrations tested..... | 77 |
| Table 12. Significant differences (Student's T-test) in all combinations of solutions tested in N2a immobilized cells in PLL in all five frequencies. * < 0.05, ** < 0.01, *** < 0.001..... | 79 |

| | |
|---|-----|
| Table 13: Correlation matrix of correlation coefficients for the means values of the 2D immobilized cells for all five frequencies tested..... | 79 |
| Table 14: Correlation matrix of correlation coefficients for the means values of the 2D immobilized cells for increasing uM DA concentrations tested..... | 80 |
| Table 15: 5-FU concentrations added to each cell culture. | 87 |
| Table 16: Significant differences among cell population densities with or without the presence of 5-FU (** < 0.01, *** < 0.001)..... | 93 |
| Table 17: Significant differences in cell viability among cell line combinations with or without the presence of 5-FU (* < 0.05, ** < 0.01, *** < 0.001)..... | 93 |
| Table 18: Significant differences in cell impedance among cell population combinations for the SK-N-SH cell line with or without the presence of 5-FU (** < 0.01, *** < 0.001)..... | 98 |
| Table 19: Significant differences in cell impedance among cell population combinations for the HEK293 cell line with or without the presence of 5-FU (* < 0.05, ** < 0.01, *** < 0.001)..... | 99 |
| Table 20: Significant differences in cell impedance among cell population combinations for the HeLa cell line with or without the presence of 5-FU (* < 0.05, ** < 0.01, *** < 0.001)..... | 100 |
| Table 21: Significant differences in cell impedance among cell population combinations for the MCF-7 cell line with or without the presence of 5-FU (* < 0.05, ** < 0.01, *** < 0.001) | 101 |

List of papers

- Th. Kountanis, G. Paivana, Th. Apostolou, S. Kintzios, G. Kaltsas, "Impedance Analysis for Cell Discrimination and Pesticides' Concentration Determination", International Conference 'Science in Technology' SCinTE 2015, Athens.
- Paivana, G.; Apostolou, T.; Kaltsas, G.; Kintzios, S.; (2017). Study of the dopamine effect into cell solutions by impedance analysis. Journal of Physics: Conference Series. 931. 012010. 10.1088/1742-6596/931/1/012010.
- Paivana, G.; Apostolou, T.; Mavrikou, S.; Barmpakos, D.; Kaltsas, G.; Kintzios, S. Impedance Study of Dopamine Effects after Application on 2D and 3D Neuroblastoma Cell Cultures Developed on a 3D-Printed Well. Chemosensors 2019, 7, 6.
- Paivana, G.; Mavrikou, S.; Kaltsas, G.; Kintzios, S. Bioelectrical Analysis of Various Cancer Cell Types Immobilized in 3D Matrix and Cultured in 3D-Printed Well. Biosensors 2019, 9, 136.
- Apostolou, T.; Mavrikou, S.; Denaxa, N.-K.; Paivana, G.; Roussos, P.A.; Kintzios, S. Assessment of Cypermethrin Residues in Tobacco by a Bioelectric Recognition Assay (BERA) Neuroblastoma Cell-Based Biosensor. Chemosensors 2019, 7, 58.
- Kaminiaris, M.D.; Mavrikou, S.; Georgiadou, M.; Paivana, G.; Tsitsigiannis, D.I.; Kintzios, S. An Impedance Based Electrochemical Immunosensor for Aflatoxin B1 Monitoring in Pistachio Matrices. Chemosensors 2020, 8, 121.
- Paivana, G.; Barmpakos, D.; Mavrikou, S.; Kallergis, A.; Tsakiridis, O.; Kaltsas, G.; Kintzios, S. Evaluation of Cancer Cell Lines by Four-Point Probe Technique, by Impedance Measurements in Various Frequencies. Biosensors 2021, 11, 345.

Chapter 1: Introduction to Toxicology

1.1 Introduction

Toxicology is mostly described as the science of intoxication and poisons. Yet, the area of fields that covers has been developed and broadened over time, hence the field of toxicology can be considered as the “science of safety” [1]. It is expected that in the near future the role of toxicology will evolve by contributing to various safety assessments of global importance, including anthropogenic changes in the atmosphere, global planning for earth resources, and modern techniques for food production [2-4]. In general, toxicology constitutes a translational science as it can transfer valuable information from basic science into practicable applications for the safety of both human health and the environment. Toxicologists are obliged to provide an integrated perspective along with superiority in their topic of basic science (e.g. chemistry, medicine, or biology) as the demands are becoming higher and higher. Nowadays, the chemical and pharmaceutical industries require universities initially to train toxicologists so that they are capable of performing research in collaboration with scientists from the industry in order to promote the future progress of safety science. The ultimate concept of novel techniques that approve safety assessments without the presence of animal testing requires the development of new approaches, especially those who aim to reduce animal experiments [5-7]. At this point, the academic community has to lead scientists to build up research networks with industry including scientists from regulatory institutes. During risks’ determination, toxicologists have to crucially evaluate findings, taking thoroughly into account knowledge from a large field of techniques and experimental abilities as well. For that reason, universities and postgraduate institutes require experienced academic staff and proper laboratories for training and research. Research that is based on the academic community is of great importance as it can provide solutions to open questions [8].

The history of toxicology provides an interesting aspect of the evolution of the science of toxicology as well as for the society's alternating approach for the prevention of disease. Famous parts of history focus on the deadly application of different poisons, for instance, the use of aconite as an arrow poison and hemlock as a technique of execution (e.g., Socrates). The word “toxicology” can have many originations, as the word “toxic” preceded the word “toxicology” [9]. Available sources suggest “toxicology” was derived from ancient Greek, where all drugs or potions were defined as “pharmaka” or “pharmakon” without any differentiation of those used for treating a disease or those causing harm [10]. Later the meaning of poison was replaced by the term pharmakon. The Greek word “toxikos” or “toxicos”

constitutes and adjective of the noun “toxon” denoting “bow”. The words “toxicos”, “toxicon”, or “toxikon” are other Greek derivations of toxicology that meant poison or poisons into which arrows were immersed [11]. The Greek word “pharmakon” or “pharmacon” was combined with the word for bow “toxicon”, in order to create the phrase for arrow poison, that is “toxicon pharmacon” [12]. More specifically, this phrase meant “arrow poison” and it was different from toxicon, regarding any other poison. The Romans limited this phrase to “toxicum”, referring to the word of poison in their Latin derivation, and furthermore, instead of the word poison, they derived the word arrow [12].

Hence, the Greek word for bow, “toxon”, describes the toxicology’s true origins, which at the beginning had no connection to poisons. It is interesting how the following derivations of the word toxon in the English language revert back to the initial Greek meaning of the word bow: toxoplasma (bow-shaped organism), toxophily (archery), toxocara (nematode with a head shaped like a bow) [11].

1.2 Toxicology as an applied science

Toxicology, as an applied science, allows the determination of risks that derive from various fields, along with humans, animals, and the environment’s exposure to industrial chemicals, biocides, plant protection products, medical drugs, and devices, etc. The protection of consumers, workers as well as the environment demand recommendations originating from scientific analysis and assessments of the toxic effects of these substances [8].

Drug toxicology, known as safety pharmacology or pharmaceutical toxicology, constitutes the study of the possible undesired outcomes of potential drugs and drugs in the therapeutic field [8]. It is a prerequisite for clinical analysis as a toxicological experiment of new drugs was traditionally implemented in accordance with typical study program [13, 14]. Lately, pre-clinical experiments have been customized to particular properties and also to the way the new drug will react. These properties could be tailored to the results from former studies [15]. This custom-made concept is adapted by the regulatory registration procedure. Novel categories of drugs, for instance, oligonucleotide therapeutics and stem cells, introduce new provocations and require recently developed testing systems and new ideas in order to evaluate the results of these studies [16].

In drug development projects, toxicology, related to pharmacology and pharmacokinetics, is critical in either success or failure of the new drug, for both early clinical and pre-clinical testing. The whole project may lead to failure if any misconception of substance features cannot be rectified even in the later stages. Hence, by eliminating ineligible drug candidates at the right time, toxicology creates value and allows trustworthy risk estimations and risk management in early clinical tests. Although it is said that toxicology “kills” drug candidates, this idea is out-of-date and the actual role of toxicology is to boost drug development projects headed for beneficial drug candidates.

Clinical toxicology connects the preventive and experimental toxicology with clinical medicine. During the last decades, this field of toxicology has endured thorough alterations. In general, clinical toxicology was related to diagnosis and therapy of acute intoxications (e.g., decrease of absorption, accelerated elimination and antidotes). Consequently, clinical toxicology was applied initially by emergency physicians [17]. Nevertheless, the frequency of occurrence of acute intoxications has been reduced in the past few decades considering the development of secure products (a worth of toxicological research), specifically more secure drugs with a large therapeutic index. Yet, the investigation of efficient antidotes for acute intoxications is still needed. This investigation demands detailed knowledge of fungal toxins and their mechanisms, including repair mechanisms in the damaged organ [18]. The research of additional toxins of plant, animal and microbial origination and contaminations has unveiled their toxic mechanisms and created new paths for future promising treatments and application in drug composition [19]. The capability in clinical toxicology is convened in poison centres that are responsible for the clinical and experimental data collection over a wide area of various substances [20]. Toxicological risk estimations are supplied by poison control centres after continuous and acute exposure that affairs subclinical or mild intoxication. The basis for recommendations of efficient therapies that contribute to medical care is specified from the fast and trustful information derived from the toxicological profile of a substance [8].

1.3 Toxicology research: Current scientific topics in toxicology

1.3.1 Toxicology in the past

Toxicological investigation was not considered a precautionary in the past. After the presence of serious health impairments detected in many people, toxicological research became an imperative need. There are a lot of examples from these health problems such as asbestos (can cause lung cancer and pleural mesothelioma), arsenic (can cause skin cancer), and contact allergies due to substances faced in everyday life and in the environment as well. In fact, results from research in asbestos presented new and valuable information not only for asbestos fibres but also for fibres in general [21-23]. It became obvious that the serious problems and diseases in people's health when they are exposed to the prior mentioned substances is due to the lack of knowledge related to the toxicological profile of those substances. In the case of adequate knowledge, the risks would be recognized as a result of actual advice and so the exposure would be minimized. Thus, the key aim of toxicological research is the determination of possible risk factors in order to prevent human's potential exposure to toxic substances, especially what the disease of damage takes place after a long latency period [8].

1.3.2 Current toxicological research – Carcinogenesis

In real life, people are often exposed to a lot of carcinogenic substances that can be found in the environment, in food, and at the workplace. In such cases, the avoidance of exposure to such substances should take place. Nevertheless, there are arguments based on mechanisms that complete prevention of exposure might not be essential [24]. This implies that the recognition of the most important carcinogens, the clarification of the molecular mechanism that indicates their adverse mode of action, and the identification of cellular repair mechanisms are factors of great importance [25]. The information provided from these mechanisms allows the decision whether the threshold levels can be determined below which no carcinogenic effects shouldn't be expected [26]. The critical step for risk management

based on science is the identification of the molecular and cellular mechanisms underlying the cancer-inducing potential of chemical substances [8].

1.3.3 Toxicity of mixtures of substances

So far, toxicological research aims attention at the investigation of mechanisms from which biological procedures can be influenced by single compounds. On the other hand, in real life, as mentioned before, people are often exposed to different types of compounds simultaneously, for instance at the workplace, from contaminants in the air, in food, or the environment. Many ideas have been suggested in order to consider combined substances [8].

Prior (non-systematic) studies showed that the addition of individual effects caused by single substances in mixtures ('additive model') leads to smaller than expected adverse results from the mixtures of toxins [27]. Notwithstanding, there are some known exceptions including substances consisting of enzymes that are able to metabolize and therefore activate chemicals. These substances are powerful compared to additive results in conjunction with their substrate chemicals. The same situation occurs for combinations of genotoxic carcinogens combined with substances that suspend DNA repair systems [28, 29].

Several approaches proposed are more or less practically oriented as they don't have a scientific basis for the toxicological evaluation of the action of a mixture of chemicals. Combined results created by mixtures of substances are particularly relevant in the combined evaluation of the human health, and additional research is required in order to set up a knowledge-based system of estimating possible adverse results that are caused by concurrent exposure to various toxic substances. The substance mixtures that require further investigation can be classified by urgency depending on the information of human exposure to those mixtures in drugs and food, in the environment, and at the workplace [30].

1.3.4 Immunotoxicity

Apart from the sensitization reactions, the immune system is trained in such a way as to identify and eliminate foreign structures. In order to predict immunotoxic

reactions, the field of basic research requires important future efforts. There is still one problem that affirms the rarely possible transfer of the results from animal models, especially mouse models, to the human situation. Recently, it became obvious that inflammatory procedures in brain are important not only for acute events in this organ (i.e. ischaemia), but also in age-dependent neurodegenerative illnesses such as Alzheimer's. Moreover, there are indications that the reaction of the brain tissue concerning substances found in everyday life are probably significant in these processes [31]. Due to the dramatic rise of neurodegenerative diseases, the interdisciplinary field of action is of a great importance and requires toxicological expertise.

1.4 In vitro methods

1.4.1 Introduction

Experimental animals have always been an alternative solution for people. Mainly, the research has aimed attention at a better comprehension of the way that cells, organs, and systems of the body behave and regulate, and also of the way a disorder can cause pathological conditions. Nevertheless, the information provided from animal studies is not expected to be connected to humans. Considering the increase of the perception that this alternative might have risky effects, the approach that relies on this attitude is changing. The need for the extrapolation into the body in vitro is increasing so as to determine the secure endpoints of an actual experiment. In 1959, Russell and Birch mentioned that "the mammalian tissue culture constitutes one of the most significant possible technologies and actually one of the most significant developments in biology", admitting the importance of cell culture as a true alternative solution to animal use [32]. Since then, due to the advances in molecular biology systems, the development and the application of the in vitro cell cultures has dramatically increased. The discovery of techniques that are able to create somatic cell pluripotency as well as the development of a high-density omics approach have controlled successfully the restrictions of in vitro studies. This proposal fits perfectly with toxicological approaches, and has considerable potential on realizing the molecular perturbations of chemicals, and eventually predicting studies that can outperform animal studies. Recently, the discovery of the possibility to induce pluripotency in somatic cell populations indicated that there is a way to

study human disease, and also there is also a probability of supplying novel biological tools and toxicological studies [33].

One of the main factors that are applied to in vitro systems is their possible application on high-content assays, combining a really well-characterized relevant cell culture system with high content, powerful and abundant information technology in order to provide a real mechanistic understanding of molecular phenomena [34]. The vast amount of epidemiological knowledge is provided by this new technology about the way cells function at the molecular level. This kind of experimental procedure depends on toxicology, which focuses on the clarification and discovery of molecular mechanisms based on the chemo-induced cellular perturbation [35]. Nonhuman mammals are individually complicated to predict for human toxicity. The improvement of present testing systems based on animals at pre-clinical levels constitutes one of the key scientific fundamentals for the development of in vitro alternatives.

1.4.2 In vitro models as alternative tests

Cell culture plays significant role as it can provide information about the identification and study in the toxicity of chemicals before their application to animal models. Cells are especially capable of modelling well-differentiated human airway epithelium and cardiac muscle cells. In addition, they can be considered as a variable tool for the study of deleterious effects of toxic inhalant chemical that are able to interact with cell surfaces in general. In order to enable quantitative comparisons of in vitro and in vivo systems, as well as to facilitate the use of these systems in human risk estimation and extrapolation, the possibility of measuring target tissue doses has been demonstrated [36].

1.4.3 Three-dimensional (3D) cell culture models

The investigation of the usefulness of in vitro systems for the prediction of acute toxicity has shown the significance of 3D in vitro models in bridging the gap among the in vitro and in vivo effects in toxicology. Both the exposure characterization and evaluation techniques are considered crucial for the successful interpretation of toxicity studies [37].

The introduction of complex biological culture systems in a 3D microfluidic design improves the physiological relevancy of *in vitro* models. The microfluidic systems are able to mimic the *in vivo* microenvironment, including exposure to fluid shear stress, and multi-compartmentalization. Recently, the developments of kidney-on-a-chip platforms were studied for current and future applications. 3D microfluidic systems that used the improved proximal tubule from the perspective of investigating cellular signalling can elucidate mechanistic aberrations that affect drug-induced toxicity. The fact that cells cultured and grown in 3D *in vitro* matrix environments appeared to have essentially different properties increases the interest of the application of 3D matrices for *in vitro* analysis in order to increase the relevance of *in vitro* studies and reduce at the same time the dependence of *in vivo* studies. Nevertheless, the recent results from the comparison of 2D and 3D cell culture models showed a different response of the cytotoxicity assay without any alteration in viability, proved by the analysis of various conversion rates. A sequential decrease in the effective concentration of the test compound and assay justifies the reduced efficiency of the drug applied to cells cultured in a 3D environment. This response increases after a short exposure period and should be explained by comparing the 2D and 3D *in vitro* culture environments [38].

Although conventional two-dimensional (2D) primary cell cultures tend to incur dedifferentiation and at the same time lose their organotypic functions, primary cell cultures have always been the standard for *in vitro* examinations. Complex cell-cell interactions are able to reflect further complex techniques, such as three-dimensional (3D) cultures and tissue engineering [39]. The first concern is to reflect the natural context of the tissues of an organ. Commercial use of these systems has already been initiated and moreover, such systems demonstrate dose-effect profiles that come closer to *in vivo* systems, compared to conventional cell culture techniques.

Various types of cells have been examined for applications in toxicity testing and drug screening. A scale-up stem cell culture is required concerning the sufficient number of cells for *in vitro* applications. In a closed system, bioreactors for dynamic 3D cell cultures can offer large cultured amounts of stem cells at high densities [34]. The evolution from 2D to 3D culture imitates *in vivo* cellular behaviour and environmental condition that both improve cell culture studies. Additional cell types and application demand modified 3D structures. Classic manual techniques can be used instead of automated procedures by applying high-throughput inspection systems [40].

The development of high predictive in vitro cell-based assays is required in order to provide trustworthy information on cancer drug toxicity and effectiveness. Lately, drug screening platforms as a developed biomaterial-based 3D cell culture model have attracted scientific attention since it was shown that 3D cancer cell models are able to sufficiently mirror the in vivo tumour conditions. Furthermore, it has been observed that the biochemical and biophysical properties of the 3D microenvironment have an important role in controlling different cancer cell fates, including their response to chemicals. In order to design more predictive in vitro platforms for toxicity screening and drug development, cell-matrix adhesions and 3D matrix stiffness are significant parameters that must be taken into account [41]. Nevertheless, in vitro studies based on tumour microenvironment and its toxicological modulation are regularly being prevented by technical challenges. These challenges are capable of creating physiological cell culture environments that combine cancer cells with the key components of their native niche in order to mirror the complex microarchitecture of cancerous tissue. A flexible perfusion culture system was developed in order to satisfy the particular needs of developing tissues crucially required in drug toxicity testing, tissue engineering and biomaterial research [42]. A novel in vitro human cell-based model for toxicity estimation was provided.

The use of in vitro neurotoxicity data was limited due to the difficulty in mirroring the complexity of the nervous system and cell-cell interactions. The biomechanical evaluation not only provides valuable information on the relevance of in vitro toxicity data but also determines particular neurotoxic warnings in order to successfully predict the neurotoxicity analysis for acute and repeated exposure in humans [43]. The potential hazardous outcomes of nanoparticles on mammalian cells grown in 2D cultures have been shown. However, various disadvantages including cell function, cell responses, changes in cell shape, and the lack of cell-cell contacts have been illustrated by 2D in vitro cell cultures and thus, it is essential to develop improved models for mimicking in vivo conditions. As some effects cannot be unveiled in 2D cell culture, the importance of 3D cell culture researches for nanoparticle safety testing is being proved from the obtained results.

Three-dimensional (3D) human cell tissue structures lead to new paths for pathophysiological applications, tissue engineering and are important for the evaluation of metastasis procedures of cancer cells, dynamic pharmacological effects of drug candidates, and toxicity expression of nano-materials, such as a 3D human tissue model rather than in vivo animal experiments. Nonetheless, most of the 3D-cellular structures have cell spheroid shape, by means of heterogeneous aggregation.

As a result, the reconstruction of the precise and sensitive 3D-location of multiple cell lines is practically impossible. Recently, new different technologies for the development of complex 3D-human tissues, including lymph and blood capillary networks, showed a reproduction of physiological human tissue responses in the nano/micro-meter spectrum.

With the application of bioreactors, recent developments in the field of dynamic cell culture are enabling the *in vivo*-like transport of compounds in an *in vivo*-like tissue context, leading to more realistic exposure scenarios. By miniaturizing such systems, the application of bioreactors is becoming widespread. The basis for the development of 'organ-on-a-chip' models is focused on these 'microfluidic' systems [44]. Such systems are using multichannel 3D microfluidic cell culture chips, which include, if not all, at least a characteristic fraction of cell lines in tissue in their natural 3D context. Depending on their dynamic culture conditions, these systems are capable of reflecting not only the activity status but also the physiological and mechanistic reactions of an organ. The following step involves various organ systems that can be combined in order to enable a systemic analysis of toxic effects.

Taking into account the limited access to human tissue, it is possible that stem cells are increasingly becoming significant as they are able to replace primary human cells. Further research is still required for the optimization of the methods that are based on induced pluripotent stem cells and embryonic cells before the activities and properties of those cell models become alike to those of the corresponding primary cells. Different types of cell types, such as cells from animals, representative cell lines, and mainly modified cells have and will continue to have a significant role in the validation of methods [5].

The prediction for the *in vivo* situation in humans with synchronous *in vitro* techniques is steadily rising. Unfortunately, although *in vitro* methods that are quite similar to *in vivo* usually fail because of technical limitations in estimation of their validity. In the case of complicated culture systems, particular key aspects of biological procedures are becoming of great interest, however, at the same time result factors including standardization, quality control and interpretation are becoming crucial. Hence, synchronous *in vitro* techniques should remain as simple as possible yet as sophisticated as essential in order to ensure satisfying responses to future scientific questions. Integrated testing strategies are expected to contribute to the efficient combination of various *in vitro* techniques [6, 45].

Chapter 2: Introduction to Sensors

2.1 Introduction

The research for sensors has always been a vital field. From the mid-1980s until now, many published studies have been focused on sensor development. Sensor research is a field that crosses over several fields and has been profited by the progress in engineering, material science, and computer technology. Thus, recently there is an enormous variety of sensors available that cover environmental, clinical, and industrial applications.

A sensor can be described as a device that produces an electrical signal by the response of an applied stimulus. This signal should correspond in a calculated way to the stimulus. Due to the wide choice of the sensor's control, the type of stimulus can be biological, chemical, optical, electrical, and mechanical [46]. A signal is converted from its physical form to a corresponding signal by the use of a transducer. This signal may have various physical forms, for instance, thermal, magnetic, mechanical, optical, electric, and chemical. The role of a transducer is essential in any kind of sensors' application and thus, various transducers are often applied in modern sensing technology [46].

Sensors, as one of the simpler approaches for chemical examination, allow direct assay of a liquid or gas sample, without any sample purification or preparation. Scientists have shown an especial interest due to the fact that sensors appear to have easy usage which makes them able to implement assays away from a central laboratory with less demand for reagents or complex equipment [47]. Recently, demanding attempts have been carried out in order to fabricate disposable, low-cost, and simple operating sensor systems for such use. A considerable number of innovative approaches concerning sensors' design has been introduced, although the progress for the advertisement of those sensor systems was slow. This resulted in the availability of complementary systems that take advantage of various physiological fundamentals and are capable of facing analytical problems. For analytically accurate and commercially profitable future sensor systems, the multiplicity of approaches is the main consideration that will be reliable for transferring the type of robust sensors. In a practical assay system, since the response of both chemical elegance and adherence to well-defined chemical fundamentals cannot warrant practical viability, the prediction of the eventual behaviour of a sensor system persists difficult, thus requiring an extended study on understanding the sensor's behaviour [47].

An accepted estimation of sensor behaviour would possibly include the quantification of selectivity, sensitivity, response times, and temperature

dependence. Such an estimation usually is accomplished under specific monitored laboratory conditions and additional delicate parameters of deficiencies in performance are either left out of the literature or are not recognized. More specifically, although biocompatibility, drift, storage and operational stability, aging effects, and hysteresis phenomena are considered as factors difficult to understand, they are important and interesting referring to the membrane element of the sensor.

Biosensors constitute chemical transducers that include a particular coating of various biologically derived molecules, which broadens the analytical range of the basic sensor due to its advantage of selective analyte recognition property [47]. The standards of sensors and sensing have been established for many years. Additional technologies and sciences have adapted plenty of basic ideas, materials, and devices. Emerging technologies of materials, microfluidics, and lab-on-a-chip science are leading to improved analytical efficiency and decreasing the sensor's price. Possible applications will be discovered for the bright future of the sensors' development.

2.2 Types of sensors

2.2.1 Chemical Sensors

The application of most chemical sensors was focused on a wide background of measurement standards as well as chemical sensitivity that are being developed through research in many areas of chemistry. The information provided from a chemical sensor concerns the chemical nature of its environment. In general, a chemical sensor consists of a chemically selective layer and a physical transducer. In order to create a determinable signal by the use of the transducer, the chemically determinable layer should interact with the environment. Factors, including sensitivity, reactivity, selectivity, response time, and lifetime are controlled by the selective layer. The sensor's composition plays a vital role as it defines its characteristics. An ideal sensor requires fast response and a signal-to-noise ratio which are both sensitive and selective.

2.2.2 Optical sensors

Optical sensors react to a chemically selective layer with a kind of interest in order to induce alterations in the optical characteristic of the sensor. Since the 1930s, when the pH indicator paper was evolved, optical sensors are very well established. The reaction to the chemically selective layer might cause an alteration in fluorescence intensity or absorbance and it is commonly detected spectrally or colorimetrically. Features, including reflectance, fluorescence, and light absorption can be exploited by optical transducers. Furthermore, optical sensors for various fumes such as ammonia, oxygen, carbon monoxide, anesthetics and chlorine have been developed.

2.2.3 Biosensors

Biosensors can be categorized into different groups, depending on the signal transduction or biorecognition standards. Based on the transduction aspect, biosensors can be sorted as optical, electrochemical, thermal, and piezoelectric sensors. Most catalytic biosensors depend on electrochemical techniques, while it is proved that in general affinity biosensors are more amenable to optical detection techniques. Based on the biorecognition aspect, biosensors are categorized into enzymatic, non-enzymatic receptors, immunochemical, DNA, and whole-cell biosensors. Enzymatic sensors depend on the selective inhibition of particular enzymes by various classes of compounds, by decreasing the activity of the immobilized enzyme in the presence of the target analyte as the factor that is usually applied for quantification. Immunosensors are characterized by selectivity, sensitivity, and versatility due to the creation of antibodies for a series of compounds that differ in their structure. DNA biosensors are applied for contaminant detection and specifically for the monitoring of contaminant interaction with the immobilized DNA layer and for the hybridization detection of nucleic acid sequences from contagious microorganisms. Whole-cell biosensors are able to recognize components by the measurement procedure of general metabolic conditions of living organisms including yeast, plant, bacteria, and animal cells or even tissue slices. The use of these kinds of biosensors is essential as they provide valuable information that concerns the determination of the toxicity of compounds to selected cells.

Electrochemical biosensors constitute integrated receptor-transducer devices that are able to provide quantitative and selective analytical information with the use of a biological recognition element. Electrochemical biosensors consist of three main categories: amperometric, conductometric, and potentiometric. Amperometric biosensors calculate the electric current that is related to electron flow that derives from redox reactions. Conductometric biosensors estimate variations in the conductivity of a medium caused by enzyme reactions that change its ionic concentration. In order to designate possible alterations in the concentration of chosen ions, potentiometric biosensors use ion selective electrodes.

2.2.4 Bioelectric sensors

The definition of bioelectric sensors specifies their position on the interface among biological factors and electronic circuits, no matter the manufacturing procedure, scale, and working principle. They are separated from electrochemical sensors in a way that they depend completely on cells, tissues, and organs as well as the biorecognition factors, rather than using just biomolecular moieties, including enzymes, antibodies, or oligonucleotides [48].

Bioelectric sensors are also known as tools used for quick access to the cellular physiologic condition. This constitutes the field where the use of both bioimpedance-based and potentiometric biosensors is significantly increased considering toxicity and/or metabolic effects screening [49-52].

A significant amount of experimental information can be provided by highly developed systems and methods. For instance, impedance frequency spectrometry can be applied for the training of dedicated software in order to identify and classify data subgroups. From the biological point of view, the process of cells' immobilization using either two-dimensional configuration onto the surface of conducting electrodes or three-dimensional configuration in the suitable gel plays a crucial role. In particular, the three-dimensional configuration appears to have an impact in considerably simplify and increase the efficacy of the operation, including the extension of the cell viability and storage stability [53].

The non-invasiveness and low cost per assay are two features that stand out among the beneficial characteristics of the bioelectric sensors. A typical example is the performance of the bioelectric profiling toxicity assays against pesticide residues

in a short time (e.g., couple of minutes) in contrast with traditional enzyme-based optical assays that may need from several hours to days [54, 55]. On the other hand, information that concerns the electric properties of living tissues and cells can be connected to particular molecular functions, if only the cellular biorecognition feature is customized to pair specific biochemical responses to a bioelectric mechanism. This is known as the case of cells with synthetic gene circuits and membrane-engineered cells [56-58]. Alternatively, the holistic screening of cellular physiology, including cell toxicity and membrane channel activity remains the desired application field for bioelectric sensors.

Alike to electrochemical sensors but also distinct from them, bioelectric sensors are characterized by the ability to monitor real-time physiological patterns, sometimes continuously, as well as transferring the results through Bluetooth/Internet to distant data storage, process and interpretation sites. In a number of cases, the monitoring is performed in a non-invasive way and especially without the procedure of sample extraction. Thereby, there is a possibility of pairing the biosensors with dedicated true point-of-test (POT) or point-of-care (POC) platforms that are integrated into various Internet of Things (IoT) networks, along with e-health applications and smartphone-based telemetry [59-64].

Bioelectric profiling is considered a superior concept for multiple applications, such as signal transduction, real-time medical diagnostics, in vitro toxicity, environmental risk evaluation, and drug development [48]. Apostolou et al. showed that mammalian cell-based assays and biosensors offer both high sensitivity and non-invasive or minimally invasive monitoring leading to a considerably increased significance in clinical analytical science. Their multipurpose catalytic capacity makes them unique as cellular biorecognition elements are enabled in order to provide valuable information regarding the actual effects of target analytes [3, 4]. Moreover, due to their quantification, speed, ease of use, assay principles have become common according to measuring cellular bioelectric properties, including impedance or membrane potential. The rapid measured alterations in the membrane potential of a cell population can be performed using the Bioelectric Recognition Assay (BERA), which can be used in multiple applications [65, 66].

Regarding the cancer case, the research focused on the field of hypoxia showed the importance of the pericellular oxygenation in the cell culture [67-69]. In particular, it was revealed that the hypoxia-regulated procedures can lead to a bad prognosis of conventional chemotherapy, hence the monitoring and control of the cellular microenvironment are both critical factors. In their article, Mavrikou et al. introduced a novel and technologically disruptive process for the monitoring of the

cell culture that can be applied as an indicator for the reaction of various chemotherapy alternatives [70]. More specifically, they presented the results of the investigation of accumulation of superoxide ions cultured in HeLa cervical cancer cells in reaction to various concentrations of the anticancer agent 5-fluorouracil (5-FU).

Despite their recent presence in diagnostic technology and relevant business, the development of novel bioelectric sensors is currently active for diagnostic and analytical needs. Bioelectric profiling constitutes an important tool for fast toxicity assays and x cell type fingerprinting, for instance in the field of food safety control [55]. In addition, the evolution of bioelectric sensors can arise as an individual field that will lead to new perspectives for the further explanation of bioelectrical phenomena and their significance for practical purposes. The new scientific subject of non-chemical distant cell interaction (NCDCl) can demonstrate another possibility in this field for the current discovery of new assumptions of biology simultaneously with the development of novel bioelectric sensing tools [71].

2.2.5 Biosensors based on impedance

The design of the biosensors is based on a biological reaction that occurs at the surface of transducers [72]. The basic detection elements include a variety of biomolecules, such as antibodies, cells, enzymes, and microorganisms. The key requirement for the development of an electrochemical biosensor is the reproducible immobilization of these biomolecules on the surface of the sensor, maintaining their biological activity [73].

2.2.6 Impedimetric Biosensors

According to impedimetric biosensors, in order to measure the capacity of biosensor systems, interdigitated electrodes are used. A biorecognition element usually modifies the dielectric permittivity among the electrodes. The use of particular binding of antibodies that change the overall permittivity can change the measured capacitance. Impedance spectroscopy can be applied for the analysis of the electrical processes that take place in the system. This method is specifically

sensitive to alterations in both bulk and surface effects. Hence, it constitutes a beneficial method for sensors application as well as for electrochemical research.

2.2.7 Cell-based impedimetric biosensors

Bacterial or prokaryotic cells have been applied for the detection systems in cell-based biosensors. More specifically, mammalian cells and higher eukaryotic cells constitute higher detection systems. The application of cells for biorecognition offers significant advantages, including the capability of external stimuli in situ analysis. Furthermore, more complex functional and comprehensive information is provided compared to immunochemical techniques as most of the tissue types of cell cultures and a wide range of growth media are commercially available [74]. Biological cells have very particular electrical properties due to the structure of cell membranes that consist of a lipid bilayer containing many proteins. Inside of a cell is present membrane-covered particulates, including vacuoles, mitochondria, and a nucleus as well as various dissolved charged molecules. Although the membrane of the cell is highly insulating, the interior of the cell appears to be highly conductive.

2.3 Conclusion

A biosensor can be defined as an independent integrated device that is able to provide particular significant or semi-significant analytical information by the application of a biological recognition element (biochemical receptor), which is directly connected to a transducer element. A bioanalytical system that demands further processing steps is required for the clear discrimination of a biosensor. Moreover, the discrimination of a biosensor can be accomplished with the use of a bioprobe, that can be either disposable (e.g., single-use), either incapable of constant monitoring of the analyte concentration. The design of impedimetric biosensors is based on the immobilization of various bioreceptors, including enzymes, antibodies, lectins, nucleic acids, bacteria, and cells at the surface of the electrode. A change in the capacitance or in the admittance at the bulk of the electrode interface takes place due to the insulating features, after the adhesion of the target molecule on the electrode's surface. The appropriate bioreceptors' immobilization on the electrode surface constitutes the most important step for the development of biosensors. Many researchers have studied various methods for the immobilization of receptors, such as physical adsorption, covalent and affinity immobilization, layer-by-layer deposition, entrapping bioreceptors in films or gels, and cross-linking.

Chapter 3: Introduction to Impedance

3.1 Introduction

Electrochemical Impedance Spectroscopy (EIS) constitutes a technique which is usually applied in different search fields such as fuel and solar cells, corrosion, and preparation of electrodes for different device assemblies and sensors. This technique is based on the principle of application of a small excitation signal (mostly an AC current) to an electrochemical system. The alterations in the cell can be described by calculating this excitation signal [75-89].

In order to investigate the interfacial and bulk electrical characteristics of electrode systems, Electrochemical Impedance Spectroscopy (EIS) is considered as an outstanding technique for this purpose as it can be applied for the determination of quantitative parameters of electrochemical procedures [90]. For instance, there is a change in interfacial characteristics from bio-recognition events, hence EIS plays an important role in the interfacial region [91]. Electrode transfers, known as electrochemical reactions, contain adsorption of electro-active species, charge transfer at the electrode surface, electrolyte resistance, and mass transfer from the bulk solution to the electrode surface. Each of these electrochemical reaction procedures can be described as an electrical circuit that contains any possible parallel or in series combination of elements such as resistance, capacitors, or constant phase. For a simple electrochemical reaction, the most common model of electrical circuit is the Randles – Ershler electrical equivalent circuit model. Every circuit component derives from a physical procedure in the electrochemical cell and has a specific impedance behaviour, thus equivalent circuit models can be if not completely partially empirical [92].

EIS is considered as a powerful tool for the investigation of interfacial characteristics connected to bio-recognition events that take place at the modified surface. The small amplitude perturbation from a steady stage of a redox couple is one of the advantages of EIS, which makes it a non-destructive method. The impedance measurements can be described as faradic and non-faradic with or without the presence of a redox couple, respectively. The faradic biosensors are able to bio-recognize events that take place at the surface of a modified electrode by calculating the alteration in the faradaic current (interfacial electron transfer resistance) due to steric hindrance that is caused by the biomolecular interaction and/or by the electrostatic repulsion between the free charges of the target molecules and the electro-active species in the supporting electrolyte.

EIS is limited by considerable requirements in order to obtain a valid impedance spectrum. In theory, stability, linearity and causality are three basic requirements for AC impedance measurements. Both technical precision of the instrumentation and the operating processes are factors relating to the accuracy of EIS measurement [92].

3.2 Bio-impedance – Theory

The definition of the term bio-impedance describes the biological tissue which is able to oppose (impede) electrical current and considered a passive electrical property. Bio-impedance measurements can be performed with the detection of the response to electric excitation (either potential or current) that is applied to biological tissue [93]. Regarding the bio-impedance measurement process, in order to measure the response, a frequency-dependent signal is applied to the system [94], which can be an electrical circuit used for the characterization of the cellular electrical properties. The cell properties are dominated by both capacitance and resistance. In a low-frequency range, the cell membrane is not affected by the electric field. On the contrary, the increase of the frequency allows the penetration of the current into the cytosol. During the bio-impedance measurement procedure, the same or other electrodes are used for the application of the excitation signal as well as for receiving the response of the signal. These electrodes are able to convert the electronic charge to ionic charge and vice versa [95].

Electrical impedance (Z) which is generally defined as the ratio of the voltage (V) and current (I), applied to alternating current (AC) (equation 1). The calculation of the measured impedance can be implemented with the contribution of all components of the tissue, which are resistive (R), capacitive (C), and inductive (L).

$$Z = \frac{V}{I} \quad (1)$$

The complex function Z can be expressed by the modulus $|Z|$ and the phase shift ϕ or the real part Z' and the imaginary part Z'' , which represents resistance and capacitance respectively. When direct current is applied, the imaginary part has zero value. The term admittance (Y) describes the inverse of impedance by means of admitting current flow. Both impedance and admittance are AC parameters and frequency-dependent.

Hence, the elements of the circuit model and specifically the resistor and the capacitor represent the cytoplasm and the membrane respectively [96], and thus the complex impedance can be calculated. In addition, the measurement of the consequential differential voltage into the tissue sample in conjunction with the injection of an alternating current across a biological tissue constitute the factors required for the determination of the electrical impedance.

More specifically, the abovementioned factors are described from the following equations:

$$I(\omega) = I_0 * \cos(\omega t + \theta) \quad (2)$$

$$V(\omega) = V_0 * \sin(\omega t + \psi) \quad (3)$$

where, the amplitude θ and the phase ψ of the current and voltage signal are represented by I_0 and V_0 respectively.

Considering the fact that the same angular frequency ω ($\omega = 2\pi f$) is used for the calculation of both I_0 and V_0 , the electrical impedance can be calculated indirectly using Ohm's law as seen in equation (4), also described as a complex number [97]:

$$Z(\omega) = \frac{V(\omega)}{I(\omega)} \quad (4)$$

The characterization of the complex impedance over a wide frequency spectrum can be determined by the EIS measurement process as shown in equation (5):

$$Z(\omega) = V(\omega)/I(\omega) = |Z|(\cos \phi + j \sin \phi) = Z' + j Z'' \quad (5)$$

where, $|Z|$ and ϕ are the amplitude and the phase difference between the phases θ and ψ respectively. The real and imaginary components of the complex impedance indicated by the terms Z' and Z'' [98] represent the resistance and the reactance respectively. The following equations are used in order to calculate the magnitude (6) and the phase angle (7):

$$|Z| = \sqrt{(Z')^2 + (Z'')^2} \quad (6)$$

$$\theta = \arctan(Z''/Z') \quad (7)$$

In the majority of cases, cells can be detected in a medium as an adherent to a substrate or suspensions [99], leading to a variety of cell measurement approaches. Therefore, there are various models of these sub-methods although they share fundamental theories [94].

3.3 Electrical properties of biological tissues

From the early 1900s, it was shown that the measurement of the electrical properties of cells could contribute to the evaluation of cells' viability [100]. In biological tissues, the frequency of the electrical signal applied as well as the conditions of the tissues, such as pathological, morphological, and physiological, are factors from which the electrical properties of the tissue depend on [101, 102].

Based on the source of the electricity, active (endogenous) and passive (exogenous) are the two types of the electrical properties of biological tissues. Active properties (bioelectricity) derive from the ionic activities inside cells (typical for nerve cells), whereas passive properties arise because of the stimulation by an external electrical excitation source [100, 103]. In biological tissues, cell with membranes are surrounded by extracellular fluids [104]. Cell membranes separate the extra and intracellular spaces by creating two electrically conducting compartments, extra and intracellular media. Both fluids provide resistive paths. However, the cell membrane has a very thin and semi-permeable lipid bilayer (~7nm), which provides the membrane a high capacitance and creates a capacitive reactance due to its insulating nature [95, 105, 106]. Furthermore, the biological tissues can demonstrate inductive properties, nevertheless, when they are compared to their resistance and reactance, in frequencies below 10 MHz the inductance has very low value, hence it can be ignored [107]. Thus, the complex electrical impedance created by biological tissues, also known as bioimpedance, is the result of the contribution of both frequency-dependent capacitance and conductance of the tissues [101, 108-112].

From the properties' analysis of the biological tissues over a wide frequency spectrum, Schwan in his study [113] realized that the dielectric properties can be described by three different dispersions:

1. α -dispersion (10 Hz to a few KHz, low frequency): Related to the tissue interfaces (e.g., membranes)

2. β -dispersion (1 KHz to several MHz, radiofrequency): Created by the polarization of cellular membranes and protein and various organic macromolecules
3. γ -dispersion (more than 10 GHz, microwave frequency): Related to the polarization of water molecules

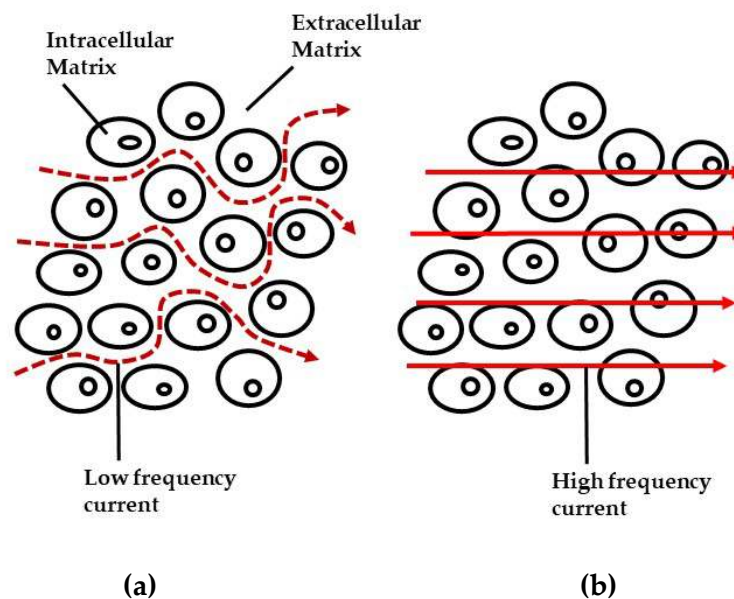


Figure 1: Electrical current's flow among biological tissue: At lower frequency range, current flows between the cells and through the extracellular fluid (a), at high frequency range, current flows through the cell membranes and penetrates intracellular and extracellular fluid (b).

Cell membranes in low frequencies can demonstrate resistive pathways and as a result, little or no current would cross the cell membranes, whereas in high frequencies the capacitive pathways of the membrane would be demonstrated and the current would pass due to the high capacitance of the cell membranes (Figure 1) [114]. Considering a very high frequency range, there is no plenty of time for the current to flow as there is no significant contribution of resistive or capacitive pathways. Therefore, the current would only be trapped between the membrane surface of the cells [110, 115].

The evident technique would be the application of an AC electric field to the cell culture and the calculation of the passive electrical response of the cells, concerning the study of the behaviour and the activity of the cells in a tissue engineered cell construct [106, 116, 117]. This can be assumed as a practical technique in order to monitor the cell growth and differentiation in a label-free and non-invasive way for tissue engineering applications [118, 119].

3.4 Common electrode configurations for bioimpedance measurements

During bio-impedance measurements, the application of alternating current on the electrode creates an impedance at its interface with the frequency-dependent tissue or solution (electrode polarization impedance). The magnitude and the phase of the electrode's impedance might be influenced by alterations in the type of material that is in contact with the electrode. Thus, the final measured impedance by the system can be defined as the electrode polarization impedance added to the impedance of the tissue or solution [95]. For a specific electrode type and material, the impedance would be specified not only by the magnitude of the excitation signal but also by the geometrical structure and the electrode dimensions [120]. For the performance of bio-impedance measurements, two electrodes are the necessary number required in order to create a closed circuit for the flow of the electrical current [95].

Various electrode configuration is needed in order to monitor the features of a tissue engineered construct. The presence of two and three electrode configurations can reflect the impedance at the interface between the electrode and electrolyte or the cell culture (electrode polarization impedance) and also affect the measurement procedure [121].

The combination of two and four electrode configurations allows further study on various volume layers of the same tissue engineered cell culture, with no significant contribution from the electrode polarization impedance [122, 123]. This combination can be applied in order to provide knowledge during the growth and differentiation procedure of the stem cells in a non-destructive way [124, 125]. Furthermore, concerning the study of the spatial distribution of cells in a 3D cell construct, more electrode pairs with different spatial distributions can be used by benefitting from the combinations of two, three, and four electrode configurations. It should not be ignored that movement and wrong positioning of electrodes are factors that may be the main error in bio-impedance measurements [120].

3.5 Electrode configurations

3.5.1 Two-electrode configuration

The two-electrode configuration constitutes the most common set-up for impedance measurements (Figure 2), where the same pair of electrodes is applied for both voltage pickup and current-carrying. The impedance calculated from this configuration contains the polarization impedance at the surface of the electrodes and provides information for the volume of the tissue around the electrodes [95]. This specific electrode set-up can be applied for unipolar measurements by using one very small and one large electrode [126]. Two-electrode set-up constitutes the simplest configuration that can be applied for impedance measurements in perfusion-based systems [121-123]. Furthermore, monolayer cell cultures can use the two-electrode configuration for impedance measurements, where the electrodes are placed at the bottom of the cell culture vessel [127]. One of the impedance techniques on cell monolayers is the Electric Cell substrate Impedance (ECIS) where two-electrode set-up is applied. In this technique, cells are grown on the surface of the sensing electrode and alterations in the impedance's value are measured between the counter and the sensing electrode. The measured impedance might depend on the cells' coverage of the electrode surface. Despite the fact that the extracted results seem to be interesting, they do not provide a precise value of the tissue volume grown on the surface of the electrode [128].

Regarding the various penetration depth in the layers of cell culture, the use of several electrode pairs as well as the change in the distance between the electrodes can be an alternative [129]. The existence of electrode polarization impedance in the output signal is considered as the main limitation of the two-electrode configuration systems and it should be assumed and extracted while the measured signal is being analysed [122, 130].

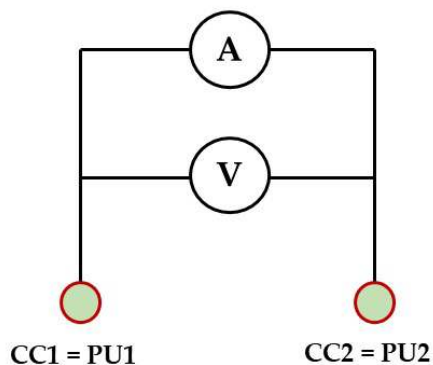


Figure 2: Schematic diagram of a two-electrode configuration set up. Both electrodes are used for current carrying (CC) and voltage pick up (PU).

3.5.2 Three-electrode configuration

The following picture (Figure 3) depicts the three-electrode set-up where between the reference (RE) and the working electrode (WE) an external voltage is applied and an electric current flow from the counter electrode (CE) to the working electrode (WE). Assuming that as no currents pass through this electrode, the potential of the reference electrode (RE) does not change its value, thus alterations in the potential of the working electrode (WE) remain same equally to the alteration in the applied voltage. In their research, Canali et al. combined two and three plate electrode configurations in order to study the spatial distribution of cells in large gelatin scaffolds [131].

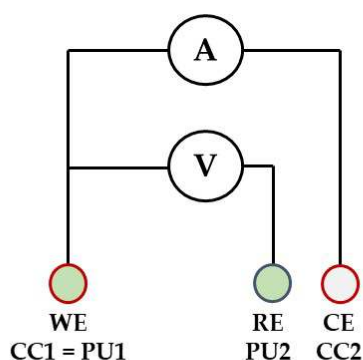


Figure 3: Schematic diagram of a three-electrode configuration set up. An external voltage is applied between the reference (RE) and the working electrode (WE), and the electric current is passed from the counter electrode (CE) to the working electrode (WE).

3.5.3 Four-electrode configuration

In late 1800s, the four-electrode configuration was proposed for the measurement of the materials' resistivity [132]. More specifically, a pair of electrodes is applied for the current flow into the tissue sample (CC), whereas the other pair of electrodes is applied for the detection of the alteration in the voltage (PU), as the results of alterations in the conductivity of the tissue (Figure 4) [122, 123]. In the four-electrode set-up the increase of the distance between the CC and PU electrode pairs might result in a decrease in the magnitude of the measured impedance [95, 133].

Compared to other electrode configurations, one of the advantages by using the four-electrode set-up is the fact that as the PU electrodes do not carry any current, the polarization impedance could be ignored, and hence the result of the contact impedance at the electrode and electrolyte or tissue could be reduced. This approach would allow the detection of the electrical properties of the biological tissue [134]. In addition, measurements using the four-electrode set-up could present a higher accuracy and sensitivity in measuring the density of the biological tissues as well as providing morphological information. On the contrary, the measurements evaluated with the two-electrode set-up can frequently be prevailed by the electrode polarization impedance which makes the contribution from the tissue hard to be extracted with sufficient sensitivity or accuracy [124, 125]. The influence of electrode polarization impedance is generally electrode-dependent regarding size, material, sample impedance, measurement frequency etc. For that reason, this consequence must be taken into account, and for its reduction, the application of various methods is required, if necessary. Although many methods have been proposed, the four-electrode configuration technique is mostly used for the reduction of the influence of the electrode polarization impedance [135].

3.6 Different types of tissue engineered constructs

For the research on biological tissues at the cellular level, two dimensional (2D) or monolayer cell cultures are typically applied [136, 137]. Because of cellular heterogeneity, the study of single cells is considered vital as cells do not necessarily represent the characteristics of the whole tissue from which they have been extracted.

Nevertheless, 2D cell culture provides an artificial environment requiring more information about the features including the concentration gradient which can be provided by a three dimensional (3D) in vitro cell culture system. Thus, a gap still exists between the 2D and 3D cell culture systems and a properly functioning biological tissue. The solution is found in the development of chip-based 3D culture systems that are able to prevail in the limitations of the 2D and 3D cell culture models [138-140].

3.6.1 Two-Dimensional (2D) cell culture

In the 2D cell culture systems, cells are gathered into a cell culture well (Figure 5), which consists of a volume of cell culture medium with a height ranging from mm to cm above the cells. This cell culture medium includes gasses and nutrients required for cells' growth as well as for carrying waste products [140]. 2D cell cultures present a simple system applied in various studies including cancer drug screening for the observation and evaluation of cellular behaviour [136, 137].

An optical microscope is used in order to evaluate the morphology of the cell monolayer or 2D cell cultures. Although studies on cell activities are usually performed using optical methods based on fluorescent staining, it appeared that fluorescent staining kills the cells. However, there is a limitation on the penetration depth of the techniques that are commonly employed for 2D cell cultures [141]. Hence, bio-impedance measurement techniques constitute an alternative approach for non-invasive, label-free and real time measurements [142].

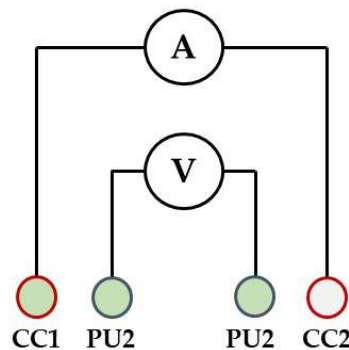


Figure 4: Schematic diagram of a four-electrode configuration set up. PU1 and PU2 are the voltage pick up electrodes where the CC1 and CC2 are the current carrying electrodes.

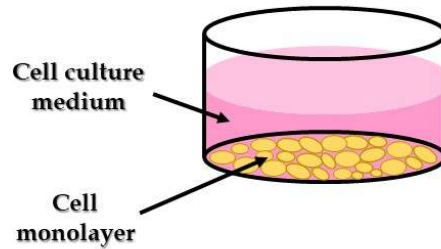


Figure 5: 2D cell culture schematic representation. Cells are seeded as individual cell into a cell culture dish.

3.6.2 Three-Dimensional (3D) cell culture

A three-dimensional (3D) environment is created from cells *in vivo*, as they interact with the extracellular matrix and neighbouring cells (Figure 6). When cells are removed from this 3D environment and transferred to a monolayer (2D), they appear to have an abnormal behaviour [136, 137]. 3D cell cultures have been developed due to the fact that they present similar *in vivo* situations and also due to the ability to provide a physiologically relevant environment [136, 143]. In order to resemble the *in vivo* environment, 3D scaffolds [144] are used for the cells' encapsulation, whose properties are considered to have a significant influence on cell physiology, including composition, stiffness, and porosity [145-147].

In a 3D cell culture system, the encapsulation of the cells in the scaffold makes direct evaluation of cellular growth and behaviour difficult and requires time [148]. Although scanning electron microscopy, histopathology, and transmission electron microscopy are techniques that can be applied for cells' study, they can be disastrous for nature as they demand cells to be frozen and fixed in that way for the evaluation by the abovementioned techniques [149]. As a result, the application of various electrode geometries and configurations can contribute in bio-impedance measurement techniques by providing non-invasive monitoring of 3D tissue-engineered constructs.

In order to create tissues in 3D scaffolds, real-time and long-term monitoring of cell growth and differentiation are factors of great importance in tissue engineering applications, as the procedure of cell culture is carried out over time [141]. In 3D culture systems, for impedance measurements cells are not cultivated as a monolayer on the surface of the electrode, on the contrary, they are encapsulated in a 3D scaffold which is in direct contact with a conductive medium [140]. Therefore, the electrodes' position can be obtained for instance outside the extracellular matrix

and in the middle for the impedance measurement process. Thus, changes in conductivity are caused due to the ionic alterations of the medium over time that would affect the measured impedance [131].

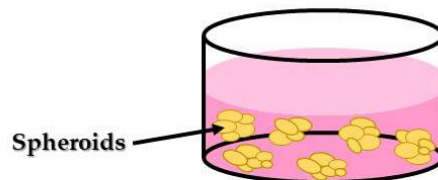


Figure 6: Scaffold free 3D cell culture schematic representation of in the form of spheroids.

3.7 EIS (Electrical/ Electrochemical Impedance Spectroscopy)

3.7.1 Description

In 1925, Fricke and Morse [150] were the first who applied Electrical Impedance Spectroscopy (EIS) to biological tissues. Since then, EIS is performed by listing the electric impedance of tissue over a specific frequency range. The electrical properties of biological tissues are frequency-dependent and they are directly connected to their morphological and physiological characteristics, hence, impedance spectroscopy can be applied as a technique for the evaluation of tissue composition [110]. Alterations between the electrode and electrolyte of the tissue that take place at the interface are described as electrochemical alterations [150] and are the results of capacitive or resistive properties of the materials, which both have a strong contribution to the measured impedance [49, 151-153]. The study of the impedance of biological tissues through a frequency spectrum has gained interest from many researchers. More specifically, studies have shown that the real and imaginary parts of the impedance are related to the resistance and capacitance of a tissue respectively. Although resistance appears to have large values at low frequencies (10 Hz or lower), both resistance and capacitance decrease with increasing frequencies [110, 115].

3.7.2 Strength and weaknesses

EIS constitutes a real-time and non-invasive monitoring technique that is inexpensive and can be applied in order to characterize the tissue-engineered constructs [110, 154]. The suitable frequency range, as well as the proper EIS technique, are required so as to obtain optimal results with this technique from the measurement sample. Factors, such as electrode oxidation and polarization, can affect the measured impedance by EIS that can cause a higher error percentage [155]. EIS is characterized by sensitivity to the permittivity of cell membranes, and thus, it can accurately estimate alterations in cell cultures when high voltage is applied, by combining advanced mathematical modelling methods [156]. As a label-free technique, EIS outstands over the rest characterization techniques that require complex procedures of preparation and dying of the samples and in general are disastrous. Nevertheless, compared to non-label-free methods, EIS is less precise as it might be hard to separate various tissue volumes, and as a result, the detection of the correct electrode configuration is of a great significance, as would provide more particular measurements [157].

3.8 ECIS (Electric Cell-substrate Impedance Sensing) / Impedance-Based Assays

3.8.1 Description

In 1984, Giæver and Keese reported that impedance spectroscopy can be used for monitoring adhesion, proliferation, and spreading of the cells on a flat surface [158]. The technique is known as Electric Cell-substrate Impedance Sensing (ECIS). In this technique, the application of a weak alternating current ($1\mu\text{A}$) results in alterations in impedance measured between a small sensing electrode that contains the cell culture, and a large counter electrode. Due to the fact that the membrane of the cells cultured on the electrode surface constrains the electrode current and forces it to flow either between the cells either under them (Figure 7), there are alterations in the measured impedance [128, 159]. Considering the low conductivity of cells at low frequencies, when they attach and start proliferating on the electrode surface, the measured impedance increases, fact that is proportional to the area of the electrode that contains the cell culture. The resistance has a maximum value when

cells become confluent. And backward, the measured impedance decreases as cells start dying and start detaching from the electrode surface [160, 161].

The resistance of the culture medium as well as both capacitance and resistance of the electrode/electrolyte interface are parameters that contribute to the impedance measurement procedure using the ECIS technique [162]. During ECIS measurements, the resistance of the cells towards the current can determine the quality of the cell barrier, whereas the capacitance describes the measure of the area of the electrode that is covered by cells [163]. The two-electrode set up is usually applied for impedance measurements in the ECIS procedure. The measured impedance depends not only on the area of the electrode that is covered by cells but also on the adherence of the cells that are cultured on the surface of the electrode [127].

3.8.2 Strength and weaknesses

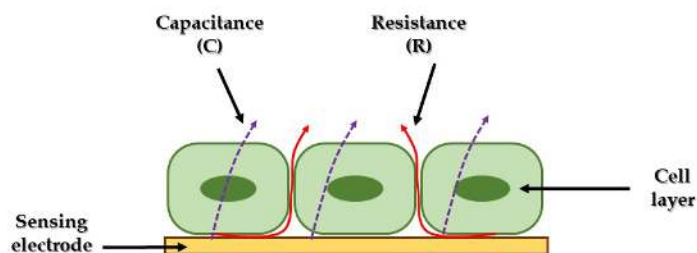


Figure 7: Schematic representation of an Electric Cell Substrate Impedance Sensing system (ECIS).

ECIS constitutes a label-free, non-invasive and continuous impedance measurement process in order to monitor cell properties with a high temporal resolution, despite the fact that impedance measurement process can be affected by small alterations in temperature, medium, or pH. Moreover, mathematical models showed that changes in the value of resistance and capacitance can be applied for the interpretation of the cellular morphology and behaviour [163, 164]. However, it should be mentioned that these mathematical models are reliable only if the cells are confluent, thus it is essential to check the maturity of the cells beforehand. Nevertheless, impedance measurements on single cells cannot be held by ECIS as the measurements are the average of signals from all the cells grown on the surface of the electrode. Furthermore, in order to obtain optimal results, parameters, including coating and seeding density of cells before ECIS measurements, should be optimized [163, 165].

Despite the fact that ECIS has proven to be a powerful tool, the difficulty in single-cell analysis, the environmental consequences, including temperature or pH, as well as the discovery of the optimal plating and coating density of cells, constitute some drawbacks that might affect impedance output responses [166]. The major limitation of ECIS is the fact that direct information on a molecular level cannot be obtained [160, 161, 167].

3.9 Conclusion

Electrochemical impedance spectroscopy has been widely applied for many research studies as a technique for the detection of DNA hybridization, and the reaction of both enzyme and antibody-agent. This technique is characterized by a low detection limit since it is a quite sensitive label-free electrochemical method for monitoring biorecognition events that occur on the surface of the electrode. The determination is quick and needs short detection time. When the immobilization of biorecognition elements takes place on the surface of the electrode with the use of strong chemical bonds, impedimetric biosensors are able to be reproduced. Cell-based impedimetric biosensors contribute to external in situ analysis. Prokaryotic, bacterial, and mammalian cells have been applied for the monitoring of the amount and activity of microorganisms. In literature, there are studies on enzyme-based

impedimetric biosensors that are able to act depending on the detection of the substrate or product of an enzyme reaction.

The translation of tissue-engineered products used in clinical application is usually restricted due to the absence of proper non-invasive imaging techniques applied for the visualization of parameters and behaviour of the constructs [168]. For the time being, there are not a lot of non-invasive techniques for general application in order to evaluate the properties or the viability of the tissue-engineered constructs. Recently, techniques and protocols used for the analysis in cell and tissue-engineering constitute mainly histological methods that need labelling and contain disastrous tests for the characterization of the cell cultures and tissue-engineered constructs [169].

The examination of the electrical features of biological materials and their applications comes from the past, where the procedure of measuring the dielectric properties of the cells could propose a method that can be applied for the evaluation of cell characteristics in a non-invasive way. On the contrary, tissue engineering is considered a relatively recent field of investigation and it has been shown that the examination of the use of electric fields for the characterization or actively monitoring tissue-engineered constructs offers significant potential [114]. Hence, impedance measurements could contribute as a non-invasive and reliable method with a high temporal resolution for real-time monitoring of tissue-engineered constructs during the production stage, making possible the monitoring of cell growth, cell viability, and cell differentiation. Still, it is necessary to optimize the measurement system as well as to enhance the frequency range.

Chapter 4: Study of the dopamine effect into cell solutions by Impedance Analysis

4. 1. Introduction

Electrical impedance spectroscopy (EIS) [170] constitutes a non-invasive technique that allows electrical impedance measurements of living cells in real-time [171]. The measured impedance can either characterize different types of cells or discriminate pathological cells from normal ones regarding the electrophysiological features of cells in the frequency range [170, 172]. In this technique, a small alternating current (AC) signal is applied on the electrochemical cell over a wide frequency spectrum in order to measure the current response. Depending on the cell's electrical response over a specific frequency spectrum, various factors can be detected, including the alterations in cell death [173], the alterations in cells' toxicity [174], as well as the impedance of the biocompatible electrodes with cells [171]. Impedance measurement method contributes to real-time analysis of complex biological systems both *in vivo* [175] and *in vitro* [158, 160, 176, 177] by demonstrating a correlation between the electrical measurements and the biological phenomena [178].

In both mammalian peripheral and central nervous systems [179], dopamine ((3, 4-dihydroxyphenyl) ethylamine, DA) constitutes one of the most significant catecholamine neurotransmitters and is the key role in the functioning of central nervous, hormonal, and renal systems [180]. In the brain, this neurotransmitter activates the five types of dopamine receptors, that are D1, D2, D3, D4, and D5 and their variants. More specifically, the basis of the treatment involves the pharmacological modification of the responsiveness of the various dopamine receptors (D1-D5) and their subtypes. In addition, the treatment involves the side effects of pathological conditions and major diseases, including Tourette syndrome, schizophrenia, Parkinson's disease, and hyperprolactinemia [181].

Over past decades, mammalian cell-based assays have gained attention in clinical analytical science as they provide the combined advantage of high-sensitivity and invasive or non-invasive monitoring. Furthermore, mammalian cell-based assays are significant due to their multipurpose catalytic capacity, which provides valuable information about the actual effects of target analytes derived from the activation of cellular biorecognition elements. This information can be provided even if the actual effects of analytes represent the cumulative or synergistic response of the interaction between this analyte and various receptor subtypes [182, 183]. Moreover, factors such as quantification, speed, and relative ease of use [184], are considered significant as they make assay principles popular, regarding the

measuring cellular bioelectric properties, including the impedance or the membrane potential.

The procedure of the cells' immobilization on the surface of the transducer becomes an increasingly easier operation and efficiently contributes to operation stability and storage. The use of immobilization processes should maintain both viability and functionality of the cells and at the same time make sure that the analyte molecules are efficiently transferred to the cells and to the product molecules produced by the intracellular enzymatic activity, on the electrode's surface.

A novel methodological concept for the development of functional assays for the in vitro interaction of DA with N2a mouse neuroblastoma cells is presented in this chapter. Sensitivity in measuring the response of the cells treated to low DA concentrations (1 μ M), reproducibility, and considerable speed (3min) are the characteristics of this novel approach.

4.2. Materials and methods

4.2.1. Cell culture

Murine neuroblastoma (N2a) cells provided by LGC Promochem, UK were prepared and used for this experiment. The cell culture was carried out under standard conditions (37°C, 5% CO₂) in Dulbecco's medium with fetal bovine serum (FBS) to a final concentration of 10% (Sigma-Aldrich, Taufkirchen, Germany), 2mM l-glutamine (Biowest, Nuaille, France), and 1U ug-1 antibiotics (penicillin/streptomycin) (Invitrogen, CA, USA). The subculture was performed in a ratio of 1:3 using T-75 flasks provided by Sarstedt AG & Co. KG, Nümbrecht, Germany. Before each experimental assay, the cells were removed carefully from the culture using trypsin-EDTA for 3-10min. After the detachment, cells were resuspended in the culture medium for the inactivation of any leftover trypsin activity and were centrifugated for 2min at 1200rpm at 25°C. Publications [179] and [185] describe in detail the whole process for the cell culture.

4.2.2. Cells' preparation/immobilization

For the cells' immobilization, bactoagar gel was used as it constitutes a 3D immobilization matrix of choice. The required mass was weighted, diluted in water, and afterward put for sterilization, having a final concentration of 1.2%. Then, the gel was heated at 37° C for the cells' immobilization, while a cell culture was carried out for preparation of cells for impedance measurements, as described in the previous section. After the completion of the culture procedure, 50.000 N2a cells were mixed with 50uL of bactoagar gel in 1% final concentration and placed together in the well of the electrode. The resulting volume of the well was 90uL after the addition of 40uL of nutrient. DA was applied in various concentrations (1uM, 10uM, 100uM, 1000uM), where each of them was prepared in double-distilled water on the day of each experimental assay. For impedance measurements, cells, immobilized or not, were placed in the electrode of the system.

4.2.3. Experimental setup

A specific electrode assay was used for the performance of impedance measurements. It consists of two silver (Ag) electrodes placed vertically into the well (Figure 8). The electrodes were connected to the inputs of the impedance meter. The handheld LCR meter U1733C provided by Keysight Technologies (CA, USA) was utilized. Each experimental process was carried out in three pre-selected frequencies given from the device (1 KHz, 10 KHz, 100 KHz). Every measurement was completed after 3min; hence, the total measurements were 180 for each run, taking into account the measurement frequency of 1 Hz.



Figure 8: Experimental setup of the specific electrode assay

4.2.4. Data analysis and experimental design

A specific electrode assembly was utilized for the impedance measurements. Every case was designed completely randomly and every experiment was carried out three times. The extracted results were presented with the mean SD values. For the statistical significance, a multiple Student's T-test was applied in order to obtain the alterations between means. The adjusted p-values < 0.05 (two-sided) were considered to be statistically significant.

4.3. Results and Discussion

The assessment of the effects of DA when applied to both immobilized and non-immobilized cells is presented in this chapter. In order to implement impedance analysis, DA was applied as a stimulant to a specific type of cells. The aim of this chapter is the extraction of calibration curves that illustrate the behaviour of the cells treated with known dopamine concentrations at different frequencies by the use of an impedance measurement device.

The results of the impedimetric assay regarding the range of DA concentrations in two different types of cell cultures are presented in this section. In all cases, the notation 0 defines the response of the control solution. Figure 9 depicts the mean impedance values ($n=3$) of the monolayer DA solution without cells in various concentrations, where Figure 10 shows the mean impedance values ($n = 3$) of the N2a neuroblastoma cells cultured in monolayer when treated with the same various DA concentrations tested in three preselected frequencies. In general, a frequency-dependent behaviour is observed as the impedance drops with the increase of the frequency range. In the case of the monolayer DA solution, with the exception of the control solution, after the addition of 1 μ M of DA, the impedance follows a decreasing pattern when both frequency and concentration increase. In both cases (monolayer DA solution and N2a monolayer cell culture), in the frequency of 100 KHz the alterations in the mean impedance values are considered minimal, though giving the highest R^2 values as shown in Table 1 ($R^2 = 0.8495$ and $R^2 = 0.9903$ respectively), with an exception of the control solution's response.

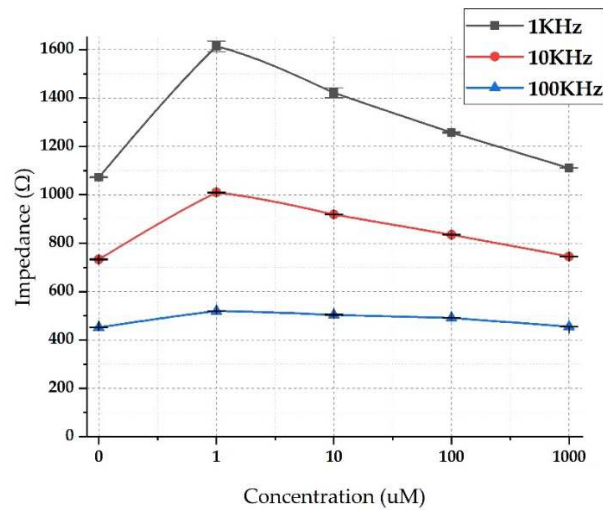


Figure 9: Response of monolayer DA solution to different frequencies (1 KHz, 10 KHz, 100 KHz) with increasing DA concentrations with \pm SD values

In addition, in the cells case, although the value of the control solution dominates in all three frequencies, the mean impedance magnitude has higher values when cells are treated with lower DA concentrations. This can be explained from the fact that in their work, Apostolou et al. [184] showed that D2-like receptors are usually activated with DA concentrations in the range of 1-1000uM. These receptors are related to inhibition of cAMP accumulation and lead to cell membrane hyperpolarization, as they increase the outward potassium currents. For comparison purposes, the same experimental procedures were followed in the case of immobilized cell culture.

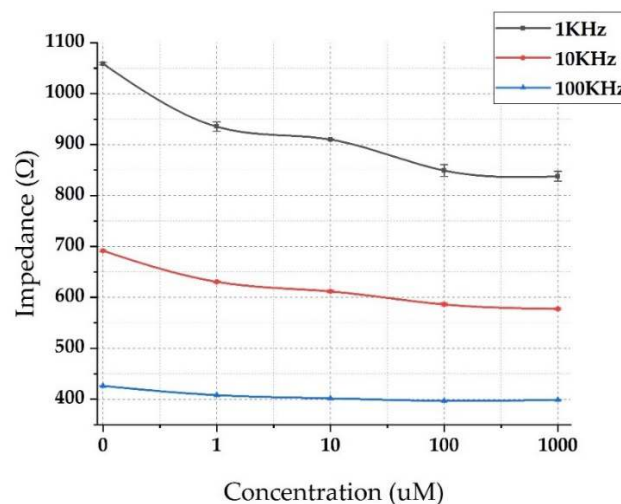


Figure 10: Response of N2a cells cultured in monolayer to different frequencies (1 KHz, 10 KHz, 100 KHz) with increasing DA concentrations with \pm SD values

Table 1: R² values for mean impedance responses regarding DA monolayer solution and N2a cell culture in monolayer treated with the same uM increasing DA concentrations in three frequencies tested (1 KHz, 10 KHz, 100 KHz).

| Frequency | R ² | |
|-----------|----------------|-----------------------|
| | DA solution | Cells treated with DA |
| 1 KHz | 0.6796 | 0.9707 |
| 10 KHz | 0.7236 | 0.9835 |
| 100 KHz | 0.8495 | 0.9903 |

In the second experimental case, in order to simulate *in vivo* conditions, N2a cells were immobilized in bactoagar gel, creating a 3D immobilization matrix. For comparison purposes, the impedance measurements of the DA solution added to the 3D immobilization matrix were also performed. The same DA concentrations were applied to the immobilized cell culture as chosen in the first experiment. Figure 11 illustrates the responses of the mean impedance values of the DA solution without cells added to the immobilization matrix and Figure 12 presents the responses of the mean impedance of immobilized cells applied to increased DA concentrations in the following frequencies: 1 KHz, 10 KHz, 100 KHz. The 3D immobilization matrix represents, though not perfectly, the actual environmental *in vivo* conditions, under *in vitro* simulative conditions. The responses of the DA solution follow the same motif after the 1uM DA concentration, similar to the previous experimental procedure. However, in Figure 11, apart from the control solution all measurements have lower values compared to the first experimental approach as a consequence of the immobilization matrix ($R^2 > 0.70$ as shown in Table 2). In Figure 12, the 3D immobilized cell culture confirms the fact that the impedance decreases with the increased frequency range. Moreover, the mean impedance values follow a similar, if not identical pattern as DA concentrations increase ($R^2 > 0.95$ as shown in Table 2). The presence of the bactoagar gel as a three-dimensional configuration obligates the cells to be surrounded by it and hence diffusion of the applied substance is created with a gradation of the concentration towards them.

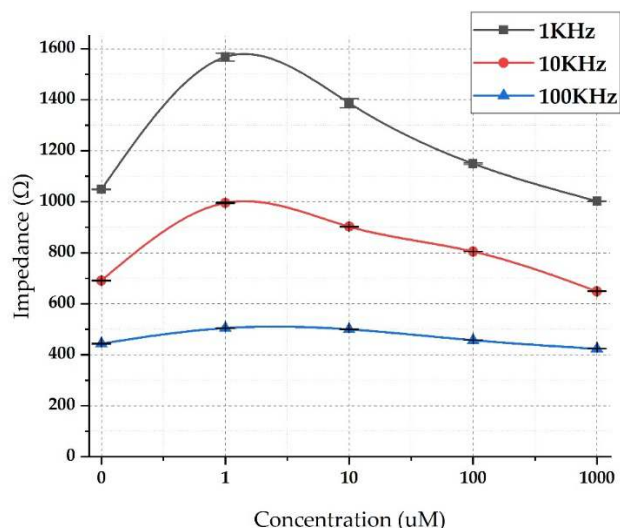


Figure 11: Response of DA solution applied to the 3D matrix in different frequencies (1 KHz, 10 KHz, 100 KHz) with increasing DA concentrations with \pm SD values

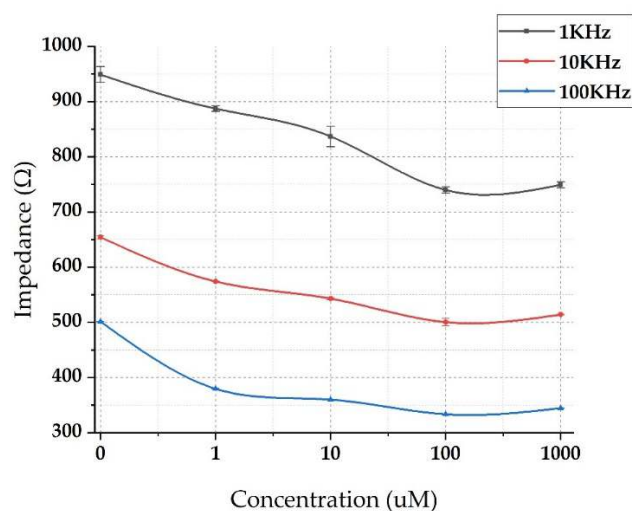


Figure 12: Response of 3D immobilized N2a cells to different frequencies (1 KHz, 10 KHz, 100 KHz) with increasing DA concentrations with \pm SD values

Table 2: R^2 values for mean impedance responses regarding DA solution applied to the 3D immobilization matrix and N2a immobilized cells treated with the same uM increasing DA concentrations in three frequencies tested (1 KHz, 10 KHz, 100 KHz).

| Frequency | R^2 | |
|-----------|-------------|-----------------------|
| | DA solution | Cells treated with DA |
| 1 KHz | 0.7128 | 0.9519 |
| 10 KHz | 0.8271 | 0.9839 |
| 100 KHz | 0.8857 | 0.9594 |

For further analysis, all combinations of DA concentrations, including the control solution, were tested using a Student's T-test in each frequency, in both cell cultures (monolayer and 3D immobilization). As shown in Table 3, in the case of 1 KHz, a small contribution of DA solutions is observed. More specifically, in the highest concentration of 1000uM, both N2a cell cultures showed no significance. In the frequency of 10 KHz (Table 4) cell cultures in monolayer and in 3D immobilization matrix contribute to all solutions with increasing DA concentrations. Table 5 shows the results of the T-test for the highest frequency of 100 KHz. It is illustrated that the control solution affects all DA concentrations in the case of monolayer cell culture, whereas in the case of 3D immobilized cells there is a total mirrored pattern between the control solution and all DA concentrations. Contrary to this observation, all combinations of 1000uM DA solutions are statistically significant.

Table 3: Significant differences (Student's T-test) in all solutions tested in different DA concentrations, including control solution, between N2a cells in monolayer and 3D immobilized N2a cells at 1 KHz frequency. * < 0.05, ** < 0.01, *** < 0.001.

| | N2a cells cultured in monolayer | 3D immobilized N2a cells |
|------------------|---------------------------------|--------------------------|
| control - 1uM | ** | * |
| control - 10uM | - | * |
| control 100uM | ** | ** |
| control - 1000uM | *** | ** |
| 1uM - 10uM | * | * |
| 1uM - 100uM | * | ** |
| 1um - 1000uM | ** | ** |
| 10uM - 100uM | * | * |
| 10uM - 1000uM | ** | * |
| 100uM - 1000uM | - | - |

Table 4: Significant differences (Student's T-test) in all solutions tested in different DA concentrations, including control solution, between N2a cells in monolayer and 3D immobilized N2a cells at 10 KHz frequency. ** < 0.01, *** < 0.001.

| | N2a cells cultured in monolayer | 3D immobilized N2a cells |
|------------------|---------------------------------|--------------------------|
| control - 1uM | ** | *** |
| control - 10uM | - | *** |
| control 100uM | *** | ** |
| control - 1000uM | - | *** |
| 1uM - 10uM | ** | ** |
| 1uM - 100uM | ** | ** |

| | | |
|----------------|----|-----|
| 1um - 1000uM | ** | *** |
| 10uM - 100uM | ** | ** |
| 10uM - 1000uM | ** | ** |
| 100uM - 1000uM | - | - |

Table 5: Significant differences (Student's T-test) in all solutions tested in different DA concentrations, including control solution, between N2a cells in monolayer and 3D immobilized N2a cells at 100 KHz frequency. * < 0.05, ** < 0.01, *** < 0.001.

| | N2a cells cultured in monolayer | 3D immobilized N2a cells |
|------------------|--|---------------------------------|
| control - 1uM | *** | - |
| control - 10uM | *** | - |
| control 100uM | *** | - |
| control - 1000uM | *** | - |
| 1uM - 10uM | *** | - |
| 1uM - 100uM | ** | - |
| 1um - 1000uM | ** | *** |
| 10uM - 100uM | * | ** |
| 10uM - 1000uM | * | ** |
| 100uM - 1000uM | - | ** |

4.4. Conclusion

For many decades, researchers have utilized EIS in order to study the interactions and the alterations in cell morphology by measuring the electrical impedance. It constitutes a widely conventional, fast, and non-invasive technique, also known as one of the most common and powerful analytical methods. The procedure of impedance measurements can provide valuable information about the sample tested. The contribution of impedance properties derived from biological cells is considered vital for the investigation of the cells themselves, and especially for the status of the body's health. Dopamine (DA) is a neurotransmitter that plays a critical role in aspects of brain function. The control of different physiological functions in both the brain and periphery depends on the level of DA as it enables its receptors (D1-D5). The regulation of many neurological diseases, including motor activity, relies on DA receptors that are coupled with G protein receptors [186].

In this chapter, the treatment of N2a cells to various DA concentrations was studied by means of impedance analysis, based on the principles of EIS. Contrary to previous reports, the innovative perspective was the investigation of the cells' immobilization using bactoagar gel as a 3D matrix. For comparison purposes, the

same experimental procedure was carried out for non-immobilized cell culture. For the reference, DA solutions were also measured with and without 3D immobilization matrix. The extracted results showed that the cells' immobilization regimes are considered essential for the impedance measurements, regarding the electrical response of the cell medium that reacts when a frequency is applied. As shown in previous articles, the frequency-dependent behavior of impedance is confirmed with or without the presence of the immobilization configuration. In general, a clear pattern is observed in both cases as the impedance value drops with both increasing frequencies and DA concentrations. The impedance response is affected by the DA solution when applied to both immobilized and non-immobilized cell cultures in all frequencies, compared to the control solution. In particular, the addition of increased DA concentrations showed a significant difference in the cells' response, and especially in the concentration of 100uM of DA. This can be explained due to the fact that increasing levels of DA can promote the stimulation of low-affinity DA receptors, including D2-like receptors, as shown in [184].

Chapter 5: Impedance Study of Dopamine Effects after
Application on 2D and 3D Neuroblastoma Cell Cultures
Developed on a 3D-Printed Well

5.1. Introduction

The generalization of the resistance can be described by the term impedance which constitutes a complex ratio of the voltage to current in a direct or alternating current circuit [94]. Electrochemical impedance spectroscopy is applied in many types of analysis as it is one of the most common impedance-related measurement methods [94]. Impedance measurements based on EIS principles are considered a powerful tool in order to characterize single cells that depend on the cellular response over a particular frequency range as well as on the cellular long-term physiological responses [96]. In addition to that, the electrical properties of the cell membrane and the cytoplasm are associated with the overall biological property of a cell [187, 188]. In many areas of biomedicine, bio-impedance is used as a non-invasive and inexpensive technology. The cells of the human body are arranged in groups by function for the formation of organs and tissues. The reaction of the cells to the alternate current flow can provide valuable information about the health status of the subject since there is a dependence between body functions and the respective cellular ones [189].

In the mammalian brain, hearing, touch, and sight are various senses that provide amounts of information received from the subject's environment, combined with signals from throughout the body. Synaptic vesicles merged with the cell membrane release neurotransmitters by exocytosis. Since amino acid neurotransmitters are considered critical for the regulation and control of different functions in the central nervous and peripheral system, they also gain attention in clinical chemistry, medical diagnostics, biomedical research, and the pharmaceutical industry [190-192].

The process of cell immobilization on the surface of the electrode is a desired integral part of whole-cell electrochemical biosensors as redox reactions occur. This can also make its operation simple and contribute to an efficient improvement in operational and storage stability. The immobilization process is able to maintain cell viability and functionality as well as to make sure that the analyte molecules can efficiently contact the cells, as well as the product molecules derived from the intracellular enzymatic activity, can access the electrode's surface [193].

During the immobilization procedure of a biorecognition element (e.g., cell) on a transducer, the anchored plasma membrane interferes above the surface of the electrode and blocks the electrical current that flows directly through the electrode.

As a result, the current that passes from the electrode to an attached cell disperses through the narrow cell-substrate spaces [194].

As mentioned in the previous chapter, one of the crucial catecholamine neurotransmitters for both mammalian peripheral and central nervous systems is dopamine ((3,4-dihydroxyphenyl) ethylamine, DA) [195]. Dopamine significantly affects the functioning of the renal, hormonal, and central nervous systems [180]. In particular, in pathological conditions and major diseases including Parkinson's disease, Tourette syndrome, schizophrenia, hyperprolactinemia, drug addiction [196], Huntington's disease [197], epilepsy, senile dementia, and HIV infection [198], DA receptors (D1-D5) along with their subtypes constitute the basis for the treatment of the abovementioned diseases, taking into account pharmacological modification of the response of the different DA receptors. The accurate and direct detection of DA neurotransmission may provide valuable information for this function. This significant comprehension may contribute to the design of treatment for diseases connected to DA systems [199].

The design of simple and fast devices for DA detection is considered vital as different techniques can be applied, such as high-performance liquid chromatography (HPLC) [200], spectrophotometry [201], and ion chromatography [202]. Despite the fact that these techniques are characterized by high sensitivity and specificity, they are time-consuming and also demand high-priced and sophisticated instrumentation. A highly sensitive, simple, and rapid solution is provided by electrochemical approaches that are able to detect multiple analytes on-line and in situ on the field [203]. The use of electrochemical methods through a two-electron oxidation reaction can make the quantitative determination possible as DA is an easily oxidizable compound [204].

Three-dimensional (3D) printing is a low-cost technology that is used in order to create sophisticated-shaped bodies in a short time period. It is used in engineering applications as it provides fast manufacturing [97-99]. For this technology, the used polymers are based on the particular characteristics that are needed for microfabricated devices, for instance, polycarbonate, polydimethylsiloxane/polyurethane (PDMS), polystyrene, polyethylene terephthalate glycol (PETG), and polymethyl methacrylate (PMMA) [205-208]. In their study, Mehta et al. [209] described an assembly consisting of PDMS and rigid polymers in order to construct a perfusion biocompatible system. In particular, they manufactured PETG channels that are connected to flexible PDMS membranes so that they can study embryonic and stem cell differentiation, ischemia, and cancer.

This chapter aims to present the performance of impedance analysis measurements on immobilized N2a neuroblastoma cells treated with DA by using two silver (Ag) electrodes embedded in a 3D-printed PETG well. Two specific immobilization methods were applied, for either 2D or 3D cell spatial ordering. Thus, the electric impedance analysis on an in vitro system able to mimic in vivo conditions is performed.

5.2. Materials and Methods

5.2.1. Cells Preparation/ Immobilization

For the cell culture, the same procedure was followed, as described in the previous chapter (see 4.2.1). In order to construct the well for the cell culture, PETG was used as a material for the 3D printing process as it is transparent and has great thermal stability [210, 211]. The resulting volume was 90uL with the addition of 40uL of nutrient in the well. All DA solutions were in double-distilled water and prepared only on the day of every assay. The DA concentrations applied for the impedance measurements were 1, 10, 100, and 1000uM. In order to measure the solution's impedance also in lower concentrations, PLL was used as a two-dimensional immobilization matrix as it is characterized by stability. 40uL of PLL were added in the well and left in the incubator chamber for 1h. Distilled water was used for the rinse of the electrode's well and after it was dried out, cells were put on the bottom of the electrode's well. Bactoagar gel was used as a three-dimensional immobilization matrix in concentration 1.2% sterilized by autoclave in 121°C for 20min for the respective cell culture. Concisely, 50uL of bactoagar gel (1% final concentration) were mixed with 50.000 N2a cells and placed together in the well of the electrode. For the experimental procedure, DA solutions were prepared and measured in the corresponding nM concentrations in order to compare the extracted results for both immobilization methods.

5.2.2. Experimental Setup

The design of a particular electrode assembly for this study was implemented. It consists of two silver (Ag) electrodes placed vertically into a custom-made transparent 3D printed well (Figure 13). The two electrodes were connected to the same handheld LCR meter U1733C, as described in 4.2.3. This device allows the direct extraction of the impedance magnitude of the sample tested in five specific frequencies (100 Hz, 120 Hz, 1 KHz, 10 KHz, 100 KHz). For the impedance measurements, $0.74 \text{ V}_{\text{rms}} \pm 50 \text{ mV}_{\text{rms}}$ of voltage were applied to the silver electrodes via the two terminals. Except for the immobilized cells, the solution in the electrode's well was either a mixture of cells applied to DA either nutrient. For the frequency of 1 Hz, the total measured values for each run were 180, taking into account that every measurement lasted three minutes, that is one measurement per second.

5.2.3. Experiment design and data analysis

All experimental cases were set up in a fully random way and every experiment was repeated three times with three replications ($n=3$). The extracted results were displayed with the mean \pm SD values. A multiple Student's T-test was utilized to test the alterations of the means for statistical significance. Significant differences were indicated as adjusted p-values < 0.05 (two-sided). Data means of immobilization matrices were also compared using correlation analysis, indicating how close the pair of means compared is related.

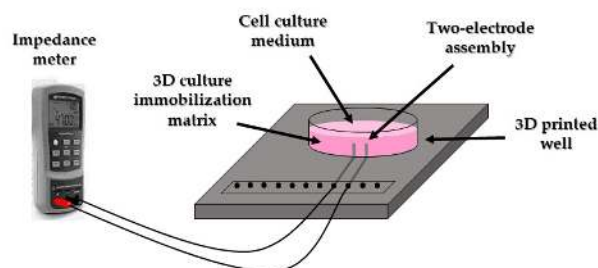


Figure 13: Experimental setup of the particular electrode assembly.

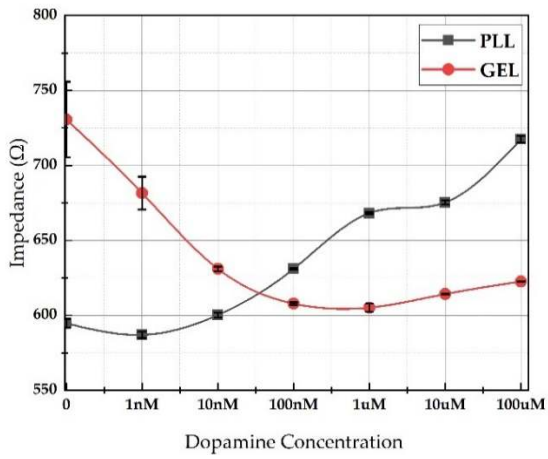
5.3. Results

In this chapter, the evaluation of the impedance interactions when mammalian cells are treated to DA under two different immobilization techniques is presented. For impedance measurements, DA was applied as a stimulant on a particular cell line in a population of 50.000. This study aims to provide a description of the behaviour of 2D and 3D cell cultures treated to known DA concentrations from the extracted calibration curves in different frequencies.

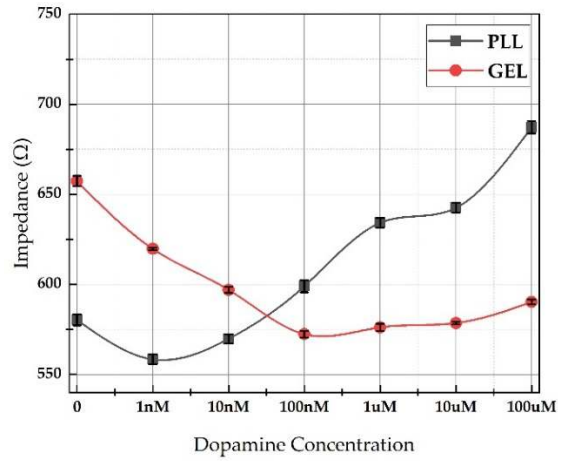
5.3.1. Impedance Comparative Results from 2D and 3D Cell Cultures

In this stage, two experimental cases were performed. The first experimental approach included the analysis of the impedance regarding immobilized cells in the 3D immobilization matrix (GEL) compared to the respective 2D (PLL). The mean impedance value ($n = 3$) of the immobilized cells when DA was applied in six known DA concentrations (1nM, 10nM, 100nM, 1uM, 10uM, 100uM) for the five frequencies given from the device is illustrated in Figure 14. In all measurements, the control solution (nutrient medium) was indicated with the notation (0).

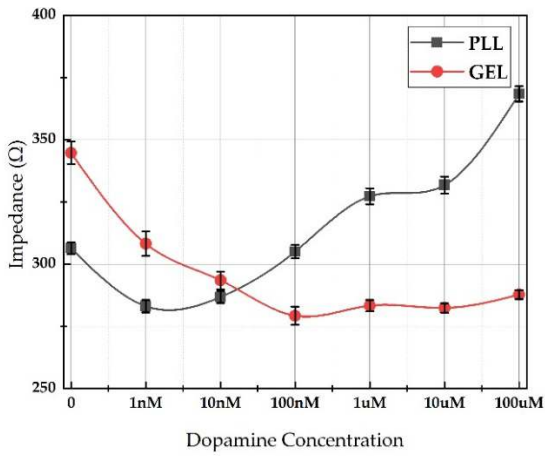
The previous chapter [212] showed that the measured impedance magnitude in different concentrations decreases with the increase of the frequency, yet compared to the 3D cell culture, the mean impedance value retains constant as the concentration increases (1nM – 100uM) corresponding to all frequencies tested, apart from the control solution. Immobilized cells in gel appeared to have a similar, if not identical response pattern with the increasing frequency range ($R^2 > 0.96$ as observed in Table 6). On the contrary, related to immobilized cells in PLL treated with DA, impedance values demonstrated a different behaviour in comparison with the other immobilization method. A clear increase in the impedance is detected for every frequency tested. In general, the presence of gel as an immobilization matrix causes a reduction in the impedance as frequency increases.



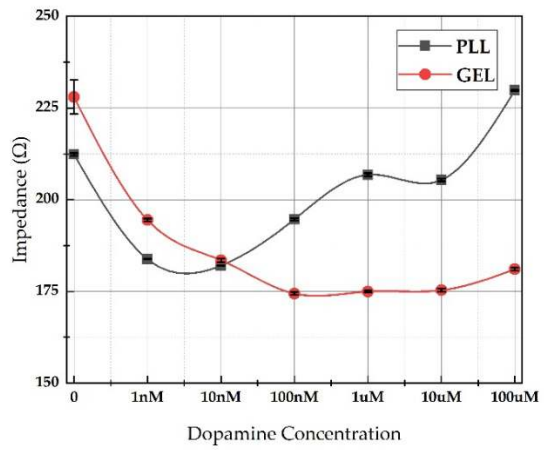
(a)



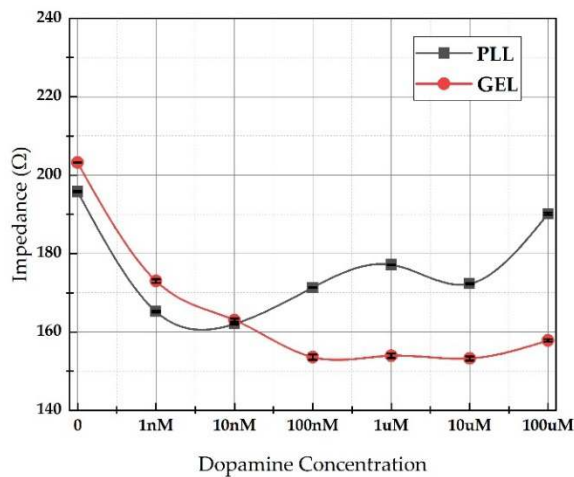
(b)



(c)



(d)



(e)

Figure 14: Mean impedance magnitude values ($n = 3$) for cells in 3D (red lines) and 2D (black lines) cultures treated with dopamine (DA) at five different frequencies: (a) 100 Hz, (b) 120 Hz, (c) 1 KHz, (d) 10 KHz, (e) 100 KHz, with \pm SD values.

Table 6: R² values for mean cell impedance responses in gel and polylysine (PLL) matrices after application of increasing DA concentrations.

| Frequency | R ² | |
|-----------|----------------|--------|
| | GEL | PLL |
| 100 Hz | 0.9882 | 0.9649 |
| 120 Hz | 0.9892 | 0.9492 |
| 1 KHz | 0.9685 | 0.9306 |
| 10 KHz | 0.9627 | 0.7987 |
| 100 KHz | 0.9672 | 0.6571 |

In addition, for frequencies, less than 1 KHz, the impedance of cells immobilized with PLL indicated essentially larger values (Table 6). The data including the error bars are presented in the following figures for all five frequencies for 3D (Figure 15) and 2D (Figure 16) immobilization matrices respectively. Furthermore, Table 7 presents the combinations of the same solutions analysed by Student’s T-test for 2D and 3D immobilization matrices respectively. As shown, with some exceptions, a clear contribution to N2a immobilized cells under different immobilization techniques is observed, especially regarding higher DA concentrations.

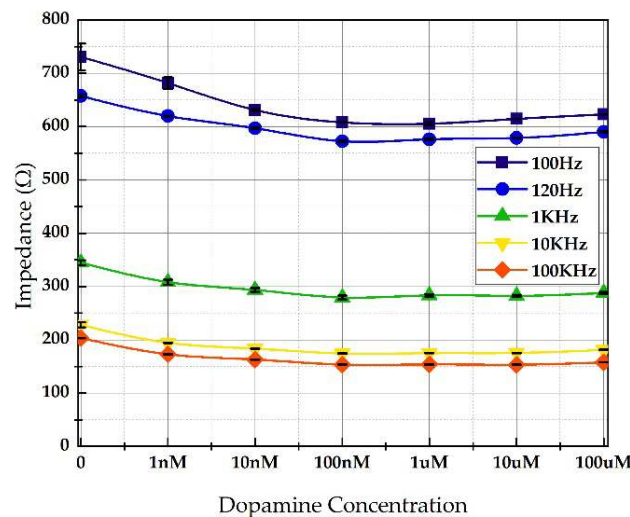


Figure 15: Mean impedance magnitude values for cells in 3D (GEL) culture treated with DA at five different frequencies (100 Hz, 120 Hz, 1 KHz, 10 KHz, 100 KHz), with \pm SD values.

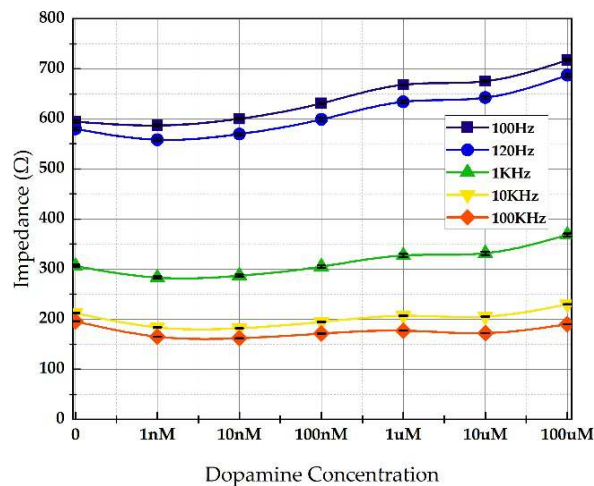


Figure 16: Mean impedance magnitude values for cells in 2D (PLL) culture treated with DA at five different frequencies (100 Hz, 120 Hz, 1 KHz, 10 KHz, 100 KHz), with \pm SD values.

5.3.2. nM DA Effects on Cells Immobilized in Bactoagar Matrix

Remarkable changes are observed with the presence of bactoagar as an immobilization matrix, especially in lower DA concentrations. Hence, in this experimental case, a different range of DA concentrations in the nM scale was prepared and tested: 1, 10, 50, 100, and 200nM. The results of the mean impedance values for the abovementioned DA concentrations are presented in Figure 17. As can be seen, the decrease of the impedance with the increase of the DA concentration for every frequency gives a quite good R^2 (Table 8), particularly up to 50nM DA. A possible explanation is due to the presence of the three-dimensional immobilization configuration. In particular, the cells don't have direct contact with the electrodes as they are surrounded by the gel, thus each substance is spread out with a gradation of concentration toward the cells.

Table 7: Significant differences (Student's T-test) in all combinations of solutions tested between N2a immobilized cells in bactoagar gel (G) and N2a immobilized cells in PLL (P) in all five frequencies. * < 0.05, ** < 0.01, *** < 0.001.

| | 100 Hz | 120 Hz | 1 KHz | 10 KHz | 100 KHz |
|-------------------------|--------|--------|-------|--------|---------|
| control(G) - control(P) | * | ** | ** | * | *** |
| 1nM(G)-1nM(P) | ** | *** | * | *** | ** |
| 10nM(G)-10nM(P) | ** | ** | - | * | - |
| 100nM(G)-100nM(P) | ** | ** | ** | *** | *** |
| 1uM(G)-1uM(P) | ** | - | *** | - | *** |
| 10uM(G)-10uM(P) | *** | *** | ** | *** | *** |
| 100uM(G)-100uM(P) | *** | *** | *** | - | *** |

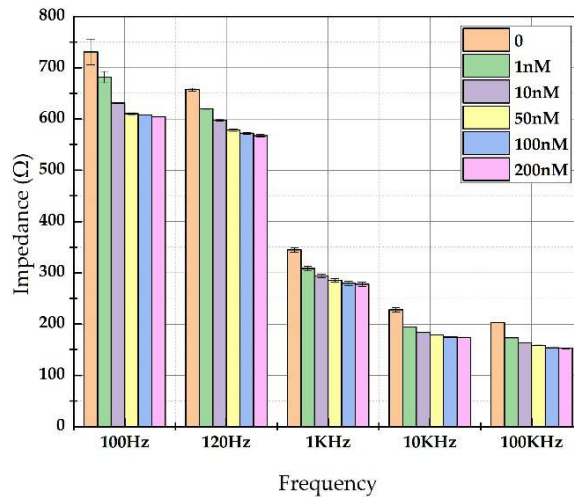


Figure 17: Mean impedance values for cells immobilized in Bactoagar matrix treated with nM DA concentrations (1, 10, 50, 100, 200 nM) at five different frequencies.

Moreover, the results of the Student's T-tests are presented in Table 9 regarding all solution combinations for the specific DA range selected in all five frequencies tested. It is observed that in most cases, the differences between the control solution and the rest of DA solutions are statistically significant in all frequencies except the frequency of 100 KHz. In addition to that, as DA concentration increases, there is a low contribution of almost all frequencies, and especially at the frequency of 1 KHz, where starting from 10nM of DA no significant differences are observed.

Table 8: R² values for mean cell impedance responses in gel for nM and PLL for uM DA concentrations.

| Frequency | R ² | |
|-----------|----------------|----------|
| | GEL (nM) | PLL (uM) |
| 100 Hz | 0.921 | 0.9468 |
| 120 Hz | 0.997 | 0.9612 |
| 1 KHz | 0.98 | 0.9358 |
| 10 KHz | 0.9608 | 0.5526 |

An additional data analysis was performed by means of correlation coefficients. Table 10 presents the results of the correlation coefficients based on the five frequencies tested whereas Table 11 illustrates the respective results based on the chosen concentrations. In both cases, the results showed a strong relationship as all frequencies appeared to have values close to 1, indicating almost a perfectly positive correlation.

Table 9: Significant differences (Student's T-test) in all combinations of solutions tested in N2a immobilized cells in bactoagar gel in all five frequencies. * < 0.05, ** < 0.01, *** < 0.001.

| | 100 Hz | 120 Hz | 1 KHz | 10 KHz | 100 KHz |
|---------------|--------|--------|-------|--------|---------|
| control-1nM | - | ** | * | * | - |
| control-10nM | * | ** | ** | ** | - |
| control-50nM | * | ** | *** | ** | - |
| control-100nM | * | *** | ** | ** | - |
| control-200nM | - | *** | ** | ** | - |
| 1nM-10nM | * | ** | * | - | ** |
| 1nM-50nM | ** | ** | ** | ** | ** |
| 1nM-100nM | ** | ** | ** | *** | - |
| 1nM-200nM | ** | ** | * | *** | *** |
| 10nM-50nM | ** | ** | - | * | ** |
| 10nM-100nM | ** | ** | - | ** | ** |
| 10nM-200nM | ** | ** | - | ** | ** |
| 50nM-100nM | - | - | - | * | ** |
| 50nM-200nM | * | - | - | * | * |
| 100nM-200nM | - | - | - | - | - |

Table 10: Correlation matrix of correlation coefficients for the means values of the 3D immobilized cells for all five frequencies tested.

| | 100 Hz | 120 Hz | 1 KHz | 10 KHz | 100 KHz |
|---------|----------|----------|----------|----------|---------|
| 100 Hz | 1 | | | | |
| 120 Hz | 0.991817 | 1 | | | |
| 1 KHz | 0.983929 | 0.990215 | 1 | | |
| 10 KHz | 0.971347 | 0.975659 | 0.996646 | 1 | |
| 100 KHz | 0.973573 | 0.980192 | 0.998192 | 0.999554 | 1 |

Table 11: Correlation matrix of correlation coefficients for the means values of the 3D immobilized cells for increasing nM DA concentrations tested.

| | control | 1nM | 10nM | 50nM | 100nM | 200nM |
|---------|----------|-----|------|------|-------|-------|
| control | 1 | | | | | |
| 1nM | 0.999887 | 1 | | | | |

| | | | | | | |
|--------------|----------|----------|----------|----------|----------|---|
| 10nM | 0.998629 | 0.999267 | 1 | | | |
| 50nM | 0.998549 | 0.999202 | 0.999998 | 1 | | |
| 100nM | 0.998841 | 0.999419 | 0.999988 | 0.999981 | 1 | |
| 200nM | 0.998972 | 0.999506 | 0.999972 | 0.999961 | 0.999996 | 1 |

5.3.3. μM DA Effects on Cells Immobilized in PLL

The results using PLL as an immobilization matrix in the DA concentration range from 1 to 100 μM illustrated almost a linear increase pattern (Figure 14) due to PLL's stability. For this reason, further analysis in additional DA μM concentrations (1, 10, 50, 100, and 200 μM) was performed (Figure 18).

The use of PLL as an immobilization matrix might not allow the lower DA concentrations to be observed from the cells because of cells' diffusion, and thus, the impedance values are not affected by the DA solution. This behaviour can be explained due to the fact that in the two-dimensional immobilization using PLL, cells are mostly concentrated in the bottom of the electrode's well and are in direct contact with the solution, which is expressed from higher DA concentrations. Hence, immobilized cells with PLL respond better with the presence of DA's molecules as the impedance increases for all five frequencies tested, and particularly for frequencies below 1 KHz, where $R^2 > 0.93$ (Table 8). A statistical analysis using Student's T-test (Table 12) indicated that, with some exceptions, the responses of solutions' combinations of N2a immobilized cells in PLL differed highly significantly among all five frequencies, with the 10 KHz and 100 KHz predominating.

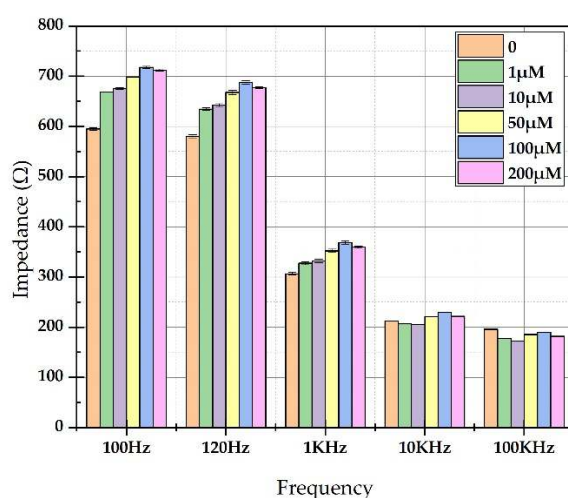


Figure 18: Mean impedance values for cells immobilized in PLL matrix treated with μM DA concentrations (1, 10, 50, 100, 200 μM) at five different frequencies.

Table 12. Significant differences (Student's T-test) in all combinations of solutions tested in N2a immobilized cells in PLL in all five frequencies. * < 0.05, ** < 0.01, *** < 0.001.

| | 100 Hz | 120 Hz | 1 KHz | 10 KHz | 100 KHz |
|--------------------------------------|--------|--------|-------|--------|---------|
| control-1 μM | *** | ** | ** | ** | - |
| control-10 μM | *** | ** | ** | ** | - |
| control-50 μM | *** | ** | *** | ** | *** |
| control-100 μM | - | ** | ** | *** | ** |
| control-200 μM | - | *** | ** | *** | *** |
| 1 μM -10 μM | * | - | - | - | *** |
| 1 μM -50 μM | - | ** | ** | - | - |
| 1 μM -100 μM | *** | ** | ** | *** | *** |
| 1 μM -200 μM | ** | *** | ** | *** | *** |
| 10 μM -50 μM | ** | ** | * | *** | - |
| 10 μM -100 μM | ** | ** | ** | *** | *** |
| 10 μM -200 μM | ** | *** | ** | *** | *** |
| 50 μM -100 μM | ** | * | * | *** | ** |
| 50 μM -200 μM | ** | - | - | - | *** |
| 100 μM -200 μM | - | - | - | *** | *** |

Again, the calculation of the correlation coefficients was carried out in the 2D immobilization case. Table 13 displays the results of the comparison regarding the five frequencies tested while Table 14 shows the respective compared results regarding the μM increasing DA concentrations tested. As observed, taking into account the frequency factor, although lower frequencies give a strong positive relationship, the higher frequencies present from weak to medium correlation strength, especially the pairs compared to 100 KHz. This pattern changes considering the concentration factor, where all the pairs tested display very strong positive correlation with values > 0.99.

Table 13: Correlation matrix of correlation coefficients for the means values of the 2D immobilized cells for all five frequencies tested.

| | 100 Hz | 120 Hz | 1 KHz | 10 KHz | 100 KHz |
|---------|----------|----------|----------|----------|---------|
| 100 Hz | 1 | | | | |
| 120 Hz | 0.994238 | 1 | | | |
| 1 KHz | 0.952346 | 0.978422 | 1 | | |
| 10 KHz | 0.582191 | 0.661629 | 0.799162 | 1 | |
| 100 KHz | -0.35927 | -0.26388 | -0.0672 | 0.545771 | 1 |

Table 14: Correlation matrix of correlation coefficients for the means values of the 2D immobilized cells for increasing uM DA concentrations tested.

| | control | 1uM | 10uM | 50uM | 100uM | 200uM |
|----------------|----------------|------------|-------------|-------------|--------------|--------------|
| control | 1 | | | | | |
| 1nM | 0.999276 | 1 | | | | |
| 10nM | 0.999051 | 0.999953 | 1 | | | |
| 50nM | 0.998891 | 0.999862 | 0.999975 | 1 | | |
| 100nM | 0.998386 | 0.999618 | 0.999839 | 0.999937 | 1 | |
| 200nM | 0.998319 | 0.999692 | 0.999877 | 0.99994 | 0.999974 | 1 |

5.4. Discussion

In bioanalytical studies, 3D printing has turned into a significant technology that allows the construction of plenty of custom-made labware and analytical devices during the last decade. Furthermore, it constitutes a valuable tool that has many advantages, including a rapid manufacturing process, ease of learning, due to its ability to create complex structures with a satisfactory resolution. In addition, biomedical engineering, tissue scaffolding, surgical preparation, pharmacodynamics/pharmacokinetics, medical and forensic science are fields that 3D printing technology is widely applied. Also, commercial manufacturers have been fascinated by the use of polymeric materials as they are characterized by low-price and easy fabrication steps in comparison with glass and silicon [213, 214].

This chapter presented the analysis of the impedance system implemented for N2a cell cultures after the addition of different DA concentrations. The alterations in impedance with the presence of 2D or 3D cell immobilization matrices were further investigated. Cell cultures were carried out in a custom-made PETG 3D printed well consisting of two silver electrodes used for the measurement process. The choice of the material used for the construction of the electrode was based on its non-polarization, and it is considered as a particular material for clinical tests regarding motion artifact, low noise, and low electrode-skin impedance [215]. The results emphasized the significance of the impedance measured under different cell immobilization conditions, as differential responses are observed when a frequency is applied. In particular, by increasing the DA concentration, impedance responses in the 2D immobilized cell culture have higher values, whereas the respective

impedance responses in the 3D immobilization matrix have lower values. This can be explained from the non-direct communication between cells and electrodes due to the presence of the bactoagar gel, as well as from the DA's effect on N2a cells, as described in the previous chapter (Figures 9 and 10) [216-218]. Moreover, it appears that with the presence of an immobilization matrix, the diffusion time of the solution could be a possible explanation, considering the fact that in a particular frequency range the solution penetrates either easily (PLL) or not (bactoagar).

As a result, due to the direct contact of more condensed cells – DA solution with the electrodes, impedance values in the 2D immobilization matrix (PLL) might increase. Many research studies have shown that ions contribute to the electric current in the external circuit [219, 220]. Considering the sinusoidal dependence of the external voltage on time, researchers have determined the impedance of a cell filled with KCl solution and examined the frequency – dependence of its real and imaginary parts. For the improvement of the efficacy of the impedance measurements, a wide frequency spectrum is generally preferred [221]. In low frequencies, and especially below 100 Hz, the impedance interface of the metal-electrolyte plays an important role [222]. This information might contribute to medical assessment that intrudes on the absorption of DA from cells, as there is an association between the activation of D2-like receptors and inhibition of cAMP accumulation [184].

5.5. Conclusions

This chapter presented an impedance analysis based on cell cultures performed on a 3D printed well. In particular, N2a neuroblastoma cells were cultured and immobilized in two immobilization matrices (2D and 3D) in a custom-made PETG 3D printed well, consisting of two silver electrodes. Each cell solution was treated with different DA concentrations. Differential responses are observed when a frequency is applied, proving that the impedance under different cell immobilization regimes plays a significant role. In the case of a 3D cell immobilization, impedance demonstrates lower values with the increase of the concentration, whereas in the 2D cell immobilization case, larger impedance values are observed with the increased concentration. Moreover, in all frequencies tested, it was shown that there is a reaction of cells in PLL to DA's molecules leading to an increase of the impedance. The results describe the responses of the cell medium in

various frequencies, indicating the significance of the impedance measured in cell immobilization matrices. The analysis and the measurements of the cell culture can contribute to a high level of additive manufacturing processes.

Chapter 6: Impedance Analysis of various cancer cell types immobilized in 3D matrix and cultured in 3D-Printed Well

6.1. Introduction

In many countries, cancer constitutes one of the main causes of death, appeared in various types, usually affecting women, for example, breast, cervical, and lung adenocarcinoma cancers. For medical care, doctors make necessary steps for the anticipation of the development of the disease which is primary prophylaxis or for the anticipation of the conception of its further development, which is secondary prophylaxis. Taking into account the measures of the secondary prophylaxis, the requirement of sophisticated procedures is necessary for the detection of possible cellular disorders at the initial stages of the disease's incubation period, considering the dependence of the efficiency on the timeliness with which the disease is detected. In general, numerous cancer diagnostic techniques use a mixture of surgical biopsy, radiological, and pathological evaluation of tissue samples that depend on morphological and immunohistochemical features [223], which makes this approach complicated, slow, invasive, and in need of proper laboratory conditions. Hence, the development of novel cancer detection techniques is required, as they are reliable, user-friendly, minimally invasive, and cost-effective [224].

Considering the significance of the biological procedure and molecular mechanisms of cancer development and progression as well, anticancer therapy has made significant improvements regarding the importance of progress in survival over the past decades [225, 226]. Despite the fact that the development of numerous approaches for cancer treatment was successful, at some point the resistance of subgroups of cancer cells will appear as an obstacle against the efficiency of most present therapeutic approaches [227]. 5-fluorouracil (5-FU) is one of the most popular applied drugs for the treatment of cancer. More specifically, it belongs to the antimetabolite group of chemotherapy drugs and also constitutes a medicine for various cancer types, such as skin cancer, breast cancer, colon cancer, etc. Due to the fact that the structure of the pyrimidine base of DNA is similar to the respective RNA, 5-FU can lead to cytotoxicity and cell death as it interposes in nucleoside metabolism [170]. Various approaches have been proposed for the optimization of the delivery of 5-FU in order to reinforce the therapeutic index with fewer side effects. The encapsulation of 5-FU in nanoparticles (e.g. liposomes) can reduce both drug clearance and relative toxicity [228].

The evaluation of the electrical impedance of the living cells can be performed by a method called Electrical Impedance Spectroscopy (EIS) in order to classify several types of cells. This method can be applied for the successful split of

pathological cells from normal ones considering the electrophysiological features of cells depending on the frequency spectrum [229, 230]. The electrical impedance of the cell can classify mechanical, physical, and biochemical functions of living biological cells. EIS aims its attention on the discrimination and the analysis of cancer cells, by exploiting the fact that depending on the electrical response over a specific frequency range, the characterization of the cells [231] can be accomplished by the impedance measurement approach. For instance, the impedance method was applied for the measurement of three-dimensional cell cultures [232] for four breast cell lines [233].

Lately, in order to perform biological measurement analysis, electrical impedance sensing has become the most preferred technology. More accurate information regarding the electrical features in the frequency range is provided as impedance signals pass through biological samples. Impedance that comes from biological samples from the cell-level impedance to the impedance of DNA is defined as bio-impedance [234, 235]. Furthermore, bio-impedance research not only can indicate the status of a single cell and the pathological status of a single cell can be indicated by bio-impedance research but also can be applied in order to determine the occurrence of toxicity, changes of environmental parameters, bacterial infections, direct or indirect detection of compounds, etc [236].

Cell immobilization can be defined as the process where whole cells are localized or physically contaminated in a specific area of space without any loss of biological activity [237]. In particular, the immobilization procedure where cells are encapsulated in an immobilization cell system is known as “microencapsulation” or “bioencapsulation”. A given immobilization system is considered suitable based not only on the type of application but also on the physical and biochemical characteristics of the immobilizing agent/matrix [238].

A considerable number of natural and synthetic polymers are applied in order to entrap gelled cells into hydrophilic matrices under mild conditions with minimum loss of viability. Despite the fact that natural polymers “dominate”, lately synthetic polymers have been used for the immobilization of living cells [49]. Gel’s features, whether hydrophilic or hydrophobic including porosity, can be controlled. Cell’s entrapment is one of the most famous techniques for the immobilization of living cells within spherical beads of calcium alginate. The success of this technique is related to the fact that immobilization is generally carried out under very mild conditions and also it is characterized by simplicity, speed, and profitability [238].

This chapter aims to provide a description related to the reaction of various cancer cell lines exposed to an anticancer agent, regarding the population density.

Impedance measurements were performed for both untreated immobilized cells and immobilized cells treated with 5-FU in order to compare the extracted results from both cases. Herein, for impedance analysis measurements, two gold-plated (Au) electrodes were installed in a 3D-printed PETG well (as described in the previous chapter) for four cancer cell cultures (SK-N-SH, HEK293, HeLa and MCF-7) immobilized in calcium alginate matrix. Cell cultures were carried out in three various population densities tested in different frequencies. Thereby, it was possible to monitor various responses between various cancer cells (control and treated with 5-FU) by a detailed application of electric impedance analysis on an in vitro system.

6.2. Materials and Methods

6.2.1. Cells Preparation/ Immobilization

Four cell types (SK-N-SH, HEK293, HeLa, and MCF-7) were prepared and cultured for this work, based on the same process as described in 4.2.1. A note that after the process of centrifugation, cells were again resuspended in the medium at concentrations 10^6 , 2×10^6 , 4×10^6 cells/ml. The procedure of cell immobilization was performed in calcium alginate as an immobilization matrix. Briefly, sodium alginate in a concentration of 1.5% was sterilized by autoclave (121 °C, 20 min) and mixed with 5×10^4 , 10^5 , and 2×10^5 cells to a final concentration of 0.75% and poured together in the well. Afterward, the addition of CaCl_2 gelling solution in a concentration of 1% lasted for 10 seconds for cross-linking and washed with phosphate-buffered saline (PBS). After washing, the scaffolds of calcium alginate combined with the cells were incubated in a culture medium for 24h. The current incubated medium was replaced with 1% FBS medium and 1% FBS with various concentrations of 5-FU, provided Sigma-Aldrich Chemie GmbH, Taufkirchen Germany.

6.2.2. Cell Viability Assay

The evaluation of cell viability was performed by 3-(4, 5-dimethylthiazol-2-yl)-2,5-diphenyltetrazolium bromide (MTT) colorimetric assay [205] using 5-FU as positive control. Table 15 presents the concentrations of 5-FU for every cell line, depending on formerly published data [206-208, 239, 240].

The selected concentrations provided at least 30% inhibition in cell proliferation after the incubation process that lasted for 24h. One day later, 0.5 mg/ml of MTT was applied to the cell culture, and afterward, cells were incubated with the dye for 3h. The incubated medium was removed after 3h and the cells consisting of alginate scaffolds were solubilized with 0.1M ethylenediaminetetraacetic acid per well. An inverted microscope (ZEISS Axio Vert.A1, Carl Zeiss Microscopy, LLC, White Plains, NY, USA) was used in order to observe cell morphology, and pictures were processed by ZEN lite software. A PowerWave240 plate reader provided by BioTek (Winooski, VT, USA) was applied for the measurement of the optical absorbance at 560nm. Each treatment was implemented three times for every experiment independently and the average OD for each treatment was expressed by the mean results.

Table 15. 5-FU concentrations added to each cell culture.

| Cell line | SK-N-SH | HEK293 | HeLa | MCF-7 |
|-------------------------|---------|--------|------|-------|
| 5-FU concentration (uM) | 7.5 | 20 | 150 | 150 |

6.2.3. Experimental Setup

For the performance of the measurement procedure based on the EIS principles, a specific electrode assembly was adjusted. In particular, two gold-coated (Au) electrodes were arranged vertically into a customized transparent 3D-printed PETG well, as displayed in Figure 19a. The handheld LCR meter U1733C (Figure 19b) was again applied for the connection of electrodes to the device (see 5.2.2). The ability of the device allows measurements in order to extract directly the impedance magnitude of the tested sample in three various frequencies: 1 KHz, 10 KHz, and 100

KHz. Once again, for the impedance measurement process, the application of a voltage of $0.74 \text{ V}_{\text{rms}} \pm 50 \text{ mV}_{\text{rms}}$ was carried out through the two terminals to the gold-coated electrodes. One measurement per second constitutes the best logging interval of the device. Herein, each experimental measurement lasted one minute, hence the total amount of values obtained from each experimental procedure were 60 with a measurement frequency of 1 Hz. The following equation (equation 8) describes the calculation of normalized values. More specifically, each normalized value was calculated by taking the mean of the absolute value of the cells for both treated and untreated with 5-FU \pm SD subtracted by the absolute value of the control, which is plain cell culture medium.

$$\text{Normalized Impedance} = \text{mean}(|\text{control value} - \text{cell value}|) \quad (8)$$

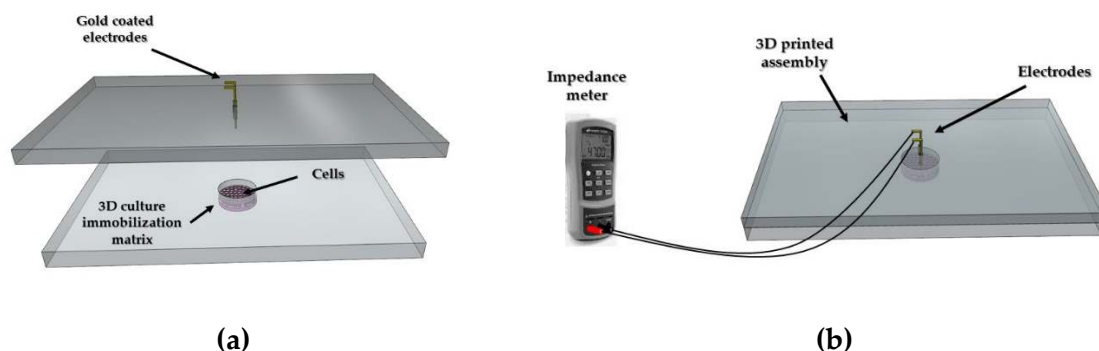


Figure 19: Experimental set up. Schematic representation of the 3D cell immobilization matrix (a); Connection of the 3D printed assembly to the LCR meter (b).

6.2.4. Experimental design and data analysis

For each cell line, all experimental cases were randomly designed and each experiment was carried out three times with three repetitions ($n=3$). Mean values including SD were utilized in order to display the results extracted. Statistical comparison of the various cancer cell lines and their populations was performed using a Student's T-test at a 95% confidence interval, describing the probability that the difference between two means is caused incidentally. Significant differences were illustrated as adjusted p-values < 0.05 (two-sided).

6.3. Results

The assessment of the applicability of EIS for the bioelectric profiling of various cancer cell types when applied to a selected anticancer agent is presented. In this section, four cancer cell lines were immobilized in calcium alginate and cultured in three particular cell population densities: 50,000, 100,000, and 200,000/100 μ L. 5-fluorouracil (5-FU) was applied as it is considered one of the most common anticancer therapeutic drugs. For each case, a specific frequency range was tested: 1 KHz, 10 KHz, and 100 KHz.

6.3.1. Cell proliferation

The evaluation of cell viability with MTT uptake assay was carried out in order to ensure that calcium alginate constituted a suitable immobilization matrix for cancer cell culture. Cell cultures were performed in the matrix for 24h for both cases (with or without application of 5-FU) and the determination of cell proliferation was implemented photometrically and microscopically after the MTT application. The microscopic observations for three various populations of four cell lines immobilized in calcium alginate after the incubation with MTT are illustrated in Figures 20 – 23.

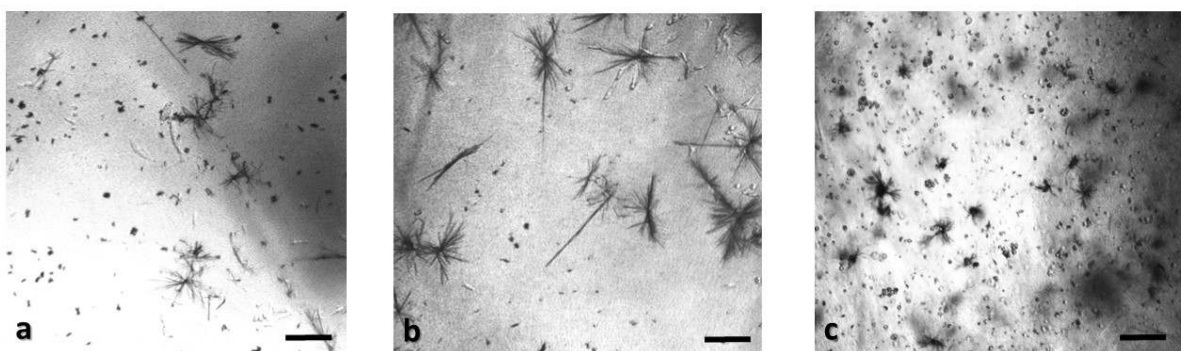


Figure 20: Panoramic view of SK-N-SH cells in 3D immobilization matrix after treatment with MTT for 24 h, indicating the viability in three various populations: 50,000 cells (a); 100,000 cells (b); and 200,000 cells (c). Scale bars = 50 μ m.

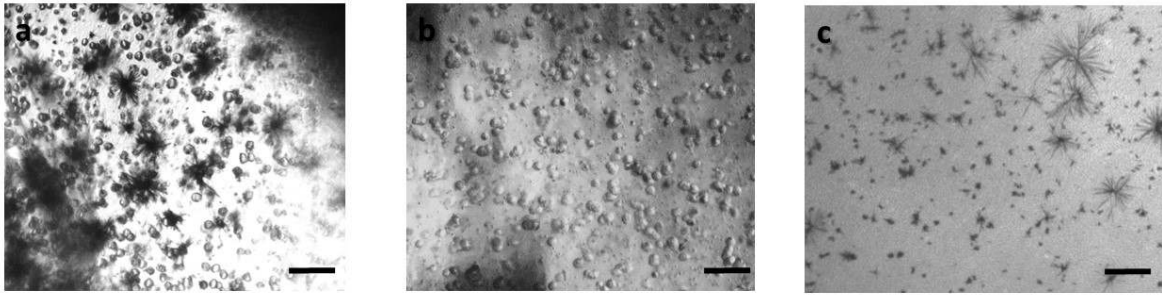


Figure 21: Panoramic view of HEK293 cells in 3D immobilization matrix after treatment with MTT for 24 h, indicating the viability in three various populations: 50,000 cells (a); 100,000 cells (b); and 200,000 cells (c). Scale bars = 50 μ m.

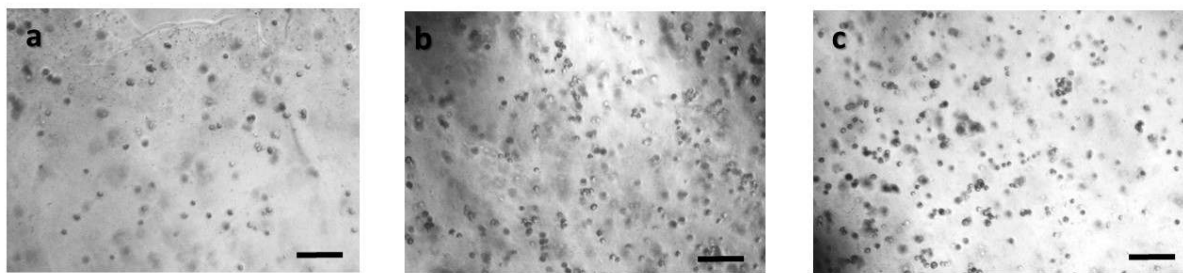


Figure 22: Panoramic view of HeLa cells in 3D immobilization matrix after treatment with MTT for 24 h, indicating the viability in three various populations: 50,000 cells (a); 100,000 cells (b); and 200,000 cells (c). Scale bars = 50 μ m.

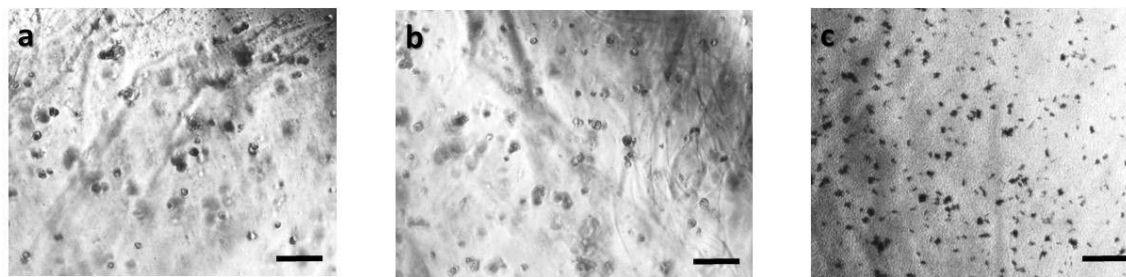


Figure 23: Panoramic view of MCF-7 cells in 3D immobilization matrix after treatment with MTT for 24 h, indicating the viability in three various populations: 50,000 cells (a); 100,000 cells (b); and 200,000 cells (c). Scale bars = 50 μ m.

The black color indicated the viable cells since the yellow formazan (MTT) by intracellular NAD(P) H-oxidoreductases [205]. The immobilization matrix in conjunction with the increase of the cell population density does not contribute the cellular proliferation. On the contrary, the photometric MTT results depicting in Figures 24 – 27 demonstrate an increase in the absorbance regarding the increase of

the cell population densities, although the viability of the cells when treated to 5-FU appeared to decrease significantly in almost every cell types (Table 16). Considering the neuroblastoma SK-N-SH cell line, the alterations in cell densities showed a limited influence in MTT absorbance with or without the presence of 5-FU (Figure 24). However, related to the cell number, the absorbance appeared to increase for the remaining cell lines, as presented in Figures 25 – 27.

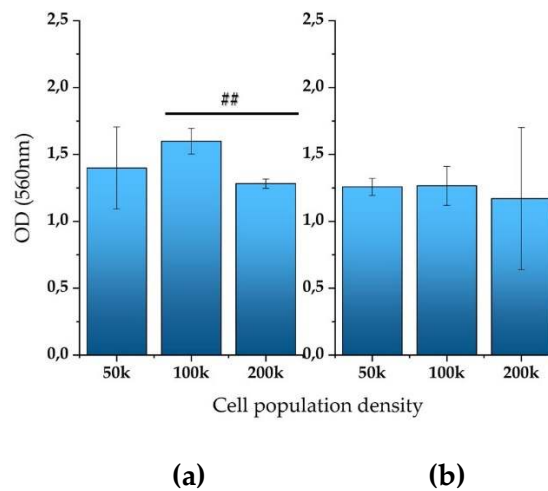


Figure 24: Cellular viability of SK-N-SH cells immobilized in 3D matrix after treatment with MTT for 24h showing the viability in three different population densities (50,000, 100,000, 200,000 cells/100 uL) ± STD: (a) untreated cells (control), (b) cells treated with 5-FU. ## < 0.01 significantly different from 100,000 cells/100 ul.

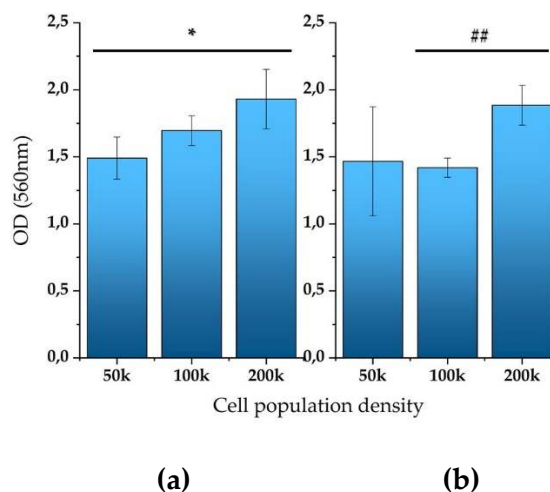


Figure 25: Cellular viability of HEK293 cells immobilized in 3D matrix after treatment with MTT for 24h showing the viability in three different population densities (50,000, 100,000, 200,000 cells/100 uL) ± STD: (a) untreated cells (control), (b) cells treated with 5-FU. * < 0.05 significantly different from 50,000 cells, ## < 0.01 significantly different from 100,000 cells/100 ul.

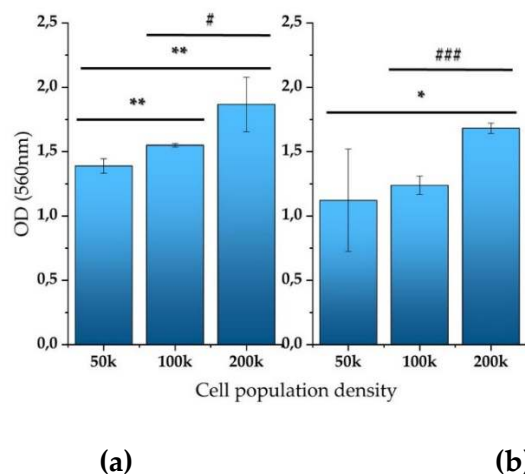


Figure 26: Cellular viability of HeLa cells immobilized in 3D matrix after treatment with MTT for 24h showing the viability in three different population densities (50,000, 100,000, 200,000 cells/100 uL) ± STD: (a) untreated cells (control), (b) cells treated with 5-FU. * < 0.05, ** < 0.01 significantly different from 50,000 cells, # < 0.05, ### < 0.001 significantly different from 100,000 cells/100 ul.

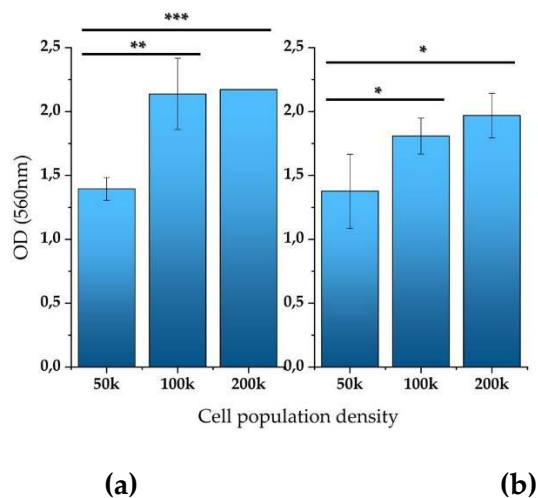


Figure 27: Cellular viability of MCF-7 cells immobilized in 3D matrix after treatment with MTT for 24h showing the viability in three different population densities (50,000, 100,000, 200,000 cells/100 uL) ± STD: (a) untreated cells (control), (b) cells treated with 5-FU. * < 0.05, ** < 0.01, *** < 0.001 significantly different from 50,000 cells/100 ul.

For comparison purposes, Table 17 presents every cell line combination analysed with Student's T-test for every population density, for treated cells with 5-FU or pure cells. In particular, in the case of 50,000 cells/100uL with the application of 5-FU, no considerable influence on MTT uptake was observed. Nevertheless, with

or without the addition of the specific anticancer agent, a clear contribution to differential viability results is observed regarding the rest two population densities.

Table 16. Significant differences among cell population densities with or without the presence of 5-FU (** < 0.01, *** < 0.001).

| Cell line | 50,000 cells | 100,000 cells | 200,000 cells |
|-----------|--------------|---------------|---------------|
| SK-N-SH | - | ** | - |
| HEK293 | - | ** | - |
| HeLa | - | *** | - |
| MCF-7 | - | - | - |

Table 17. Significant differences in cell viability among cell line combinations with or without the presence of 5-FU (* < 0.05, ** < 0.01, *** < 0.001).

| | Cell line combination | | | Cell line combination with the application of 5-FU | | |
|------------------|-----------------------|---------------|---------------|--|---------------|---------------|
| | 50,000 cells | 100,000 cells | 200,000 cells | 50,000 cells | 100,000 cells | 200,000 cells |
| SK-N-SH – HEK293 | - | - | * | - | - | * |
| SK-N-SH – HeLa | - | - | ** | - | - | - |
| SK-N-SH – MCF-7 | - | * | *** | - | *** | * |
| HEK293 – HeLa | - | * | - | - | ** | * |
| HEK293 – MCF-7 | - | * | - | - | ** | - |
| HeLa – MCF-7 | - | ** | * | - | ** | * |

6.3.2. Impedance results in comparison to various immobilized cell lines

In this experimental case, an analysis of the impedance measurements was performed based on different cancer cell lines in various population densities. For every cancer cell type, calcium alginate was again used as a 3D immobilization matrix. The following figures (Figures 28 – 31) illustrate the compared results for each cell line tested in three various frequencies (1 KHz, 10 KHz, 100 KHz). For the calculation of the absolute values, the mean impedance values were subtracted from the mean blank values, corresponding to the control solution (as described in equation 4).

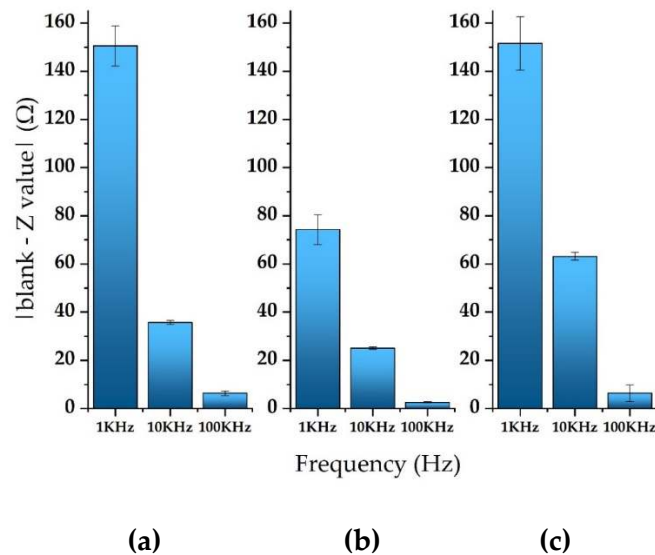


Figure 28: Normalized values of the mean impedance magnitude for untreated (control) immobilized SK-N-SH cancer cell lines tested at three frequencies (1 KHz, 10 KHz, 100 KHz) for three different population densities \pm STD: (a) 50,000 cells, (b) 100,000 cells and (c) 200,000 cells/100 ul.

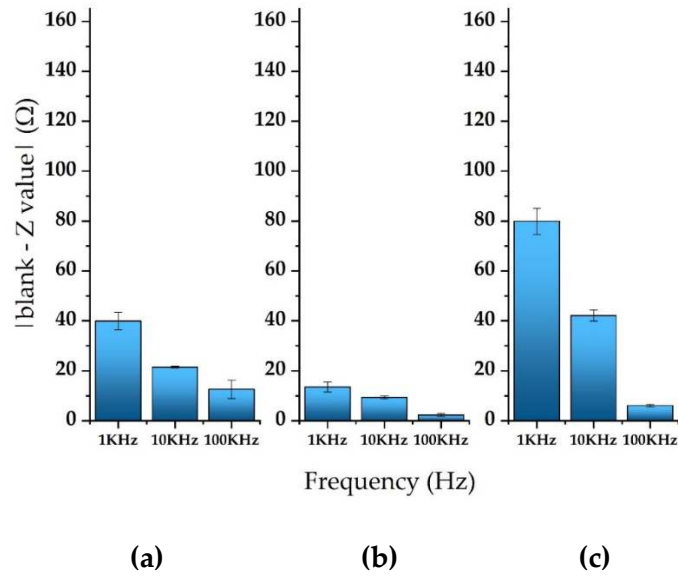


Figure 29: Normalized values of the mean impedance magnitude for untreated (control) immobilized HEK293 cancer cell lines tested at three frequencies (1 KHz, 10 KHz, 100 KHz) for three different population densities \pm STD: (a) 50,000 cells, (b) 100,000 cells and (c) 200,000 cells/100 ul.

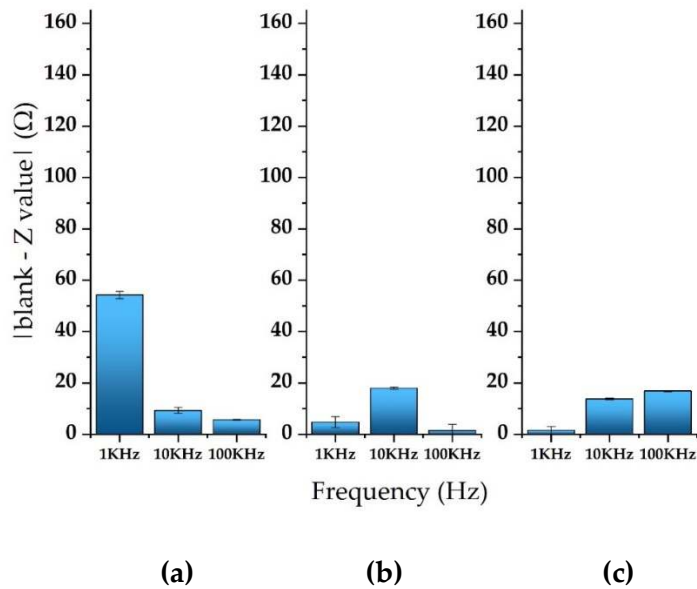


Figure 30: Normalized values of the mean impedance magnitude for untreated (control) immobilized HeLa cancer cell lines tested at three frequencies (1 KHz, 10 KHz, 100 KHz) for three different population densities \pm STD: (a) 50,000 cells, (b) 100,000 cells and (c) 200,000 cells/100 ul.

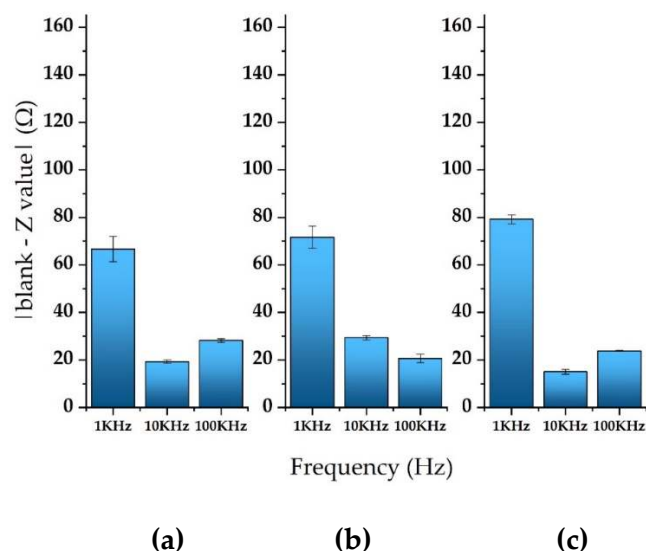


Figure 31: Normalized values of the mean impedance magnitude for untreated (control) immobilized MCF-7 cancer cell lines tested at three frequencies (1 KHz, 10 KHz, 100 KHz) for three different population densities: (a) 50,000 cells, (b) 100,000 cells and (c) 200,000 cells/100 ul.

The results depicted a frequency-dependent impedance response, as shown in numerous studies. In every frequency tested, a different motif in the measured impedance magnitude is observed for every combination regarded the cell line population density. More specifically, in the case of neuroblastoma SK-N-SH cell line (Figure 28), the increase in cell population from 50,000 cells to 100,000 cells and afterward to 200,000 cells/100uL causes a decrease in the normalized impedance. In the case of HEK293 cell culture (Figure 29), although an equivalent motif is seen, the mean impedance takes higher value at the population of 200,000 cells/100uL, compared to the corresponding impedance observed at 50,000 cells population. Figures 30 and 31 display a completely different behaviour for the HeLa and MCF-7 cell lines respectively. In particular, although the initial response of the HeLa cells was high (54.23 Ohm) in the frequency of 1 KHz, the measured impedance dropped dramatically (1.60 Ohm) as the cells' population increased. However, the response of the MCF-7 cell culture performed a totally reversed pattern, beginning from 66.72 Ohm for the population of 50,000 cells and concluding to 79.23 Ohm for the population of 200.000 cells. In addition, for both cell lines, differential alterations were detected for the rest two frequencies. In general, the characterization of every combination regarded the cell line population density appeared to have its own unique EIS identity.

6.3.3. Impedance results in comparison to various immobilized cell lines treated with 5-FU

In this experimental case, the assessment of the application of 5-FU to the abovementioned cancer cell lines was performed by EIS analysis for the investigation of the impact of the specific anticancer agent. The following figures (Figures 32 – 35) illustrate the results regarding the normalized values of the mean impedance values subtracted from the mean blank values, corresponding to the control solution. These results were calculated for every cell line tested treated or not with 5-FU in three various frequencies. The results of all combinations of cell population densities are displayed in Tables 18 – 21, indicating the statistical significance in each pair.

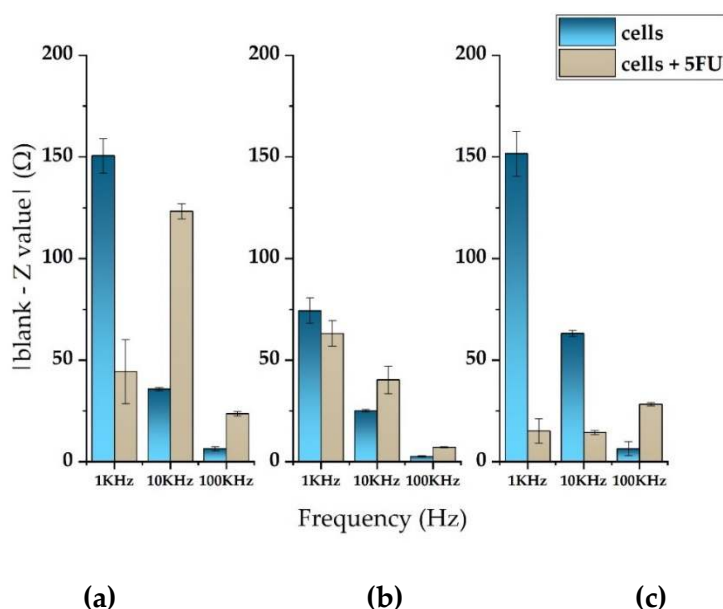


Figure 32: Normalized values of the mean impedance magnitude for control immobilized SK-N-SH cells (blue bars) and immobilized SK-N-SH cells treated with 5-FU (grey bars), tested at three different cell population densities \pm STD: (a) 50,000, (b) 100,000 and (c) 200,000/100uL for three different frequencies (1 KHz, 10 KHz, 100 KHz).

The application of the 5-FU for 24h gave higher values in normalized impedance for most of the cases compared to the pure immobilized cells. More specifically, regarding the SK-N-SH cell line (Figure 32), a reversed motif is observed with the presence of the specific anticancer agent in comparison with the remaining cell lines, particularly in the lower frequency (1 KHz). In the tested frequency range, the measured impedance magnitude appeared to drop in the population of 200,000

cells/100uL, compared to the respective case with the addition of 5-FU, where the impedance magnitude had higher values.

Table 18. Significant differences in cell impedance among cell population combinations for the SK-N-SH cell line with or without the presence of 5-FU (** < 0.01, *** < 0.001)

| | Cell population combination | | | Cell population combination with the application of 5-FU | | |
|-------------------|-----------------------------|--------|---------|--|--------|---------|
| | 1 KHz | 10 KHz | 100 KHz | 1 KHz | 10 KHz | 100 KHz |
| 50,000 – 100,000 | *** | *** | ** | ** | *** | *** |
| 50,000 – 200,000 | - | *** | - | *** | *** | *** |
| 100,000 – 200,000 | *** | *** | - | *** | ** | *** |

The summary of the results of the HEK293 cell line is presented in the following figure (Figure 33). Again, a considerable drop of impedance is observed with the increase of the frequency in every cell population tested, and also the application of the specific anticancer agent resulted in higher normalized values, as seen in Table 19. However, there are two exceptions seen from the extracted results illustrating higher values for the control solutions compared to the respective with the addition of 5-FU, considering the case of 50,000 cells/100uL at 10 KHz and 100 KHz as well as the case of 200,000 cells/100uL at 10 KHz.

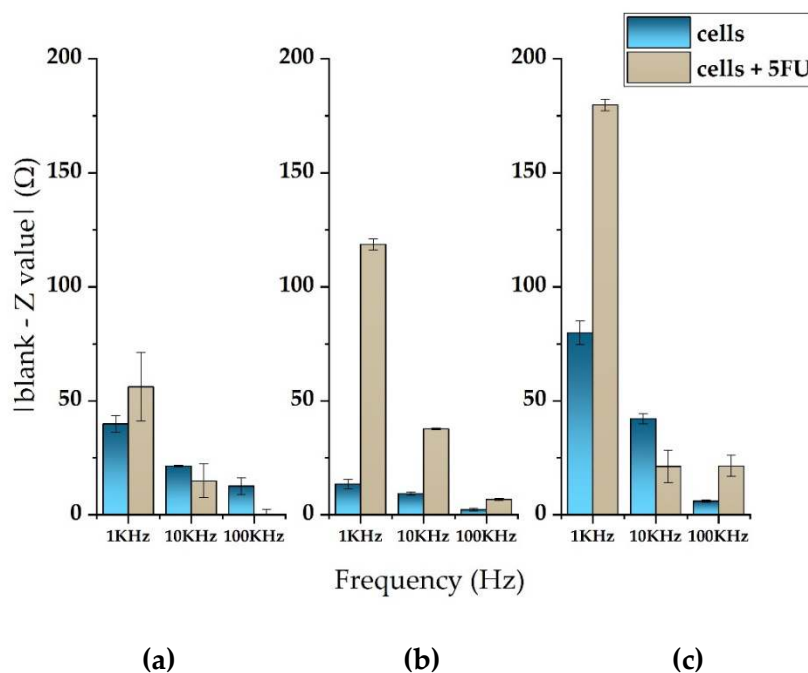


Figure 33: Normalized values of the mean impedance magnitude for control immobilized HEK293 cells (blue bars) and immobilized HEK293 cells treated with 5-FU (grey bars), tested at three different cell population densities \pm STD: (a) 50,000, (b) 100,000 and (c) 200,000/100uL for three

different frequencies (1 KHz, 10 KHz, 100 KHz).

Table 19. Significant differences in cell impedance among cell population combinations for the HEK293 cell line with or without the presence of 5-FU (* < 0.05, ** < 0.01, *** < 0.001)

| | Cell population combination | | | Cell population combination with the application of 5-FU | | |
|-------------------|-----------------------------|--------|---------|--|--------|---------|
| | 1 KHz | 10 KHz | 100 KHz | 1 KHz | 10 KHz | 100 KHz |
| 50,000 – 100,000 | *** | *** | ** | *** | *** | ** |
| 50,000 – 200,000 | *** | *** | * | *** | - | ** |
| 100,000 – 200,000 | *** | *** | *** | *** | * | ** |

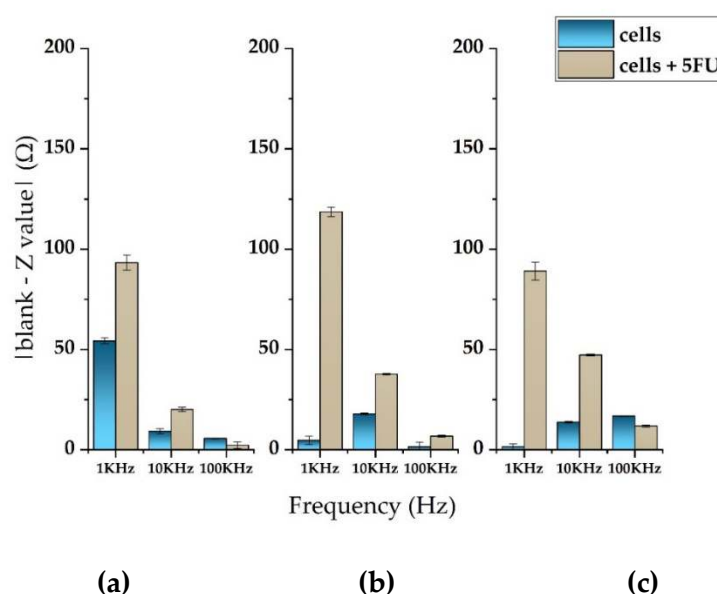


Figure 34: Normalized values of the mean impedance magnitude for control immobilized HeLa cells (blue bars) and immobilized HeLa cells treated with 5-FU (grey bars), tested at three different cell population densities \pm STD: (a) 50,000, (b) 100,000 and (c) 200,000/100uL for three different frequencies (1 KHz, 10 KHz, 100 KHz).

Figure 34 presented the results for HeLa cells when treated to the specific anticancer agent. As depicted, although for each population density a frequency-dependent pattern is observed, pure cells don't follow the same motif as mean impedance value drops at the population of 50,000 cells/100uL. The behaviour of the impedance response varies as at the population of 100,000 cells/100uL the impedance follows a non-linear pattern and also at the last population density tested impedance keeps an increasing trend. Again, in almost all instances the response of the mean

impedance when cells are treated with 5-FU has a considerably higher value compared to the control solution, as seen in Table 20. There is only one exception regarding two population densities (50,000 and 200,000 cells/100uL) in the frequency of 100 KHz, where low impedance values were observed with or without the presence of the specific anticancer agent.

Table 20. Significant differences in cell impedance among cell population combinations for the HeLa cell line with or without the presence of 5-FU (* < 0.05, ** < 0.01, *** < 0.001)

| | Cell population combination | | | Cell population combination with the application of 5-FU | | |
|-------------------|-----------------------------|--------|---------|--|--------|---------|
| | 1 KHz | 10 KHz | 100 KHz | 1 KHz | 10 KHz | 100 KHz |
| 50,000 – 100,000 | *** | *** | * | *** | *** | ** |
| 50,000 – 200,000 | *** | ** | *** | - | *** | *** |
| 100,000 – 200,000 | * | *** | *** | *** | *** | *** |

Figure 35 presented the results for the last cell line tested (MCF-7). As it can be seen, high impedance values are illustrated with the addition of 5-FU for each cell population compared to pure cells, particularly at 1 KHz. These values are considered significant as they increase with the increase of population density (Table 21). In the case of the cells without the presence of the 5-FU, impedance values displayed low alterations among various cell populations. In general, the normalized impedance values decrease with the increase of the frequency magnitude.

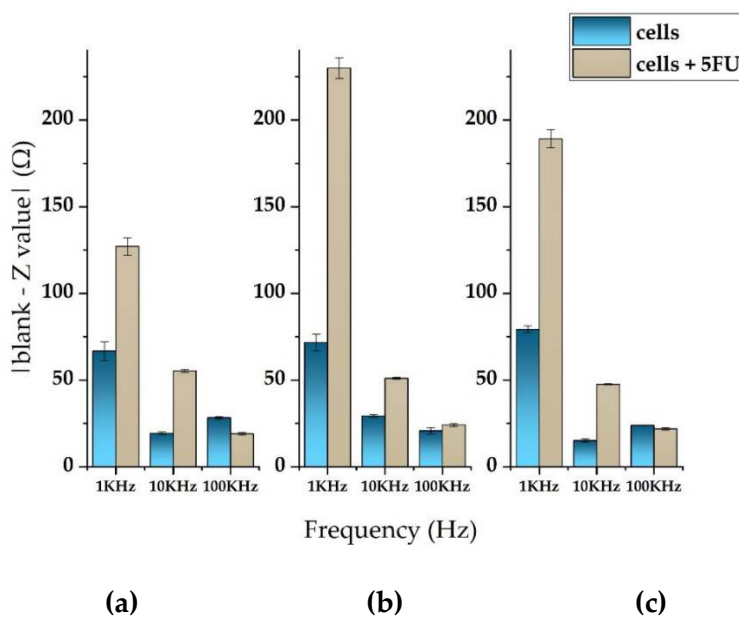


Figure 35: Normalized values of the mean impedance magnitude for control immobilized MCF-7 cells (blue bars) and immobilized MCF-7 cells treated with 5-FU (grey bars), tested at three

different cell population densities \pm STD: (a) 50,000, (b) 100,000 and (c) 200,000/100uL for three different frequencies (1 KHz, 10 KHz, 100 KHz).

Table 21. Significant differences in cell impedance among cell population combinations for the MCF-7 cell line with or without the presence of 5-FU (* < 0.05, ** < 0.01, *** < 0.001)

| | Cell population combination | | | Cell population combination with the application of 5-FU | | |
|-------------------|-----------------------------|--------|---------|--|--------|---------|
| | 1 KHz | 10 KHz | 100 KHz | 1 KHz | 10 KHz | 100 KHz |
| 50,000 – 100,000 | - | *** | ** | *** | *** | *** |
| 50,000 – 200,000 | ** | *** | *** | *** | *** | *** |
| 100,000 – 200,000 | * | *** | * | *** | *** | ** |

6.4. Discussion

Till now, for the performance of either historic and/or pathologic analysis, the direct tumour biopsies could initially control the development of cancer diagnostics. Novel advanced molecular biology methods including genomics bioinformatics analysis and next-generation DNA sequencing have been developed for the transition from conventional microscopy of tissue samples to molecular genomics for the identification of cancer. These current novel techniques combined with the outstanding advances in drug development and effectiveness contributed to the beginning of an era relevant for personalized cancer identification and treatment. Hence, the advances regarding cancer management and therapy made vital the need for the pursuit of avant-garde non-invasive approaches in order to implement precise detection and monitoring.

In this regard, the investigation of the alterations between the electric properties of various in vitro 3D cancer cell cultures, including breast, kidney, and cervical tumour models was studied in this work. Mainly, because of the further dimensionality of 3D culture in comparison with the 2D culture [241], numerous alterations are observed in cell activities considering proliferation, morphology, and protein and gene expression. Hydrogels, for instance, collagen (COL), alginate (SA), and agarose (AG) have gained more attention as they promise to provide matrices for bio-inks due to their low cytotoxicity, native biocompatibility, and high water content [95, 242, 243]. The application of SA as a bio-ink for cells is due to the fact that it allows quick gelling in the presence of Ca²⁺ or additional cations as well as it can be simple and fast encapsulated and interlayer attached during the layer-by-layer printing procedure [244-246].

An optical inverted microscope was used for the observation of alterations in cell morphology among the four various cell lines after conducting the MTT colorimetric assay [205]. Many studies reported similar results related to epithelial cancer cells in 3D culture [247-249]. The results in this work demonstrated no significant changes in the cell viability regarding the immobilization matrix. Moreover, an increase in cellular proliferation considering the cell population density was indicated from the photometric MTT determination. However, the addition of the anticancer agent 5-fluorouracil (5-FU) displayed a decrease in the cell viability, which means that the influx of the compound in the SA is not affected by the 3D immobilization matrix.

The completion of the biochemical cytotoxic assays was followed by the performance of an impedance spectroscopic analysis on every cancer cell line in combination with the respective electrodes in the 3D alginate matrix. A methodology that unifies various spectral impedance measurement methods in order to provide significant information about the relevant characteristics of cancerous cell cultures was presented. The proposed protocol was split into two cases depending on the various aspects of the cell cultures for investigation. In the first case, the record of impedance measurements was implemented related to various cell population densities of the previously described cell lines in 3D cultures in plain medium, whereas in the second case, the corresponding impedance measurements were recorded for regarding the 3D cell cultures after the application of the anticancer agent 5-FU for 24h.

In order to determine the contrasts among the unique cell lines, the extracted characteristic features were used by means of normalized impedance magnitudes. This technique has been notably efficient for the cytotoxic impact of the anticancer compound along with the discrimination of cells derived from different tissue origin. Valuable information can be obtained by this technique since the assay provides significant information concerning the response of the cells when a particular frequency spectrum is applied, allowing researches to use it as an alternative cancer diagnostic method. This methodology could be optimized by further research related to additional cell lines, normal or cancer ones. Analogous studies have been carried out on breast [147], skin [250], cervical [224], and esophagus cancer cells [251].

In this chapter, a discrimination technique was proposed for the performance of a measurement process and data processing, methods that are quite simple to handle, despite the fact that obtained samples by invasive means are required in order to use this technique for cancer diagnosis or evaluation of effective

chemotherapy treatment. However, in many instances, the evaluation of a real tissue sample is based on a definite diagnosis of a malignant tumour. Despite that, although a small number of cells (e.g., obtainable through liquid biopsy) was tested, the results of this study could be evaluated by EIS for the performance of their bioelectric profile regarding their susceptibility to chosen anticancer agents.

In order to analyse the electrical properties of various cell types, frequencies from 1 KHz up to 100 KHz were tested. At the frequency of 1 KHz, especially high impedance normalized values were obtained for both treated and non-treated cells with 5-FU in almost all cell types. Taking into account the abovementioned frequency range, the properties of either plain cell culture medium and / or the specific anticancer drug seemed to be affected by the cell-hydrogel interface considering the relevance of the contribution of the cell structure. Therefore, the detection sensitivity might have a vital role in the cell structure. In cancerous tissues, at frequencies higher than 1 KHz a decrease of the impedance has been detected, whereas there are no alterations observed in the frequency range up to 100 KHz [252]. Moreover, lower impedance values have been reported in abnormal tissues including breast cancer tissue [253], in comparison with healthy tissues [254].

6.5. Conclusions

In this chapter, the development of a supplementary non-invasive cell analysis technique was reported in order to evaluate the responses of 3D cultured cancer cell lines that come from different tissues after the application cytotoxic concentrations of a commonly used anticancer agent 5-FU by the use of electrical impedance spectroscopy. 3D printed PETG well assembled with two perpendicular gold-coated electrodes placed on the top of the structure constitutes the key element of the proposed cell-based impedance sensor. The assessment of our cell bio-system configuration presented considerable efficiency regarding various cell type determination with sufficient sensitivity. For the optimization of both sensitivity and selectivity depending on very low cell population densities (up to single-cell analysis), the fabrication of a novel electrode configuration, for instance screen-printed, is required for the implementation of single-cell impedance spectroscopy [255-257].

Chapter 7: Summary – Discussion

Toxicology, commonly described as the “science of safety”, constitutes the scientific investigation of the harmful effects that appear in living organisms with the presence of chemicals. Generally, it involves detection mechanisms and treatments of toxic substances along with pharmaceutical compounds applied for medical use. The field of the sensors research has gained great interest since 1980. Many scientists, taken advantage of the progress in material science, engineering, and computer technology, have been focused on the development of a variety of sensors for various applications, including clinical, industrial, and environmental applications. The device that creates an electrical signal caused by the response of an applied stimulus gives the main description of a sensor. The type of stimulus can vary because of the wide range in the sensor’s control (e.g., optical, chemical, biological, mechanical, etc.).

Electrochemical Impedance Spectroscopy (EIS) is a technique that depends on the principle of the application of a small excitation signal to an electrochemical system, and it involves the preparation of the electrodes for various sensors and device assemblies. In literature, it is commonly described as a non-invasive, conventional, and user-friendly method. The study of interfacial characteristics that are connected to bio-recognition events is mostly performed by EIS. For AC impedance measurements, the three basic requirements are causality, linearity, and stability. The accuracy of the impedance measurement procedure is related to the technical precision of the instrumentation as well as to the operating processes.

Electrical impedance spectroscopy (EIS) is mostly applied as an impedance – based non-invasive material characterization method in numerous fields of technology, engineering, and applied sciences, as it focuses on the frequency response of the electrical impedance of the sample tested [258]. The characterization of biological cells, cell culture monitoring, and tissue engineering are typical examples that EIS has been applied lately [115, 126, 154, 259-266]. The application of the electric field with high voltage pulses can lead to a breakdown in the cell membrane that causes alterations in the resistivity and integrity of the cell membrane [263]. The impedance spectrum can be influenced by the properties of the cell membrane, as well as by intra and extracellular spaces. Hence, information regarded to the quantitative alterations of cells (e.g. cell population) is provided by the measurement of electrical impedance of a volume of a biological tissue across a frequency range [264].

Impedance spectroscopy constitutes a technique used in order to monitor the differentiation and the growth of stem cells in various tissue engineering applications, such as the study of the development of Human mesenchymal stem

cells [118, 267]. By the use of EIS, an important increase in the value of the measured impedance magnitude of osteogenic treated human mesenchymal stem cells is observed compared to the control samples [118]. EIS is used in additional applications, including the number and classification of cell type and shape, and the quantification of cell size [157, 268], the real-time monitoring of cell attachment and spreading on substrates as well as the study of alterations in endothelial monolayers [269]. Information related to cell toxicity, and cell inflammation or invasion can be obtained from this technique. Another application of EIS includes the characterization of cell suspensions in a bioreactor or a cell monolayer [265, 266], which points to the evaluation of the effect of growth factors and culture medium on cell differentiation [157, 268].

Biological tissues constitute three dimensional materials that are mostly developed with biological cells. These cells are developed with intracellular fluid, surrounded by the cell envelope. In addition, cells are organized in a 3D structure and their suspension can be obtained in extracellular fluid [49, 270-272]. When an alternating electrical excitation signal is applied, the cell membrane provides some capacitance, where both intracellular and extracellular fluids give low resistive properties [49, 273]. Hence, under an alternating electrical excitation signal, a biological cell surrounded by the extracellular fluid provides a complex electrical impedance. This electrical impedance can be defined as bioelectrical impedance, also known as bioimpedance [49]. In general, bioimpedance is described as the method which allows the biological tissue to oppose electrical current. The detection of the response to electric excitation which is applied to a biological tissue can be implemented by bioimpedance measurements. Valuable information can be obtained from impedance measurements concerning the tested sample. In particular, the impedance properties of biological cells have a great impact on the investigation of the cells themselves. The tissue anatomy, the tissue composition as well as the frequency of the applied excitation signal are the main parameters that the electrical impedance of the biological tissue depends on [49]. Furthermore, the bioimpedance values vary with the frequency of the applied signal, as the capacitive reactance of the membrane is frequency – dependent. As a result, frequency affects the current penetration as well as the conduction paths to a large extent [273].

In order to develop tissue-engineered constructs, non-invasive, and real-time monitoring and characterization are crucial factors. This evaluation procedure becomes more difficult due to the complex structure of 3D cell cultures. Many researchers have studied every possible way to find the reliable non-invasive method in order to examine the properties of various tissue-engineered cell cultures

as well as for various research objectives, for instance, evaluation stem cell differentiation protocols [120, 148, 160, 274]. Optical techniques based on light absorbance, fluorescence, and scattering are techniques for cell suspensions, but it is hard to be incorporated for evaluations of cells in microporous scaffolds [275]. For its evaluation, scanning electron microscopy needs slide cuts of the cell culture so it can be disastrous to the tissue engineered construct. Despite the fact that magnetic and nuclear resonance imaging offer a reliable monitoring technique, both are expensive and of low portability and also, they can injure the cell culture because of their ionizing nature [276]. Based on capacitance measurements, the biomass monitor is a useful technique for monitoring immobilized cells in bioreactors, yet because of its design, measurements within microporous scaffolds are not feasible [277].

Therefore, for the evaluation of cell growth, indirect techniques that calculate the metabolic/protein content, for instance, the rate of oxygen-uptake, ATP, or DNA are being applied. Such indirect techniques including MTT assay that ends up in cell death as well as Alamar blue dye are examples of indirect measurements applied for the evaluation of cytotoxicity [278], though they need to be performed in various phases and they are not suitable for on-line monitoring of cell cultures. However, electrical impedance measurements constitute a simple and reliable technique for the evaluation and characterization of cell cultures, including shape and size, the status of intra and extracellular media, and the state of cell membranes [110, 154]. Small alterations in the electrical properties can be observed because of the nature of the impedance measurement technique [114]. For instance, impedance measurements have been applied for continuous monitoring of tissue spheroids [148, 279, 280], along with proliferation [148], the estimation of the cell size [279, 280], the cell viability [281, 282], and the evaluation of cell concentration [283]. Moreover, this technique has been applied for monitoring cells behaviour by attaching cells to a substrate [284], applying bulk [285] or thin-film electrodes, on trapped single cell [286], or on cells in suspension [287].

A specific environment for cell cultures can be provided from microsystems where the non-invasive monitoring of cell behaviour by applying electrical methods is feasible [288, 289]. Monitoring cellular functions including cell growth and cell death [290], counting and discrimination of cell population [291, 292], cell cycle [293], and detecting alterations in electrical properties of cells [294, 295] are applications that can be performed by these microsystems. As a result, the impedance measurement is a reliable and non-disastrous method used for monitoring the behaviour of cell cultures with a high temporal resolution.

Electrical cell-substrate impedance sensing (ECIS) is mostly used as a real-time and label-free technique for the characterization of the cellular behaviour and the responses of the cells when drugs are applied to the cells. It allows fast and precise drug screening as it provides valuable information regarding cell proliferation, migration, differentiation, apoptosis, adherence, and necrosis, as well as therapeutic investigations of neuroprotective consequences [296, 297].

There are two ways that the ECIS measurement process can be performed. In the first one, a current is applied at a specific frequency and the impedance of the cell-covered electrode is measured. Hence, the magnitude and phase of the voltage as a function of time can be observed. The results provided information related to cells' morphological alterations and metabolic activities [159, 298]. In the second one, the measurement process of the impedance of the electrode covered with cells is performed at a different frequency range. The results provided information related not only to cells grown on the electrode's surface but also to the resistance of the cell barriers and capacitance of the cell membranes [159, 299, 300]. Valuable information about the dynamic properties of the cells grown on the surface of the electrode can be obtained by ECIS. In addition, spreading, density, cell adhesion, and barrier function including cell micromotion and motility can be examined by this technique [163, 301].

In literature, many researchers have used impedance measurements for their research, as this method can be applied in many fields, for instance, body fat calculation [302], characterization of cells [297], biomedical applications [303], diagnosis of pre-malignant and malignant conditions [304], discovery of modulators of intraocular pressure [305], etc. There are multiple of choices regarding impedance analysers and meters that can be utilized for the respective measurements. Impedance spectrum analysers perform the impedance process in real-time and allow the extraction of numerous parameters in a wide frequency spectrum (from Hz to GHz) with high accuracy [306]. The use of such devices allows adjusting the excitation signal (current, voltage) applied to the sample for test.

Handheld impedance meters constitute an alternative for the impedance measurements, as they are rapid, cost-effective and easy-to-use devices. The user-friendly software allows the user to plan their experiment by means of many factors, such as the number of intervals, frequency, extracted parameters etc. In our methodology, for every experimental procedure, the impedance measurements were performed by using a handheld LCR meter provided by Keysight Technologies (CA, USA). The utilization of such instrument can provide valuable information about the resistance, the capacitance, the inductance, or the total impedance of the sample

under test. Despite the fact that most handheld meters are cheap and fast operating, they are limited considering the frequency range (only five preselected frequencies) and the extracted results (only one parameter extracted per run).

In the first section, the study for the impedance analysis regarding mammalian neuroblastoma N2a cells treated to different dopamine concentrations was presented. A comparison with previous studies showed the importance of the cells' immobilization using a 3D matrix. The obtained results highlighted that for the impedance measurements, the cells' immobilization regimes are crucial, considering the reaction of the electrical response of the cell medium when a frequency is applied. In particular, the 3D immobilization matrix provides better resolution in higher frequencies, whereas in lower frequency range, the alterations of the impedance values are considered minimal, due to the effect from the medium.

Furthermore, in all frequencies tested, when lower DA concentrations are applied to the cell culture, although the control solution seems to dominate, the mean impedance magnitude has higher values. In the 1000uM DA concentration, the system enters saturation when cells are 3D immobilized. Regarding the cell suspension, the impedance responses are between 400 – 1050 Ohm, when the respective 3D case provided lower responses (from 350 to 950 Ohm). In both DA cases (suspension and 3D immobilized), the solution appeared to have approximately the same response values between 400 – 1600 Ohm, following almost the same pattern. The electrical response interferes with the absorption of dopamine from cells and can be applied for medical assessment (e.g., schizophrenia, Parkinson's disease, etc.). Moreover, this methodological approach can be further improved considering the effects of the electrode material, various immobilization matrices, in conjunction with the frequency range, especially in lower frequencies. An optimized impedimetric system can be developed for immobilized cells in order to analyze various types of target analytes with bioactive properties.

The second section included an impedance analysis on cell cultures carried out on a 3D printed well. More specifically, N2a neuroblastoma cells were immobilized in two different immobilization matrices (2D and 3D) in a custom-made PETG 3D printed well, involving two silver vertically-placed electrodes. For every cell solution, DA was applied in various concentrations. The application of a frequency proved the significant role of the impedance under various cell immobilization regimes. The impedance measured in the 3D cell immobilization indicated lower values as the concentration increases, whereas larger values were obtained in the 2D cell immobilization with the increase of the concentration.

In order to enhance the attachment on the electrodes, PLL was chosen as a 2D immobilization matrix as it improves the functionality of the cell culture, providing a beneficial microenvironment [307]. For all the frequencies chosen, an increase in impedance was due to the reaction of the cells immobilized in PLL to dopamine molecules. The extracted results from the cell medium in a specific frequency range displayed the significance of the impedance measured in cell immobilization matrices. In particular, in the 100 Hz and 120 Hz frequencies, the impedance responses follow the same pattern.

Although the impedance responses increase in the 2D immobilization matrix, they converge up with the respective 3D at the DA concentration of 10 μ M. Regarding 3D immobilization, the impedance values have range from 150 up to 750 Ohm and drop from the 100 μ M DA concentration. However, the opposite behaviour is observed in the PLL immobilization case, where the impedance has same value range and increasing as the concentration increases, intensively in lower frequencies. In order to investigate further frequency characteristic patterns, nM and μ M DA concentration levels were tested for the 3D and 2D immobilization matrices respectively. In particular, in the nM DA case, there is a linear drop up to 50nM in almost all frequencies, whereas, in the respective μ M DA range, the impedance appeared to be concentration-dependent, especially in frequencies below 10 KHz. The optimization of the proposed immobilized system can be improved by investigating further a wider frequency spectrum, particularly for lower frequencies. This study can be of a great impact in order to analyse different analytes with bioactive properties.

The last section of the thesis reported a supplementary non-invasive cell analysis method that was developed for the evaluation of the responses of 3D immobilized cancer cell lines derived from various tissues (SK-N-SH, HEK293, HeLa, and MCF-7) after treated with cytotoxic concentrations of an anticancer agent. More specifically, all cancer cell types were immobilized in calcium alginate matrix in several population densities (50,000, 100,000, and 200,000 cells/100 μ L). For the investigation of the ability of the proposed methodology to determine the effect of chemotherapeutic schemes, 5 – fluorouracil (5-FU) was applied to every cell culture as a chemotherapeutic agent. All cancer cell lines and populations were measured before and after the treatment of 5-FU.

For the impedance measurements, the proposed cell-based impedance sensor was utilized, consisting of two parts. The top part included two gold-coated electrodes placed perpendicularly on the top of the system where the bottom part was constituted by a custom-made 3D printed PETG well. The evaluation of this cell-

based bio-system configuration introduced a significant efficacy related to different cell type determination with good sensitivity. Considering the evaluation of the cell viability, the microscopical results after the MTT application showed that the immobilization matrix combined with the increase in the cell population density does not indicate any contribution to the cellular proliferation. However, taking into account the increase in the cell population, the respective photometric results illustrated an increase in the absorbance, despite the fact that the cells' viability considerably dropped in almost all the cell lines after the application of 5-FU. The prospect of the performance of a complementary assay on in vivo samples could be assessed by additional investigations.

Our attention was concentrated on the fact that during the whole measurement process, the extracted results could initiate the highlighting of the diversities in the electrical behaviour of pure and cancerous 3D cell cultures. In particular, the results of the SK-N-SH cell line showed a decrease in the normalized impedance with the increase of the population density. Although HEK293 cancer cells followed a similar motif, the population of 200,000 cells/100uL gave the higher impedance value. Both HeLa and MCF-7 cancer cell lines presented totally different behaviours. In the HeLa case, the measured impedance decreased dramatically with the increase in the cells' population, whereas in the MCF-7 case, a completely reversed motif was observed, giving with the higher impedance value for the 200,000 cells population.

The 24h application of the anticancer agent 5-FU demonstrated higher values considering the normalized impedance for most of the cases, in comparison with untreated cell cultures. The SK-N-SH cell line presented a reversed pattern after the application of 5-FU, particularly in the frequency of 1 KHz. In the case of HEK293 with the addition of 5-FU, the impedance again drops with the increase of the frequency in every cell population measured, however with some exceptions where the control solutions gave higher values in the higher frequencies for 50,000 and 200,000 cells/100uL. Despite the fact that in the HeLa cell culture a frequency-dependent motif was followed, the impedance responses at 100,000 cells/100uL don't follow a linear pattern. MCF-7 cancer cell line gave higher impedance values for every population tested compared to the respective pure cells, especially for the lower frequency of 1 KHz. Generally, in almost all cases, the increase in the frequency range was followed by the decrease in the normalized impedance.

The evaluation of additional heterogeneous models with further characteristics including capacitance or resistance could contribute in order to improve the resolution capacity of the system. Despite the fact that the proposed

methodology was successful in the determination of various cancer cell lines, the adjustment of cancer cells can specify their existence in cocultures with normal ones by using suitably placed electrodes in a single well. Furthermore, in order to improve the selectivity as well as the sensitivity of the sensor configuration on the basis of low cell populations up to single-cell analysis, a novel electrode assembly could be designed.

The innovations and development of this thesis focus on the cell growth conditions, cell population and proliferation, emphasizing the similarities and differences between 2D and 3D cell culture systems. In particular, both above-mentioned cell culture systems were carried out and measured in terms of impedance, providing significant information regarding the differentiation and growth of each cell culture tested. By applying electrical impedance measurements, significant alterations in the measured impedance value (increasing or decreasing) of various cell types, including cancer cell lines were obtained, compared to the control solutions. Although, 3D cultures appear to be complicated for cells, a high-resolution screening could be the solution for this type of cell culture. Moreover, electrical sensing constitutes another alternative for both 2D and 3D cell cultures, in order to obtain real-time, dynamic and label-free monitoring of cells [308].

3D printing was used as a cheap and rapid technology in order to construct a custom-made well for the cell culture, allowing the design of any kind of structure based on the experiment's needs. A PETG-based material was chosen due to its stability and biocompatibility, thus being able to mimic environmental conditions. In all experimental configurations, the electrodes were placed perpendicularly in order to have direct contact with the cell culture. An issue that still remains is the suitable electrode system, by means of material, size, shape, etc. It has been mentioned that the continuous use of Ag electrodes cannot provide reliable measurements [309]. Hence, Ag electrodes were replaced by Au-coated electrodes as they are characterized by thermodynamic stability [310].

Based on the number of electrodes, the most common-used electrode configurations for bio-impedance measurements are two and four electrode setups. The two-electrode configuration which measures the voltage at the same current injection electrodes, was utilized in this study in order to monitor and measure the cell cultures by means of electrochemical impedance spectroscopy (EIS). However, as the electrode-medium is connected in series with the bio-impedance, significant errors might occur. A four-electrode setup gives the solution to this problem, as the external electrodes are used for the current injection and the internal for the voltage measurement [309].

A recent publication [311] presented an evaluation of various cancer cell lines by using four-electrode configuration and measuring the impedance in various frequencies. Four cancer cell lines were cultured in two population densities and measured with or without the application of the anticancer agent doxorubicin. In this study, the limitation on the frequency range (especially below the 1 KHz) was overcome, due to the implementation of a custom-made electronic circuit able to perform real-time frequency sweep (increasing and decreasing). The results indicated a drop in the impedance as the frequency increases. When cells were treated with the chemotherapeutic agent, each cell line demonstrated a different behaviour. Each cancer cell type can provide a signature in order to detect their response to the anticancer agent again by means of non-invasive cell status monitoring.

To sum up, the bio-impedance measurements can reveal significant information relating to the electrical and mechanical properties of the cells, including motility, activity, viability and growth [312, 313]. In the cell cultures, the detection of interactions with drugs [314] and the in vivo investigation of cancer models [309, 315] can be performed by bio-impedance measurements. The results of bio-impedance measurements were presented in this thesis, providing significant information regarding every cell culture tested, especially for the cancer cell lines after the treatment with the anticancer agent. This can lead to a dependent relationship between the bio-impedance values and the frequency, which can give valuable information about the pathology and physiology of the cells and tissues.

References

1. F.S. Collins, G.M. Gray, and J.R. Bucher, *Toxicology. Transforming environmental health protection*. Science 2008. **319**(5865): p. 906-907.
2. A. Manciocco, G. Calamandrei, and E. Alleva, *Global warming and environmental contaminants in aquatic organisms: the need of the etho-toxicology approach*. Chemosphere 2014. **100**: p. 1-7.
3. R.R.M. Paterson and N. Lima, *How will climate change affect mycotoxins in food?* Food Research International, 2010. **42**: p. 1902-1914.
4. UN, *Back to our common future sustainable development in the 21st century (SD21) project Summary for policymakers*. 2015.
5. S. Adler, et al., *Alternative (non-animal) methods for cosmetics testing: current status and future prospects*. Archives of Toxicology, 2011. **85**(5): p. 367-485.
6. P. Jennings, et al., *SEURAT-1 liver gold reference compounds: a mechanism-based review*. Archives of Toxicology, 2014. **88**(12): p. 2099-2133.
7. T.B. Knudsen, et al., *FutureTox II: in vitro data and in silico models for predictive toxicology*. Toxicological Sciences, 2015. **143**(2): p. 256-267.
8. U. Gundert-Remy, et al., *Toxicology: a discipline in need of academic anchoring--the point of view of the German Society of Toxicology*. Archives of Toxicology, 2015. **89**(10): p. 1881-1893.
9. I.A. Ramoutsaki, et al., *The roots of toxicology: An etymology approach*. Veterinary and human toxicology 2000. **42**: p. 111.
10. Bailey, M.D., *Magic and Superstition in Europe: A Concise History from Antiquity to the Present*. 2007, New York: Rowman and Littlefield Publishers.
11. A.N. Hayes and S.G. Gilbert, *Historical milestones and discoveries that shaped the toxicology sciences*. Molecular, Clinical and Environmental Toxicology, 2009. **1**: p. 1-35.
12. Hutchinson, J., *Words to the wise: Poison arrows*. The British Medical Journal, 1997. **314**(7082).
13. L.B. Kinter and J.P. Valentin, *Safety pharmacology and risk assessment*. Fundamental and Clinical Pharmacology, 2002. **16**(3): p. 175-182.
14. Pugsley, M.K., *Methodology used in safety pharmacology: appraisal of the state-of-the-art, the regulatory issues and new directions*. Journal of Pharmacological and Toxicological Methods, 2005. **52**(1): p. 1-5.
15. M.K. Pugsley, et al., *Innovation in safety pharmacology testing*. Journal of Pharmacological and Toxicological Methods, 2011. **64**(1): p. 1-6.
16. P.Y. Muller and M.N. Milton, *The determination and interpretation of the therapeutic index in drug development*. Nature Reviews Drug Discovery, 2012. **11**(10): p. 751-761.
17. Hahn, A., *Poison control centers*, in *Information resources in toxicology*, P. Wexler, et al., Editors. 2009, Elsevier: Amsterdam. p. 701-710.
18. D. Müller and H. Desel, *Common causes of poisoning: etiology, diagnosis and treatment*. Deutsches Ärzteblatt International, 2013. **110**(41): p. 690-699.
19. H. Barth and B.G. Stiles, *Binary actin-ADP-ribosylating toxins and their use as Molecular Trojan Horses for drug delivery into eukaryotic cells*. Current Medicinal Chemistry, 2008. **15**: p. 459-469.

20. M.E. Sutter, et al., *The role of clinical toxicologists and poison control centers in public health*. American Journal of Preventive Medicine, 2010. **38**(6): p. 658-662.
21. G.W. Gibbs and C.Y. Hwang, *Dimensions of airborne asbestos fibres*. IARC Scientific Publications, 1980. **30**: p. 69-78.
22. W.N. Rom, W.D. Travis, and A.R. Brody, *Cellular and molecular basis of the asbestos-related diseases*. The American Review of Respiratory Disease, 1991. **143**: p. 408-422.
23. T. Gebel, et al., *Manufactured nanomaterials: categorization and approaches to hazard assessment*. Archives of Toxicology, 2014. **88**: p. 2191-2211.
24. G.E. Johnson, et al., *Non-linear dose-response of DNA-reactive genotoxins: recommendations for data analysis*. Mutation Research, 2009. **678**: p. 95-100.
25. A. Oberemm, et al., *Toxicogenomic analysis of N-nitrosomorpholine induced changes in rat liver: comparison of genomic and proteomic responses and anchoring to histopathological parameters*. Toxicology and Applied Pharmacology, 2009. **241**(2): p. 230-245.
26. H.M. Bolt, et al., *Carcinogenicity categorization of chemicals-new aspects to be considered in a European perspective*. Toxicology Letters, 2004. **151**: p. 29-41.
27. R.C. Hertzberg, et al., *A four-step approach to evaluate mixtures for consistency with dose addition*. Toxicology, 2013. **313**(134-144).
28. A. Kortenkamp, et al., *Investigation of the state of science on combined actions of chemicals in food through dissimilar mode of actions and proposal for science-based approach for performing related cumulative risk assessment*, in *Scientific Report submitted to EFSA Supporting Publications 2012*. 2012. p. 232.
29. S. Ermler, M. Scholze, and A. Kortenkamp, *Genotoxic mixtures and dissimilar action: concepts for prediction and assessment*. Archives of Toxicology, 2014. **88**(3): p. 799-814.
30. D.J. Carlin, et al., *Unraveling the health effects of environmental mixtures: an NIEHS priority*. Environmental Health Perspectives, 2013. **121**(1): p. a6-a8.
31. M.T. Heneka, et al., *Neuroinflammation in Alzheimer's disease*. The Lancet Neurology, 2015. **14**: p. 388-405.
32. W.M.S. Russell and R.L. Burch, *The Principles of Humane Experimental Technique 1959*, London: Methuen Publishing.
33. K. Takahashi, et al., *Induction of pluripotent stem cells from adult human fibroblasts by defined factors*. Cell, 2007. **131**(5): p. 861-872.
34. A. Wilmes, et al., *Application of integrated transcriptomic, proteomic and metabolomic profiling for the delineation of mechanisms of drug induced cell stress*. Journal of Proteomics, 2013. **79**: p. 180-194.
35. P. Jennings, et al., *An overview of transcriptional regulation in response to toxicological insult*. Archives of Toxicology, 2013. **87**: p. 49-72.
36. J.G. Teeguarden, et al., *Comparative iron oxide nanoparticle cellular dosimetry and response in mice by the inhalation and liquid cell culture exposure routes*. Particle and Fibre Toxicology, 2014. **11**(46).
37. W.J. Wills, et al., *Genetic toxicity assessment of engineered nanoparticles using a 3D in vitro skin model (EpiDerm™)*. Particle and Fibre Toxicology, 2016. **13**(50).
38. A. Casey, et al., *Chemotherapeutic efficiency of drugs in vitro: Comparison of doxorubicin exposure in 3D and 2D culture matrices*. Toxicology in Vitro, 2016. **33**: p. 99-104.
39. N. Alépée, et al., *State-of-the-art of 3D cultures (organs-on-a-chip) in safety testing and pathophysiology*. ALTEX 2014. **31**(4): p. 441-477.
40. R. Lehmann, et al., *Biomek Cell Workstation: A flexible system for automated 3D cell cultivation*. Journal of Laboratory Automation, 2016. **21**: p. 568-578.

41. S.P. Zustiak, et al., *Three-dimensional matrix stiffness and adhesive ligands affect cancer cell response to toxins*. *Biotechnology and Bioengineering*, 2016. **113**: p. 443-452.
42. W. Feng, et al., *Human normal bronchial epithelial cells: a novel in vitro cell model for toxicity evaluation*. *PLoS One* 2015. **10**: p. e0123520.
43. G. Pomponio, et al., *Amiodarone biokinetics, the formation of its major oxidative metabolite and neurotoxicity after acute and repeated exposure of brain cell cultures*. *Toxicology in Vitro*, 2015. **30**: p. 92-202.
44. J.M. Kelm and R. Marchan, *Progress in 'body-on-a-chip' research*. *Archives of Toxicology*, 2014. **88**(11): p. 1913-1914.
45. C. Rovida, et al., *Integrated testing strategies (ITS) for safety assessment*. *ALTEX*, 2015. **31**(1): p. 25-40.
46. Regan, F., *Sensors Overview*. Reference Module in Chemistry, Molecular Sciences and Chemical Engineering, 2018.
47. Vadgama, P., *Membrane based sensors: A review*. *Journal of Membrane Science*, 1990. **50**: p. 141-152.
48. Kintzios, S., *Bioelectric Sensors: On the Road for the 4.0 Diagnostics and Biomedtech Revolution*. *Biosensors*, 2020. **10**(96).
49. Bera, T.K., *Bioelectrical Impedance Methods for Noninvasive Health Monitoring: A Review*. *Journal of medical engineering*, 2014. **38**1251.
50. L.M.S. Nascimento, et al., *Sensors and Systems for Physical Rehabilitation and Health Monitoring - A Review*. *Sensors* 2020. **20**: p. 4063.
51. J.Liu, et al., *Recent Progress in Flexible Wearable Sensors for Vital Sign Monitoring*. *Sensors* 2020. **20**: p. 4009.
52. S. Brosel-Oliu, et al., *Impedimetric transducers based on interdigitated electrode arrays for bacterial detection - A review*. *Anal Chim Acta*, 2019. **1088**: p. 1-19.
53. M.I. Neves, L. Moroni, and C.C. Barrias, *Modulating Alginate Hydrogels for Improved Biological Performance as Cellular 3D Microenvironments*. *Frontiers in Bioengineering and Biotechnology*, 2020. **8**: p. 665.
54. K.P. Ferentinos, et al., *Pesticide residue screening using a novel artificial neural network combined with a bioelectric cellular biosensor*. *BioMed Research International*, 2013. **2013**: p. 813519.
55. G. Moschopoulou, et al., *Assessment of pesticides cytotoxicity by means of bioelectric profiling of mammalian cells*. *Environmental Nanotechnology, Monitoring and Management*, 2017. **8**: p. 254-260.
56. A. Kokla, et al., *Visualization of the membrane engineering concept: Evidence for the specific orientation of electroinserted antibodies and selective binding of target analytes*. *Journal of Molecular Recognition*, 2013. **26**: p. 627-632.
57. J.A. Dewey and B.C. Dickinson, *Split T7 RNA polymerase biosensors to study multiprotein interaction dynamics*. *Methods in Enzymology*, 2020. **641**: p. 413-432.
58. J. Wiechert, et al., *Inducible Expression Systems Based on Xenogeneic Silencing and Counter-Silencing and Design of a Metabolic Toggle Switch*. *ACS synthetic biology*, 2020. **9**(8): p. 2023-2038.
59. Kintzios, S., *Consumer Diagnostics*, in *Portable Biosensors and Point-of-Care Systems*, S. Kintzios, Editor. 2017, Institution of Engineering and Technology: London, UK. p. 309-331.

60. G.P. Kanakaris, C. Sotiropoulos, and L.G. Alexopoulos, *Commercialized point-of-care technologies*, in *Portable Biosensors and Point-of-Care Systems*, S. Kintzios, Editor. 2017, Institution of Engineering and Technology: London, UK. p. 256-330.
61. J. Guo, et al., *A photoelectrochemical biosensor for rapid and ultrasensitive norovirus detection*. *Bioelectrochemistry*, 2020. **136**: p. 107591.
62. S. Campuzano, et al., *Beyond sensitive and selective electrochemical biosensors: Towards continuous, real-time, antibiofouling and calibration-free devices*. *Sensors* 2020. **20**: p. 3376.
63. D. Rodrigues, et al., *Skin-Integrated Wearable Systems and Implantable Biosensors: A Comprehensive Review*. *Biosensors* 2020. **10**(79).
64. P. Yáñez-Sedeño, S. Campuzano, and J.M. Pingarrón, *Screen-Printed Electrodes: Promising Paper and Wearable Transducers for (Bio) Sensing*. *Biosensors* 2020. **10**(76).
65. P.A. Kramer, et al., *A review of the mitochondrial and glycolytic metabolism in human platelets and leukocytes: Implications for their use as bioenergetic biomarkers*. *Redox Biology*, 2014. **2**: p. 206-210.
66. T. Apostolou, et al., *Assessment of Cypermethrin Residues in Tobacco by a Bioelectric Recognition Assay (BERA) Neuroblastoma Cell-Based Biosensor*. *Chemosensors*, 2019. **7**(4): p. 58.
67. M.L. Zhang, et al., *Involvement of glutathione peroxidases in the occurrence and development of breast cancers*. *Journal of translational medicine*, 2020. **18**(1): p. 247.
68. S. Brassart-Pasco, et al., *Tumor Microenvironment: Extracellular Matrix Alterations Influence Tumor Progression*. *Frontiers in oncology*, 2020. **10**: p. 397.
69. L. Gao, et al., *Targeting ROS-Mediated Crosstalk Between Autophagy and Apoptosis in Cancer*. *Advances in experimental medicine and biology*, 2020. **1260**: p. 1-12.
70. S. Mavrikou, et al., *Detection of Superoxide Alterations Induced by 5-Fluorouracil on HeLa Cells with a Cell-Based Biosensor*. *Biosensors* 2019. **9**(126).
71. T. Apostolou and S. Kintzios, *Cell-to-Cell Communication: Evidence of Near-Instantaneous Distant, Non-Chemical Communication between Neuronal (Human SK-N-SH Neuroblastoma) Cells by Using a Novel Bioelectric Biosensor*. *Journal of Consciousness Studies*, 2018. **25**: p. 62-74.
72. S. Helali, et al., *A disposable immunomagnetic electrochemical sensor based on functionalised magnetic beads on gold surface for the detection of atrazine*. *Electrochimica Acta*, 2006. **51**: p. 5182-5186.
73. B. Rezaei, N. Askarpour, and A.A. Ensafi, *A novel sensitive doxorubicin impedimetric immunosensor based on a specific monoclonal antibody-gold nanoparticle-sol-gel modified electrode*. *Talanta*, 2014. **119**: p. 164-169.
74. P. Banerjee and A.K. Bhunia, *Mammalian cell-based biosensors for pathogens and toxins*. *Trends in Biotechnology*, 2009. **27**: p. 179-188.
75. B. He, et al., *Investigation of Pulsating Electrochemical Dissolution of Nickel in Rotating Processes*. *Journal of The Electrochemical Society*, 2019.
76. R.B. Figueira, et al., *Alcohol-Aminosilicate Hybrid Coatings for Corrosion Protection of Galvanized Steel in Mortar*. *Journal of The Electrochemical Society*, 2014. **161**(6): p. C349-C362.
77. E. Schindelholz, B.E. Risteen, and R.G. Kelly, *Effect of relative humidity on corrosion of steel under sea salt aerosol proxies: II. MgCl₂, artificial seawater*. *Journal of The Electrochemical Society* 2014. **161**(10): p. C460.

78. Y. Hoshi, et al., *Non-Contact Measurement to Detect Steel Rebar Corrosion in Reinforced Concrete by Electrochemical Impedance Spectroscopy*. Journal of The Electrochemical Society, 2019. **166**(11): p. C3316.
79. D.H. Xia, et al., *Detection of Atmospheric Corrosion of Aluminum Alloys by Electrochemical Probes: Theoretical Analysis and Experimental Tests*. Journal of The Electrochemical Society, 2019. **166**(12): p. B1000.
80. M. Whelan, et al., *Optimization of Anodic Oxidation of Aluminum for Enhanced Adhesion and Corrosion Properties of Sol-Gel Coatings*. Journal of The Electrochemical Society, 2016. **163**(5): p. C205.
81. D. Chung and B. Gray, *Editors' Choice—Development of Screen-Printed Flexible Multi-Level Microfluidic Devices with Integrated Conductive Nanocomposite Polymer Electrodes on Textiles*. Journal of The Electrochemical Society, 2019. **166**: p. B3116-B3124.
82. B.Suthar, et al., *Method to Determine the In-Plane Tortuosity of Porous Electrodes*. Journal of The Electrochemical Society, 2018. **165**(10): p. A2008-A2018.
83. F. Pogăcean, et al., *Graphene/TiO₂-Ag based composites used as sensitive electrode materials for amaranth electrochemical detection and degradation*. Journal of The Electrochemical Society 2018. **165**(8): p. B3054–B3059.
84. C.D. Lee, et al., *Low-Impedance, high surface area pt-ir electrodeposited on cochlear implant electrodes*. Journal of The Electrochemical Society 2018. **165**(12): p. G3015.
85. N.C. Hoyt, et al., *Electrochemical Impedance Spectroscopy of Flowing Electrosorptive Slurry Electrodes*. Journal of the electrochemical society, 2018. **165**(10): p. E439.
86. F. DeKu, et al., *Electrodeposited iridium oxide on carbon fiber ultramicroelectrodes for neural recording and stimulation*. Journal of The Electrochemical Society, 2018. **165**(9): p. D375.
87. P.F. Méndez, et al., *Voltammetric and Electrochemical Impedance Spectroscopy Study of Prussian Blue/Polyamidoamine Dendrimer Films on Optically Transparent Electrodes*. Journal of The Electrochemical Society, 2017. **164**: p. H85.
88. Nahir, T.M., *Impedance Spectroscopy: Theory, Experiment, and Applications*. 2nd ed. Vol. xvii. 2005, Hoboken, NJ: John Wiley & Sons, Inc.
89. K. Doi, et al., *Effects of Oxygen Pressure and Chloride Ion Concentration on Corrosion of Iron in Mortar Exposed to Pressurized Humid Oxygen Gas*. Journal of The Electrochemical Society, 2018. **165**(9): p. C582-C589.
90. E.B. Bahadır and M.K. Sezgintürk, *A review on impedimetric biosensors*. Artificial cells, nanomedicine, and biotechnology, 2016. **44**(1): p. 248-262.
91. R. Maalouf, et al., *Amperometric and impedimetric characterization of a glutamate biosensor based on Nafion and a methyl viologen modified glassy carbon electrode*. Biosensors and Bioelectronics, 2007. **22**: p. 2682-2688.
92. X. Yuan, et al., *Electrochemical Impedance Spectroscopy in PEM Fuel Cells Fundamentals and Applications* 2010, London: Springer-Verlag.
93. M. Amini, J. Hisdal, and H. Kalvøy, *Applications of bioimpedance measurement techniques in tissue engineering*. Journal of Electrical Bioimpedance, 2018. **9**: p. 142-158.
94. Y. Xu, et al., *A review of impedance measurements of whole cells*. Biosensors and Bioelectronics, 2016. **15**(77): p. 824-36.
95. S. Grimnes and O. Martinsen, *Bioimpedance & Bioelectricity Basics*. 3rd ed. 2014: Elsevier Science.
96. S.L.Tsai and M.H.Wang, *24-h observation of a single HeLa cell by impedance measurement and numerical modeling*. Sensor. Actuat. B-Chem., 2016. **229**: p. 225-231.

97. P.J.Kitson, et al., *Configurable 3D-Printed millifluidic and microfluidic 'lab on a chip' reactionware devices*. Lab Chip, 2012. **12**: p. 183267-71.
98. A.Waldbaur, et al., *Let there be chip—towards rapid prototyping of microfluidic devices: One-step manufacturing processes*. Analytical Methods, 2011. **3**: p. 2681–2716.
99. A.S.Munshi and R.S.Martin, *Microchip-Based Electrochemical Detection using a 3-D Printed Wall-Jet Electrode Device*. Analyst, 2016. **141**: p. 862-869.
100. R. Pethig and D.B. Kell, *The passive electrical properties of biological systems: Their significance in physiology, biophysics and biotechnology*. Physics in Medicine and Biology, 1987. **32**(933).
101. D. Miklavcic, N. Pavselj, and F.X. Hart, *Electric Properties of Tissues*, in *Wiley Encyclopedia of Biomedical Engineering*. 2006.
102. Schwan, H.P. *Electrical properties of tissue and cell suspensions: Mechanisms and models*. in *16th Annual International Conference of the IEEE Engineering in Medicine and Biology Society*. 1994. Baltimore, MD, USA.
103. U.G. Kyle, I. Bosaeus, and A.D.D. Lorenzo, *Bioelectrical impedance analysis part I: review of principles and methods*. Clinical Nutrition, 2004. **23**: p. 1226-43.
104. B. Alberts, A. Johnson, and J. Lewis, *Transport into the cell from the plasma membrane: Endocytosis*. 4th ed. Molecular Biology of the Cell. 2002: Garland Science.
105. Asami, K., *Characterization of heterogeneous systems by dielectric spectroscopy*. Progress in Polymer Science, 2002. **27**: p. 1617-59.
106. K. Heileman, J. Daoud, and M. Tabrizian, *Dielectric spectroscopy as a viable biosensing tool for cell and tissue characterization and analysis*. Biosensors and Bioelectronics, 2013. **49**: p. 348-59.
107. Riu, P.J., *Comments on "Bioelectrical parameters of the whole human body obtained through bioelectrical impedance analysis"*. Bioelectromagnetics, 2004. **25**: p. 69-71.
108. C. Gabriel, S. Gabriel, and E. Corthout, *The dielectric properties of biological tissues: I. Literature survey*. Physics in Medicine and Biology, 1996. **41**: p. 2231-49.
109. O. Martinsen, S. Grimnes, and H.P. Schwan, *Interface phenomena and dielectric properties of biological tissue*, in *Encyclopedia of Surface and Colloid Science*. 2002. p. 2643-53.
110. D.A. Dean, et al., *Electrical Impedance Spectroscopy Study of Biological Tissues*. Journal of Electrostatics, 2008. **66**(3-4): p. 165-77.
111. H. Kwon, et al., *A local region of interest imaging method for electrical impedance tomography with internal electrodes*. Computational and Mathematical Methods in Medicine, 2013. **9**.
112. J.K. Seo, et al., *Effective Admittivity of Biological Tissues as a Coefficient of Elliptic PDE*. Computational and Mathematical Methods in Medicine, 2013. **2**.
113. Schwan, H.P., *Electrical properties of tissues and cell suspensions* Advances in Biological and Medical Physics, 1957. **5**: p. 147-209.
114. Markx, G.H., *The use of electric fields in tissue engineering. A review*. Organogenesis, 2008. **4**(1): p. 11-7.
115. U. Pliquet and M.R. Prausnitz, *Electrical impedance spectroscopy for rapid and non-invasive analysis of skin electroporation*. Electrochemotherapy, Electrogenetherapy and Transdermal Delivery , Electrically Mediated Delivery of Molecules to Cells. Totowa, NJ: Humana Press.

116. P. Ducommun, et al., *On-line determination of animal cell concentration in two industrial high-density culture processes by dielectric spectroscopy*. *Biotechnology and Bioengineering*, 2002. **77**: p. 316-23.
117. C. Justice, et al., *Process control in cell culture technology using dielectric spectroscopy*. *Biotechnology*, 2011. **29**(391-401).
118. C. Hildebrandt, et al., *Detection of the osteogenic differentiation of mesenchymal stem cells in 2D and 3D cultures by electrochemical impedance spectroscopy*. *Biotechnology*, 2010. **148**(1): p. 83-90.
119. H. Wu, et al., *Exploring the Potential of Electrical Impedance Tomography for Tissue Engineering Applications*. *Materials*, 2018. **11**(6): p. 31.
120. S.F. Khalil, M.S. Mohktar, and F. Ibrahim, *The Theory and Fundamentals of Bioimpedance Analysis in Clinical Status Monitoring and Diagnosis of Diseases. A Review*. *Sensors*, 2014. **14**.
121. C. Canali, et al. *Impedance-Based Monitoring for Tissue Engineering Applications*. in *Latin American Conference on Bioimpedance*. 2016. New York: Springer.
122. A. Yúfera and A. Rueda, *A Method for Bioimpedance Measure With Four- and Two-Electrode Sensor Systems*, in *30th Annual International IEEE EMBS Conference Vancouver*. 2008: British Columbia, Canada.
123. T.S. Carvalho, et al., *Comparison of bipolar and tetrapolar techniques in bioimpedance measurement*, in *XXIV Congresso Brasileiro de Engenharia Biomédica – CBEB*. 2014.
124. R. Bragos, et al., *Four versus two-electrode measurement strategies for cell growing and differentiation monitoring using electrical impedance spectroscopy*, in *Annual International Conference of the IEEE Engineering in Medicine & Biology Society*. 2006. p. 2106-9.
125. E. Sarro, et al. *Four electrode EIS measurement on interdigitated microelectrodes for adherent cell growing and differentiation monitoring*. in *13th International Conference on Electrical Bioimpedance and the 8th Conference on Electrical Impedance Tomography - IFMBE Proceedings*. 2007. New York: Springer.
126. H. Kalvøy, et al., *Impedance-based tissue discrimination for needle guidance*. *Physiological Measurements* 2009. **30**.
127. S.M. Radke and E.C. Alocilja, *Design and Fabrication of a Microimpedance Biosensor for Bacterial Detection*. *IEEE Sensor Journal*, 2004. **4**: p. 434-40.
128. Giaever, I., *Use of Electric Fields to Monitor the Dynamical Aspect of Cell Behaviour in Tissue Cultures*. *IEEE Transaction on Biomedical Engineering*, 1986. **32**: p. 242-7.
129. P. Linderholm, A. Bertsch, and P. Renaud, *Resistivity probing of multi-layered tissue phantoms using microelectrodes*. *Physiological Measurement*, 2004. **25**: p. 645-58.
130. Huang, X., *Simulation of Microelectrode Impedance Changes Due to Cell Growth*. *IEEE Sensors Journal*, 2004. **4**: p. 576-83.
131. C. Canali, S. Mohanty, and A. Heiskanen, *Impedance Spectroscopic Characterisation of Porosity in 3D Cell Culture Scaffolds with Different Channel Networks*. *Electroanalysis*, 2015. **27**(1): p. 193-9.
132. T. Ragheb and L.A. Geddes, *The Polarization Impedance of Common Electrode Metals Operated at Low Current Density*. *Annals of Biomedical Engineering*, 1991. **19**: p. 151-63.
133. L.A. Geddes and R. Roeder, *Criteria for the selection of materials for implanted electrodes*. *Annals of Biomedical Engineering*, 2003. **31**(7): p. 879-90.
134. Holder, D., *Electrical Impedance Tomography: Methods, History and Applications*. 2005, Bristol: Institute of Physics Publishing.

135. H. Kalvøy, et al., *New Method for Separation of Electrode Polarization Impedance from Measured Tissue Impedance*. The Open Biomedical Engineering Journal, 2011. **5**: p. 8-13.
136. M.W. Tibbitt and K.S. Anseth, *Hydrogels as extracellular matrix mimics for 3D cell culture*. Biotechnology and Bioengineering, 2009. **103**(4): p. 655-63.
137. H.J. Mulhall, et al., *Epithelial cancer cells exhibit different electrical properties when cultured in 2D and 3D environments*. Biochimica et Biophysica Acta, 2013. **1839**(11): p. 5136-41.
138. D. Huh, et al., *Microengineered physiological biomimicry: organs-on-chips*. Lab Chip, 2012. **12**(12): p. 2156-64.
139. B. Zhang and M. Radisic, *Organ-on-a-chip devices advance to market*. Lab Chip, 2017. **17**(14): p. 2395-420.
140. J. Kieninger, et al., *Microsensor systems for cell metabolism – from 2D culture to organ-on-chip*. Lab Chip, 2018. **18**: p. 1274-91.
141. H.C. Wu, et al., *Electrical impedance tomography for real-time and label-free cellular viability assays of 3D tumour spheroids*. Analyst, 2018. **143**(17): p. 4189-98.
142. S.M. Lee, et al., *Realtime monitoring of 3D cell culture using a 3D capacitance biosensor*. Biosensors and Bioelectronics, 2016. **77**: p. 56-61.
143. E. Knight and S. Przyborski, *Advances in 3D cell culture technologies enabling tissue-like structures to be created in vitro: Review Article*. Journal of Anatomy, 2015. **227**(746-56).
144. Abbott, A., *Cell culture: Biology's new dimension*. Nature, 2003. **424**: p. 870-2.
145. A.J. Engler, et al., *Matrix Elasticity Directs Stem Cell Lineage Specification*. Journal of Biomechanical Engineering, 2006. **126**: p. 677-89.
146. L.G. Griffith and M.A. Swartz, *Capturing complex 3D tissue physiology in vitro*. Nature Reviews Molecular Cell Biology, 2006. **7**: p. 211-24.
147. D. Antoni, et al., *Three-Dimensional cell culture: A breakthrough in Vivo*. International Journal of Molecular Sciences, 2015. **16**(3): p. 5517-27.
148. Lei, K.F., *Review on Impedance Detection of Cellular Responses in Micro/Nano Environment* Micromachines, 2014. **5**: p. 1-12.
149. L.E. Smith, R. Smallwood, and S. Macneil, *A comparison of imaging methodologies for 3D tissue engineering*. Microscopy Research and Technique, 2010. **73**(12): p. 1123-33.
150. H. Fricke and S. Morse, *The electrical resistance and capacity of blood for frequencies between 800 Hz and 4.5 MHz*. The Journal of General Physiology, 1925. **9**: p. 153-67.
151. J.S. Daniels and N. Pourmand, *Label-Free Impedance Biosensors: Opportunities and Challenges: A Review*. Electroanalysis, 2007. **19**(12): p. 1239-57.
152. T.K. Bera and J. Nagaraju, *Electrical Impedance Spectroscopic Studies on Broiler Chicken Tissue Suitable for the Development of Practical Phantoms in Multifrequency EIT*. Journal of Electrical Bioimpedance, 2011. **2**: p. 48-63.
153. D. Bouchaala, O. Kanoun, and N. Derbel, *High accurate and wideband current excitation for bioimpedance health monitoring systems*. Measurement, 2015. **79**: p. 339-48.
154. I.O. K'Owino and O.A. Sadik, *Impedance spectroscopy: A powerful tool for rapid biomolecular screening and cell culture monitoring*. Electroanalysis, 2005. **17**(23): p. 2101-13.
155. L. Holhjem, et al., *Development of a conductometric biocompatible sensor for detecting ischemia*, in *Microelectronics Packaging Conference (EMPC)*. 2013.
156. D. El Khaled, et al., *Dielectric and Bioimpedance Research Studies: A Scientometric Approach Using the Scopus Database. A Review*. MDPI Publications, 2018. **6**(6).

157. J. Martínez-Teruel, et al., *Electrical Impedance Spectroscopy cell monitoring in a miniaturized bioreactor* in *19th IMEKO TC 4 Symposium and 17th IWADC Workshop Advances in Instrumentation and Sensors Interoperability*. 2013: Barcelona, Spain.
158. I.Giaever and C.R.Keese. *Monitoring fibroblast behavior in tissue culture with an applied electric field*. in *Proceedings of the National Academy of Sciences of the United States of America*. 1984. USA.
159. I. Giaever and C.R. Keese, *Micromotion of mammalian cells measured electrically*. *Proceedings of the National Academy of Sciences of the United States of America: Cell Biology*, 1991. **88**: p. 7896-900.
160. P. Daza, et al., *Monitoring living cell assays with bio-impedance sensors*. *Sensors and Actuators B: Chemical*, 2013. **176**: p. 605-10.
161. S.H. Jeong, et al., *A study of electrochemical biosensor for analysis of three-dimensional (3D) cell culture*. *Biosensors and Bioelectronics*, 2012. **35**: p. 128-33.
162. J. Wegener, M. Sieber, and H.J. Galla, *Impedance analysis of epithelial and endothelial cell monolayers cultured on gold surfaces*. *Journal of Biochemical and Biophysical Methods*, 1996. **32**(3): p. 151-70.
163. R. Szulcek, H.J. Bogaard, and G.P.V.N. Amerongen, *Electric Cell-substrate Impedance Sensing for the Quantification of Endothelial Proliferation, Barrier Function, and Motility*. *Journal of Visualized Experiments*, 2014. **85**: p. 51300.
164. O. Pänke, et al., *Impedance spectroscopy and biosensing*. *Advances in Biochemical Engineering / Biotechnology*, 2008. **109**: p. 195-237.
165. J.Wegener, C.R. Keese, and I. Giaever, *Electric cell-substrate impedance sensing (ECIS) as a noninvasive means to monitor the kinetics of cell spreading to artificial surfaces*. *Experimental Cell Research*, 2000. **259**(1): p. 158-66.
166. L.L. Crowell, et al., *Electrical Impedance Spectroscopy for Monitoring Chemoresistance of Cancer Cells*. *Micromachines*, 2020. **11**(9): p. 832.
167. Nguyen, D.T., et al., *Electrode-Skin contact impedance: In vivo measurements on an ovine model*. *Journal of Physics: Conference Series*, 2013. **434**: p. 012023.
168. J. Frese, et al., *Non-invasive Imaging of Tissue-Engineered Vascular Endothelium with Iron Oxide Nanoparticles*. *Biomedical Engineering*, 2012. **57**.
169. L. Jaatinen, et al., *Bioimpedance Measurement Setup for the Assessment of Viability and Number of Human Adipose Stem Cells Cultured as Mono layers*, in *World Congress on Medical Physics and Biomedical Engineering, Biomaterials, Cellular and Tissue Engineering, Artificial Organs*, O. Dossel and W.C. Schlegel, Editors. 2009, IFMBE Proceedings. p. 286-288.
170. J.L.Hong, K.Ch.Lan, and L.Sh.Jang, *Electrical characteristics analysis of various cancer cells using a microfluidic device based on single-cell impedance measurement*. *Sensor. Actuat. B-Chem.*, 2012. **173**: p. 927-934.
171. H.S. Jun, et al., *Effect of cell senescence on the impedance measurement of adiposetissue-derived stem cells*. *Enzyme Microb. Tech.* , 2013. **53**: p. 302-306.
172. J.Morucci, et al., *Bioelectrical impedance techniques in medicine. Part I. Bioimpedance measurement*. *Crit. Rev. Biomed. Eng.*, 1996. **24**: p. 257-351.
173. P.Patel and G.H.Markx, *Dielectric measurement of cell death*. *Enzyme and Microbial Technology* 2008. **4**(3): p. 463-70.
174. C.Xiao and J.H.T.Luong, *Assessment of cytotoxicity by emerging impedance spectroscopy*. *Toxicol. Appl. Pharm.*, 2005. **206**: p. 102-12.

175. P.W.Weijenborg, et al., *Electrical tissue impedance spectroscopy: a novel device to measure esophageal mucosal integrity changes during endoscopy*. J. Neurogastroenterol., 2013. **25**: p. 574-e458.
176. K.F.Lei, et al., *Development of a micro-scale perfusion 3D cell culture biochip with an incorporated electrical impedance measurement scheme for the quantification of cell number in a 3D cell culture construct*. Microfluid. Nanofluid., 2012. **12**: p. 117-125.
177. K.F. Lei, et al., *Real-time and non-invasive impedimetric monitoring of cell proliferation and chemosensitivity in a perfusion 3D cell culture microfluidic chip*. Biosensors and Bioelectronics, 2014. **51**: p. 16-21.
178. Ch.Canali, et al., *Bioimpedance monitoring of 3D cell culturing – Complementary electrode configurations for enhanced spatial sensitivity*. Biosensors and Bioelectronics, 2015. **63**: p. 72-79.
179. Wang, H.S., et al., *Highly selective and sensitive determination of dopamine using a Nafion/carbon nanotubes coated poly(3-methylthiophene) modified electrode*. Biosensors and Bioelectronics, 2006. **22**: p. 664-669.
180. W. Song, et al., *Dopamine sensor based on molecularly imprinted electrosynthesized polymers*. Journal of Solid State Electrochemistry, 2010. **14**: p. 1909-1914.
181. A.D.Abraham, K.A.Neve, and K.M.Lattal, *Dopamine and extinction: a convergence of theory with fear and reward circuitry*. Neurobiol. Learn Mem., 2014. **108**: p. 65-77.
182. S.Kintzios, *Cell-based biosensors in clinical chemistry* Mini-Rev. Med. Chem. , 2007. **7**: p. 1019-26.
183. P.Banerjee, S.Kintzios, and B.Prabhakarpanidyan, *Biotoxin detection using cell-based sensors* Toxins, 2013. **5**: p. 2366-83.
184. Apostolou, T., et al., *Assessment of in vitro dopamine-neuroblastoma cell interactions with a bioelectric biosensor: perspective for a novel in vitro functional assay for dopamine agonist/antagonist activity* Talanta, 2017. **170**: p. 69-73.
185. A.DiMauro, et al., *Spontaneous deposition of polylysine on surfaces: Role of the secondary structure to optimize noncovalent strategies*. J. Colloid Interf. Sci., 2015. **437**: p. 270-276.
186. A. Mishra, S. Singh, and S. Shukla, *Physiological and Functional Basis of Dopamine Receptors and Their Role in Neurogenesis: Possible Implication for Parkinson's disease*. Journal of experimental neuroscience, 2018. **12**: p. 1179069518779829.
187. H.Morgan, et al., *Single cell dielectric spectroscopy*. J. Phys. D Appl. Phys. , 2007. **40**: p. 61-70.
188. A.Valero, T.Braschler, and P.Renaud, *A unified approach to dielectric single cell analysis: impedance and dielectrophoretic force spectroscopy*. Lab Chip, 2010. **10**(17): p. 2216-2225.
189. N.Noveletto, et al. *Low-Cost Body Impedance Analyzer for Healthcare Applications*. in IFMBE. 2016.
190. G.Salvadore, et al., *An investigation of amino-acid neurotransmitters as potential predictors of clinical improvement to ketamine in depression*. Int. J. Neuropsychop., 2012. **15**: p. 1063-1072.
191. Marc, D.T., et al., *Neurotransmitters excreted in the urine as biomarkers of nervous system activity: validity and clinical applicability*. Neurosci. Biobehav. R., 2011. **35**: p. 635-644.
192. S.Nurullah, S.E.Tague, and C.Lunte, *Analysis of amino acid neurotransmitters from rat and mouse spinalcords by liquid chromatography with fluorescence detection*. J. Pharmaceut. Biomed., 2015. **107**: p. 217-222.

193. T.Yoetz-Kopelman, et al., "Cells-on-Beads": A novel immobilization approach for the construction of whole-cell amperometric biosensors. *Sensor. Actuat. B-Chem.*, 2016. **232**: p. 758-764.
194. F.Asphahani and M.Zhang, *Cellular Impedance Biosensors for Drug Screening and Toxin Detection*. *Analyst*, 2007. **132**(9): p. 835-841.
195. H.S.Wang, et al., *Highly selective and sensitive determination of dopamine using a Nafion/carbon nanotubes coated poly(3-methylthiophene) modified electrode*. *Biosens. Bioelectron.*, 2006. **22**(5): p. 664-669.
196. Glezer, A. and M.D. Bronstein, *Hyperprolactinemia*, in *Endotext*, L.J. De Groot, et al., Editors. 2000-, MDText.com, Inc.: South Dartmouth (MA).
197. S.Komathi, Al.Gopalan, and K.P.Lee, *Nanomolar detection of dopamine at multi-walled carbon nanotube grafted silica network/gold nanoparticle functionalised nanocomposite electrodes*. *Analyst*, 2010. **135**(2): p. 397-404.
198. A.S.Adekunle, et al., *Electrocatalytic detection of dopamine at single-walled carbon nanotubes-iron (III) oxide nanoparticles platform*. *Sensor. Actuat. B-Chem.*, 2010. **148**: p. 93-102.
199. R.M.Wightman, L.J.May, and A.C.Michael, *Detection of dopamine dynamics in the brain* *Analytical Chemistry*, 1988. **60**(13): p. 769-779.
200. C.Muzzi, et al., *Simultaneous determination of serum concentrations of levodopa, dopamine, 3-O methyl dopa and -methyl dopa by HPLC*. *Biomedical Pharmacotherapy*, 2008. **62**: p. 235-258.
201. Q.Li, J.Li, and Z.Yanga, *Study of the sensitization of tetradecyl benzyl dimethyl ammonium chloride for spectrophotometric determination of dopamine hydrochloride using sodium 1,2-naphthoquinone-4-sulfonate as the chemical derivative chromogenic reagent*. *Anal Chim Acta*, 2007. **583**(1): p. 147-152.
202. C.A.Heidbreder, et al., *Development and application of a sensitive high performance ion-exchange chromatography method for the simultaneous measurement of dopamine, 5-hydroxytryptamine and norepinephrine in microdialysates from the rat brain*. *Journal of neuroscience methods*, 2001. **112**(2): p. 135-144.
203. S.Jo, et al., *Modified platinum electrode with phytic acid and single-walled carbon nanotube: Application to the selective determination of dopamine in the presence of ascorbic and uric acids*. *Microchem. J.*, 2008. **88**(1): p. 1-6.
204. M.C.Henstridge, et al., *Voltammetric selectivity conferred by the modification of electrodes using conductive porous layers or films: The oxidation of dopamine on glassy carbon electrodes modified with multiwalled carbon nanotubes*. *Sensor. Actuat. B-Chem.*, 2010. **145**(1): p. 417-427.
205. K.W.Kwon, et al., *Soft lithography for microfluidics: a review*. *Biochip Journal*, 2008. **2**: p. 1-11.
206. K.Liu and Z.H.Fan, *Thermoplastic microfluidic devices and their applications in protein and DNA analysis*. *Analyst*, 2011. **136**: p. 1288-1297.
207. H.Becker, M.Nevitt, and B.L.Gray. *Selecting and designing with the right thermoplastic polymer for your microfluidic chip: A close look into cyclo-olefin polymer*. in *SPIE*. 2013.
208. A.Bhattacharyya and C.M.Klapperich, *Thermoplastic microfluidic device for on-chip purification of nucleic acids for disposable diagnostics*. *Analytical Chemistry*, 2006. **78**: p. 788-792.
209. G.Mehta, et al., *Hard top soft bottom microfluidic devices for cell culture and chemical analysis*. *Analytical Chemistry*, 2009. **81**(3714-3722).

210. T.Chen, J.Zhang, and H.You, *Photodegradation behavior and mechanism of poly(ethylene glycol-co-1,4-cyclohexanedimethanol terephthalate) (PETG) random copolymers: Correlation with copolymer composition*. RSC Adv., 2016. **6**: p. 102778-102790.
211. T.Chen and J. Zhang, *Surface hydrophilic modification of acrylonitrile-butadiene-styrene terpolymer by poly(ethylene glycol-co-1,4-cyclohexanedimethanol terephthalate): Preparation, characterization, and properties studies*. Appl. Surf. Sci., 2016. **388**: p. 133-140.
212. G.Paivana, et al., *Study of the dopamine effect into cell solutions by impedance analysis*, in *Conference on Bio-Medical Instrumentation and related Engineering and Physical Sciences*. 2017: Athens.
213. B.C.Gross, et al., *Evaluation of 3D printing and its potential impact on biotechnology and the chemical sciences*. Anal. Chem. , 2014. **86**(7): p. 3240-3253.
214. C.L.Ventola, *Medical applications for 3D printing: current and projected uses*. P.T., 2014. **39**(10): p. 704-711.
215. Albulbul, A., *Evaluating Major Electrode Types for Idle Biological Signal Measurements for Modern Medical Technology*. Bioengineering, 2016. **3**(20).
216. T.Valero, et al. *Electrical impedance analysis of N2a neuroblastoma cells in gel matrices after ACh-receptor triggering with an impedimetric biosensor*. in *Euroensors XXIII conference 2009*. Procedia Chemistry.
217. M.H. da Luz, et al., *Dopamine induces the accumulation of insoluble prion protein and affects autophagic flux*. Frontiers in cellular neuroscience, 2015. **9**(12).
218. Valero, M.T., *Studies on neural differentiation and monitoring with novel biosensor tools in Faculty of Biotechnology*. 2013, Agricultural University of Athens: Athens, Greece.
219. G. Barbero, L.R. Evangelista, and I. Lelidis, *Ionic contribution to the electric current in an electrolytic cell submitted to an external voltage*. Physical Review E, 2006. **74**(2).
220. E. Tognoni, et al., *Scanning Ion Conductance Microscopy-Morphology and Mechanics*, in *Encyclopedia of Interfacial Chemistry*, K. Wandelt, Editor. 2018. p. 465-474.
221. L. Yang, et al., *The Frequency Spectral Properties of Electrode-Skin Contact Impedance on Human Head and Its Frequency-Dependent Effects on Frequency-Difference EIT in Stroke Detection from 10Hz to 1MHz*. PLOS ONE, 2017.
222. M.Becchi, et al., *Impedance Spectroscopy of Water Solutions: The Role of Ions at the Liquid-Electrode Interface* J. Phys. Chem. B 2005. **109**: p. 23444-23449.
223. A.T. Lindsey, et al., *Global Cancer in Women: Burden and Trends*. Cancer Epidemiology. Biomarkers & Prevention, 2017. **26**(4).
224. C.S. Dela Cruz, L.T. Tanoue, and R.A. Matthay, *Lung Cancer: Epidemiology, Etiology, and Prevention*. Clinics in Chest Medicine, 2011. **32**(4).
225. S. Izetbegovic, et al., *Prevention of Diseases in Gynecology*. International Journal of Preventive Medicine, 2013. **4**(12): p. 1347-1358.
226. Nigel S. Key, et al., *Venous Thromboembolism Prophylaxis and Treatment in Patients With Cancer: ASCO Clinical Practice Guideline Update*. Journal of Clinical Oncology, 2019.
227. Montagnana, M. and G. Lippi, *Cancer diagnostics: current concepts and future perspectives*. Annals of Translational Medicine, 2017. **5**(13): p. 268.
228. Arruebo, M., et al., *Assessment of the Evolution of Cancer Treatment Therapies*. Cancers, 2011. **3**(3): p. 3279-3330.
229. Park, S.Y., J.B.Choi, and S. Kim, *Measurement of cell-substrate impedance and characterization of cancer cell growth kinetics with mathematical model*. International Journal of Precision Engineering and Manufacturing, 2015. **16**(8): p. 1859-1866.

230. Dan Liu, et al., *Neural regulation of drug resistance in cancer treatment*. BBA - Reviews on Cancer, 2019. **1871**: p. 20-28.
231. Paivana, G., et al., *Study of the dopamine effect into cell solutions by impedance analysis in Conference on Bio-Medical Instrumentation and related Engineering and Physical Sciences*. 2017, Journal of Physics: Athens.
232. Paivana, G., et al., *Impedance Study of Dopamine Effects after Application on 2D and 3D Neuroblastoma Cell Cultures Developed on a 3D-Printed Well*. Chemosensors, 2019. **7**(6).
233. A.K. Yadav, et al., *Development and characterization of hyaluronic acid decorated PLGA nanoparticles for delivery of 5-fluorouracil*. Drug Delivery, 2010. **17**(8): p. 561-572.
234. T. Kilic, et al., *Organs-on-chip monitoring: sensors and other strategies*. Microphysiological Systems, 2018. **2**(5).
235. G. Qiao, et al., *Electrical properties of breast cancer cells from impedance measurement of cell suspensions*. Journal of Physics Conference Series, 2010. **224**(1).
236. Ren Chaoshi, et al. *Development of electrical bioimpedance technology in the future*. in *Proceedings of the 20th Annual International Conference of the IEEE Engineering in Medicine and Biology Society*. 1998. Hong Kong, China.
237. Altinagac, E., S. Taskin, and H. Kizil. *Single Cell Array Impedance Analysis for Cell Detection and Classification in a Microfluidic Device*. in *10th International Joint Conference on Biomedical Engineering Systems and Technologies*. 2017. Portugal.
238. Hanbin, M., et al., *An impedance-based integrated biosensor for suspended DNA characterization*. Scientific Reports, 2013. **3**.
239. Sharma, S. and S.A. Goel, *Three-Dimensional Printing and its Future in Medical World*. Journal of Medical Research and Innovation, 2018. **3**(1).
240. Garcia, J., et al., *3D printing materials and their use in medical education: a review of current technology and trends for the future*. BMJ Simulation & Technology Enhanced Learning, 2018. **4**: p. 27-40.
241. L. Yuan, S. Ding, and C. Wen, *Additive manufacturing technology for porous metal implant applications and triple minimal surface structures: A review*. Bioactive Materials, 2019. **4**: p. 56-70.
242. J.J. Otero, A. Vijverman, and M.Y. Mommaerts, *Use of fused deposit modeling for additive manufacturing in hospital facilities: European certification directives*. Journal of Cranio-Maxillofacial Surgery, 2017. **45**: p. 1542-1546.
243. E. Barsoukov and J.R. Macdonald, *Impedance Spectroscopy Theory, Experiment, and Applications*. 2nd ed. 2005, New Jersey: Wiley Interscience Publication.
244. R.G. Ramírez-Chavarría, et al., *Ex-vivo biological tissue differentiation by the Distribution of Relaxation Times method applied to Electrical Impedance Spectroscopy*. Electrochimica Acta, 2018. **276**: p. 214-222.
245. Mosmann, T., *Rapid colorimetric assay for cellular growth and survival: Application to proliferation and cytotoxicity assays*. Journal of Immunological Methods, 1983. **65**(1-2): p. 55-63.
246. Li, J., et al., *Enhanced anticancer activity of 5-FU in combination with Bestatin: Evidence in human tumor-derived cell lines and an H22 tumor-bearing mouse*. Drug Development and Therapeutics, 2015. **9**(1): p. 45-52.
247. Maney, V. and M. Singh, *The Synergism of Platinum-Gold Bimetallic Nanoconjugates Enhances 5-Fluorouracil Delivery In Vitro*. Pharmaceuticals, 2019. **11**(9): p. 439.

248. Hemaiswarya, S. and M. Doble, *Combination of phenylpropanoids with 5-fluorouracil as anti-cancer agents against human cervical cancer (HeLa) cell line*. *Phytomedicine*, 2013. **20**(2): p. 151-158.
249. Kazi, J., et al., *Design of 5-fluorouracil (5-FU) loaded, folate conjugated peptide linked nanoparticles, a potential new drug carrier for selective targeting of tumor cells*. *Medicinal Chemistry Communications*, 2019. **10**: p. 559-572.
250. Pasquier, E., et al., *Propranolol potentiates the anti-angiogenic effects and anti-tumor efficacy of chemotherapy agents: implication in breast cancer treatment*. *Oncotarget*, 2011. **2**(10): p. 797-809.
251. J.A. Weisman, et al., *Antibiotic and chemotherapeutic enhanced three-dimensional printer filaments and constructs for biomedical applications*. *International Journal of Nanomedicine*, 2015. **10**: p. 357-370.
252. Schwartz, M.A. and C.S. Chen, *Deconstructing dimensionality* *Science*, 2013. **339**: p. 402-404.
253. Chung, J.H.Y., et al., *Bio-ink properties and printability for extrusion printing living cells*. *Journal of Biomaterials Science: Polymer Edition*, 1, 2013. **7**: p. 763-773.
254. Frampton, J.P., et al., *Fabrication and optimization of alginate hydrogel constructs for use in 3D neural cell culture*. *Biomedical Materials*, 2011. **6**(1).
255. Guillotin, B. and F. Guillemot, *Cell patterning technologies for organotypic tissue fabrication*. *Trends in Biotechnology*, 2011. **29**(4): p. 183-190.
256. Axpe, E. and M.L. Oyen, *Applications of Alginate-Based Bioinks in 3D Bioprinting*. *International Journal of Molecular Sciences*, 2016. **17**(12).
257. Yeo, M.G. and G.H. Kim, *A cell-printing approach for obtaining hASC-laden scaffolds by using a collagen/polyphenol bioink*. *Biofabrication*, 2017. **9**(2).
258. T.K. Bera, J. Nagaraju, and G. Lubineau, *Electrical impedance spectroscopy (EIS)-based evaluation of biological tissue phantoms to study multifrequency electrical impedance tomography (Mf-EIT) systems*. *Journal of Visualization*, 2016. **19**: p. 691-713.
259. Kerner, T.E., *Electrical impedance spectroscopy of the breast: clinical imaging results in 26 subjects*. *IEEE Transactions on Medical Imaging*, 2002. **21**(6): p. 638-45.
260. Aberg, P., *Skin cancer identification using multifrequency electrical impedance—a potential screening tool*. *IEEE Transaction on Biomedical Engineering*, 2004. **51**: p. 2097-102.
261. Osterman, K.S., *Non-invasive assessment of radiation injury with electrical impedance spectroscopy*. *Physics in Medicine and Biology*, 2004. **49**: p. 665-83.
262. Brown, B.H., *Detection of cervical intraepithelial neoplasia using impedance spectroscopy: a prospective study*. *BJOG: An International Journal of Obstetrics & Gynaecology*, 2005. **112**: p. 802-6.
263. T. Süsselbeck, et al., *Intravascular electric impedance spectroscopy of atherosclerotic lesions using a new impedance catheter system*. *Basic Research in Cardiology*, 2005. **100**: p. 446-52.
264. Soley, A., *On-line monitoring of yeast cell growth by impedance spectroscopy*. *Journal of Biotechnology*, 2005. **118**: p. 398-405.
265. R. Strand-Amundsen, et al., *In vivo characterization of ischemic small intestine using bioimpedance measurements*. *Physiological Measurement*, 2016. **37**(2): p. 257-75.
266. R. Strand-Amundsen, J.O. Høgetveit, and C. Tronstad, *Small intestinal ischemia and reperfusion – Bioimpedance measurements*. *Physiological Measurement*, 2018. **39**(2).
267. C. Hildebrandt and H. Thielecke, *Non-invasive Characterization of the Osteogenic Differentiation of hMSCs in 3D by Impedance Spectroscopy*, in *World Congress on Medical*

- Physics and Biomedical Engineering, Biomaterials, Cellular and Tissue Engineering, Artificial Organs.*, O. Dossel and W.C. Schlegel, Editors. 2009, IFMBE Proceedings: Munich, Germany. p. 81-84.
268. Y. Xu and X. Xie, *Review of impedance measurements of whole cells*. Biosensors and Bioelectronics, 2015. **77**(77).
 269. N. DePaola, et al., *Electrical impedance of cultured endothelium under fluid flow*. Annals of Biomedical Engineering, 2001. **29**(8): p. 648-56.
 270. M.D. Van Loan, et al., *Use of bioimpedance spectroscopy to determine extracellular fluid, intracellular fluid, total body water, and fat-free mass, in Human body composition 1993*, Springer US. p. 67-70.
 271. Y.P. Lin, et al., *The extracellular fluid-to-intracellular fluid volume ratio is associated with large-artery structure and function in hemodialysis patients*. American journal of kidney diseases, 2003. **42**(5): p. 990-999.
 272. T.K. Bera, N. Jampana, and G. Lubineau, *A LabVIEW-based electrical bioimpedance spectroscopic data interpreter (LEBISDI) for biological tissue impedance analysis and equivalent circuit modelling*. Journal of Electrical Bioimpedance., 2016.
 273. Bera, T.K., *Bioelectrical Impedance and The Frequency Dependent Current Conduction Through Biological Tissues: A Short Review*. IOP Conference Series: Materials Science and Engineering, 2018. **331**: p. 012005.
 274. J.A. Serrano, et al. *Practical Characterization of cell-electrode electrical models in bioimpedance assays in Proceedings of the 11th International Joint Conference on Biomedical Engineering Systems and Technologies (BIOSTEC)*. 2018.
 275. S.Y. Nam, L.J. Suggs, and S.Y. Emelianov, *Imaging strategies for tissue engineering applications*. Tissue Engineering, 2015. **21**(1).
 276. A.A. Appel, et al., *Imaging challenges in biomaterials and tissue engineering*. Biomaterials, 2013. **34**(28): p. 6615-30.
 277. P. Ducommun, P.A. Ruffieux, and A. Kadouri, *Process Development in a Packed Bed Bioreactor*. Animal Cell Technology: From Target to Market, 2002.
 278. H. Gloeckner, T. Jonuleit, and H.D. Lemke, *Monitoring of cell viability and cell growth in a hollow-fiber bioreactor by use of the dye Alamar Blue*. Journal of Immunological Methods, 2001. **252**: p. 131-8.
 279. S.C. Bürgel, et al., *Automated, Multiplexed Electrical Impedance Spectroscopy Platform for Continuous Monitoring of Microtissue Spheroids*. Analytical Chemistry, 2016. **88**(22).
 280. Y.R.F. Schmid and S.C. Burgel, *Electrical Impedance Spectroscopy for Microtissue Spheroid Analysis in Hanging-Drop Networks*. ACS Sensors, 2016. **1**(8).
 281. Sharma, R., *On-chip microelectrode impedance analysis of mammalian cell viability during biomanufacturing*. Biomicrofluidics, 2014. **8**(5).
 282. J. Stolwijk, et al., *Impedance analysis of adherent cells after in situ electroporation: non-invasive monitoring during intracellular manipulations*. Biosensors and Bioelectronics, 2011. **26**: p. 4720-7.
 283. Krommenhoek, E.E., *Monitoring of yeast cell concentration using a micromachined impedance sensor*. Sensors and actuators B: Chemical, 2006. **115**(1).
 284. P. Linderholm, et al., *Two-dimensional impedance imaging of cell migration and epithelial stratification*. Lab Chip, 2006. **6**: p. 1155-62.
 285. V. Senez, et al., *Integrated 3-D Silicon Electrodes for Electrochemical Sensing in Microfluidic Environments: Application to Single-Cell Characterization* IEEE Sensors Journal, 2008: p. 548-57.

286. Jang, L.-S. and M.-H. Wang, *Microfluidic device for cell capture and impedance measurement*. *Biomedical Microdevices*, 2007. **9**: p. 737-43.
287. Gawad, S., *Dielectric spectroscopy in a micromachined flow cytometer: theoretical and practical considerations*. *Lab on a Chip*, 2004. **3**.
288. S. Ostrovidov, Y. Sakai, and T. Fujii, *Integration of a pump and an electrical sensor into a membrane-based PDMS microbio reactor for cell culture and drug testing*. *Biomedical Microdevices*, 2011. **13**(5): p. 847-64.
289. T. Sun, et al., *On-chip electrical impedance tomography for imaging biological cells*. *Biosensors and Bioelectronics*, 2010. **25**: p. 1109-15.
290. C.R. Keese, et al., *Electrical woundhealing assay for cells in vitro*. *Proceedings of the National Academy of Sciences of the United States of America*, 2004. **101**(6).
291. G. Schade-Kampmann, et al., *On-chip non-invasive and label-free cell discrimination by impedance spectroscopy*. *Cell Proliferation in basic and clinical sciences*, 2008. **41**(5).
292. Holmes, D., *Leukocyte analysis and differentiation using high speed microfluidic single cell impedance cytometry* *Lab on a Chip*, 2006. **20**.
293. Wang, P. and Q. Liu, *Cell-based Biosensors: Principles and Applications*. 2010: Artech House.
294. F. Asphahani and M. Zhang, *Cellular impedance biosensors for drug screening and toxin detection*. *Analyst*, 2007. **132**(9): p. 835-41.
295. D. Malleo, et al., *Continuous differential impedance spectroscopy of single cells*. *Microfluidics and Nanofluidics*, 2010. **9**: p. 191-198.
296. Krukiewicz, K., *Electrochemical impedance spectroscopy as a versatile tool for the characterization of neural tissue: A mini review*. *Electrochemistry Communications*, 2020. **116**: p. 106742.
297. H.T. Ngoc Le, et al., *A Review of Electrical Impedance Characterization of Cells for Label-Free and Real-Time Assays*. *BioChip Journal*, 2019.
298. C.M. Lo, C.R. Keese, and I. Giaever, *Monitoring motion of confluent cells in tissue culture*. *Experimental Cell Research*, 1993. **204**(1): p. 102-3.
299. I. Giaever and C.R. Keese, *A morphological biosensor for mammalian cells*. *Nature*, 1993. **366**: p. 591-2.
300. C.M. Lo, C.R. Keese, and I. Giaever, *Impedance analysis of MDCK cells measured by electric cell-substrate impedance sensing*. *Biophysical Journal*, 1995. **69**(6): p. 2800-7.
301. S. Rahim and A. Uren, *A Real-time Electrical Impedance Based Technique to Measure Invasion of Endothelial Cell Monolayer by Cancer Cells*. *Journal of Visualized Experiments*, 2011. **50**.
302. J. Lyons-Reid, et al., *Bioelectrical Impedance Analysis-An Easy Tool for Quantifying Body Composition in Infancy?* *Nutrients*, 2020. **12**(4): p. 920.
303. C. Petchakup, K. Li, and H. Hou, *Advances in Single Cell Impedance Cytometry for Biomedical Applications*. *Micromachines*, 2017. **8**(3): p. 87.
304. A.A. Pathiraja, et al., *The clinical application of electrical impedance technology in the detection of malignant neoplasms: a systematic review*. *Journal of Translational Medicine*, 2020. **18**(1).
305. T.R. Vollmer, et al., *Application of Cell Impedance as a Screening Tool to Discover Modulators of Intraocular Pressure*. *Journal of Ocular Pharmacology and Therapeutics*, 2020.

306. S. Chabchoub and M. Nakkach. *Conception of Impedance Spectroscopy Analyzer and validation using yeast cell*. in *ICEMIS '18: Proceedings of the Fourth International Conference on Engineering & MIS*. 2018.
307. J.S. Heo, et al., *Poly-L-lysine Prevents Senescence and Augments Growth in Culturing Mesenchymal Stem Cells Ex Vivo*. *BioMed research international*, 2016. **2016**: p. 8196078.
308. Y.D. Yalcin and R. Luttge, *Electrical monitoring approaches in 3-dimensional cell culture systems: Toward label-free, high spatiotemporal resolution, and high-content data collection in vitro*. *Organs-on-a-Chip*, 2021. **3**(2021): p. 100006.
309. D. Naranjo-Hernández, J.Reina-Tosina, and M. Min, *Fundamentals, Recent Advances, and Future Challenges in Bioimpedance Devices for Healthcare Applications*. *Journal of Sensors*, 2019. **2019**: p. 42.
310. M. Pinto Sandra, et al., *Electrode cleaning and reproducibility of electrical impedance measurements of HeLa cells on aqueous solution*. *Revista de la Academia Colombiana de Ciencias Exactas, Físicas y Naturales*, 2020. **44**(170): p. 257-268.
311. G. Paivana, et al., *Evaluation of Cancer Cell Lines by Four-Point Probe Technique, by Impedance Measurements in Various Frequencies*. *Biosensors* 2021. **11**: p. 345.
312. R.E. Fernandez, et al., *Flexible bioimpedance sensor for label-free detection of cell viability and biomass*. *IEEE Transactions on NanoBioscience*, 2015. **14**(7): p. 700-706.
313. G. Huertas, et al., *The bio-oscillator: a circuit for cell-culture assays*. *IEEE Transactions on Circuits and Systems II: Express Briefs*, 2015. **62**(2): p. 164-168.
314. F.A. Alexander, D.T. Price, and S. Bhansali, *From cellular cultures to cellular spheroids: is impedance spectroscopy a viable tool for monitoring multicellular spheroid (MCS) drug models?* *IEEE Reviews in Biomedical Engineering*, 2013. **6**: p. 63-76.
315. S. Khan, et al., *Prostate cancer detection using composite impedance metric*. *IEEE Transactions on Medical Imaging*, 2016. **35**(12): p. 2513-2523.